Evapotranspiration from Groundwater Dependent Plant Communities:

Comparison of Micrometeorological and Vegetation-Based Measurements

A Cooperative Study Final Report Prepared by The County of Inyo Water Department and Los Angeles Department of Water and Power

Robert Harrington, Aaron Steinwand, Paula Hubbard, and Dave Martin
with contributions from Jim Stroh, The Evergreen State College
and Dani Or, Univ. of Connecticut

September 15, 2004

TABLE OF CONTENTS

LIST OF FIGURES

LIST OF TABLES

EXECUTIVE SUMMARY

In 2000, Inyo County and LADWP began a cooperative study designed to compare methods of forecasting plant water requirements based on vegetation leaf area with independent micrometerological measurements of evapotranspiration (ET). Towers equipped with eddy covariance (EC) sensors to measure the vertical flux of heat and water vapor were installed at seven sites over four growing seasons. As in other studies using the EC technique, the amount of energy accounted for by heat flow and evaporation was less than total available energy. To address this discrepancy, an additional experiment comparing results from Bowen ratio and EC stations was successfully completed to develop a procedure to adjust the EC measurements.

Two transpiration models to determine plant water requirements, the current Green Book (GB) method and a similar method based on transpiration coefficients (Kc), were compared with measured ET. The GB and Kc models best agreed with measured values of ET for essentially equal numbers of site-years, but the Kc model and its leaf area component performed marginally better than the GB model. The preferred transpiration model for management could not be determined, however, as both models tended to underestimate growing season ET. Failure to identify the superior model was partially due to the narrow range of site conditions that meet assumptions in the models and also due to the small difference between the models relative to the precision of the ET measurement. Often neither model predicted ET well and average deviation from measured ET was relatively large, approximately 8 to 9 cm over the growing season, despite the attempt to select sites that met the assumptions of the transpiration models. Reliance on forecasted plant water requirements for groundwater management is not advised without provisions to consider the potentially large error in the forecasts.

Introduction

Pumping is managed under the Inyo/Los Angeles Water Agreement (Agreement) based on data collected at permanent monitoring sites located in wellfield areas throughout the Owens Valley. Operational status of Los Angeles Department of Water and Power (LADWP) pumping wells near the permanent monitoring sites is determined by comparing predicted transpiration with the amount of plant-available soil water stored in the root zone. The transpiration predictions are derived from vegetation measurements and functions that describe the seasonal trends in transpiration per leaf area and leaf area index (LAI). Details of the measurement methods and models are contained in a technical appendix to the Agreement titled the Green Book (GB). An alternative method to prepare the transpiration predictions based on empirically-derived transpiration coefficients (Kc) has been proposed for adoption to revise the Green Book (Steinwand et al., 2001; Steinwand, 1999b). Both the Kc and GB methods were developed from similar field measurements and involve scaling up from measurements made on individual leaves or small branches to the scale of the monitoring sites. Relying on computations involving variables measured at small scales to make large-scale forecasts requires verification against concurrent measurements made at larger spatial scales.

There are several methods of measuring evapotranspiration (ET) using micrometeorological measurements (Brutsaert, 1982; Shuttleworth, 1993). All such methods measure variables near the land surface (i.e., a few meters above the plant canopy) to determine fluxes of energy, momentum, or trace gases. The eddy covariance (EC) method has gained predominance among micrometeorological methods recently because of its minimal theoretical assumptions and improved instrumentation (Shuttleworth, 1993). An advantage of the eddy covariance method is that it is the most direct measurement of sensible and latent heat fluxes that is possible with micrometeorological methods. Previous studies in the Owens Valley have used micrometeorological methods to measure water vapor fluxes from phreatophytic vegetation (Duell, 1990; Gay, 1992; Duell, 1992), but these measurements were not made concurrently with the necessary vegetation cover or leaf area measurements to perform a comparison with the GB or Kc vegetation-based transpiration models.

Since 2000, Inyo County and LADWP have jointly conducted a cooperative study entitled "Evapotranspiration (ET) from groundwater dependent plant communities: Comparison of micrometeorological and vegetation-based measurements". The purpose of the study is to measure ET from groundwater dependent plant communities in the Owens Valley using EC methods, and to compare those measurements with plant leaf area based methods of forecasting plant water requirements. In 2002, Inyo County received funding from California Department of Water Resources to purchase and operate two additional EC stations. Because of the similar study design, data from sites equipped with those instruments are included in this report.

Materials and Methods

Site selection

Sites were selected based on plant species composition, depth to the water table, site security, and fetch. Eddy covariance stations were placed in both mixed and monocultural sites ranging from alkali meadow to scrub vegetation communities. Except for one site (PLC018), the intent was to select sites with DTW sufficient to subirrigate the vegetation, but deep enough to

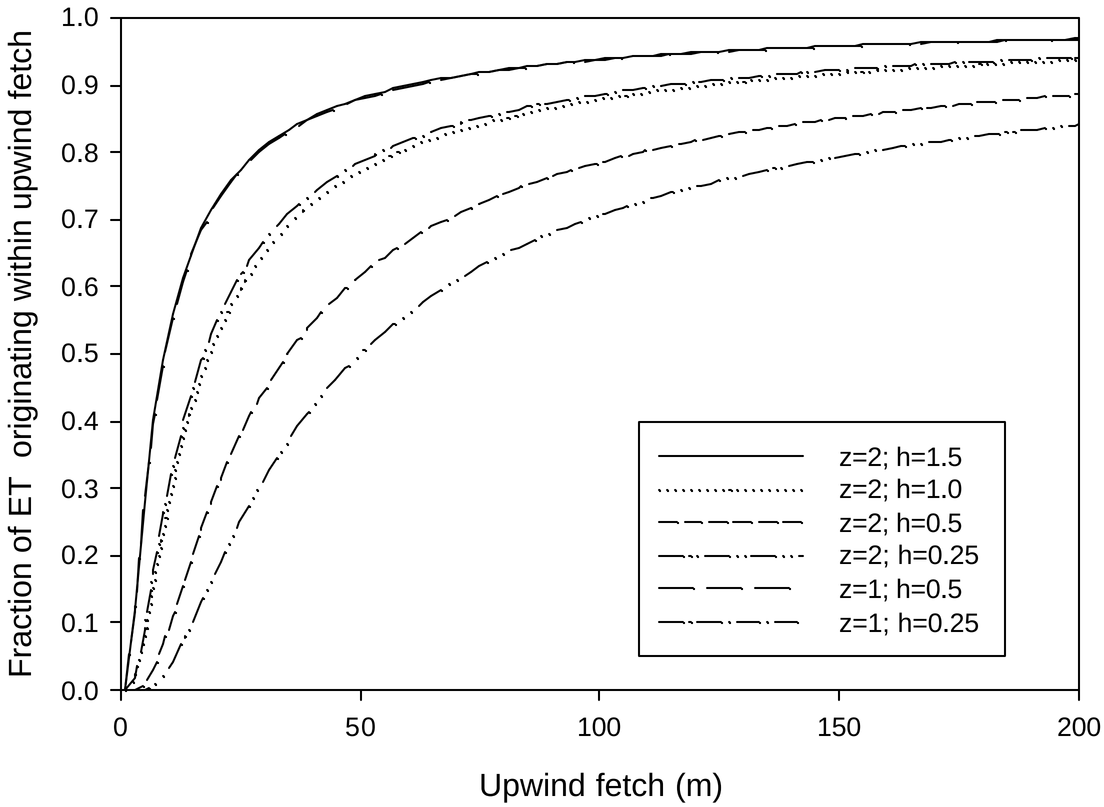

Figure 1. Approximate contributing area upwind of an eddy-covariance station in unstable conditions according to Gash (1986). Reasonable values were assumed for roughness height, stability, wind speed, and zero-plane displacement. *z* is instrument height and *h* is canopy height.

minimize surface evaporation. Bare soil evaporation must be minimal to allow comparison of eddy covariance results (ET) with vegetation based estimates of transpiration (T). Soil water and water table measurements were included in this study to examine how well these assumptions were met. Sites PLC018 and PLC045 were typical of abandoned farmland on sandy soils and relatively deep water tables near Bishop that are now vegetated with near-monocultures of rabbitbrush or saltbush. Although probably not appropriate to compare to GB or Kc models,

Table 1. Eddy covariance site characteristics. Depth to water change during the growing season is given, and precipitation values are annual totals beginning October 1 the previous year.

Year	Site	Vegetation type	Dominant Species^	Depth to water (m)	Precipitation (mm)
2000	BLK100	alkali meadow	SPAI, DISP2	2.0-2.5	35.6
2001	BLK100	alkali meadow	SPAI, DISP2	2.2-3.0	71.1
	BLK009	Rabbitbrush meadow	CHNA2, SPAI	2.6-3.2	71.1
	PLC045	Nev.saltbush scrub	ATTO	3.8-4.1(est.)	105.9
2002	BLK100	alkali meadow	SPAI, DISP2	2.3-3.2	32.5
	FSL138	alkali meadow	DISP2, LETR, SPAI	1.2-2.1	21.8
	PLC018	Rabbitbrush scrub	CHNA2	>5.0	34.5
	PLC074	Nev. saltbush meadow	SAVE4, ATTO, DISP2	2.1-2.4	31.5
	PLC185	desert sink scrub	SAVE4	4.0	31.5
2003	BLK100	alkali meadow	SPAI, DISP2	2.1-3.3	301.8
	PLC074	Nev. saltbush meadow	SAVE4, ATTO, DISP2	2.1-2.4	91.7
	PLC185	desert sink scrub	SAVE4	>4.0	150.9

^: grasses: SPAI, *Sporobolus airoides;* DISP2, *Distichlis spicata;* LETR5, *Leymus triticoides.* shrubs*: C*HNA2, *Chysothamnus nauseosus;* ATTO *Atriplex lentiformis* ssp. *torreyi;* SAVE4, *Sarcobatus vermiculatus.* The rabbitbrush subspecies at PLC018 may be *hololeuca.*

EC data from those sites were valuable to interpret results from other sites and may be useful for groundwater modeling efforts in another cooperative study. Methods in Gash (1986) were used to estimate the size of the potential area contributing to the EC measurements to guide selection of sites (Figure 1). Sites with obvious boundaries between dissimilar vegetation and hydrologic conditions within approximately 150 m of the site were avoided. All sites were undisturbed by water spreading or irrigation.

Locations of the EC sites are shown on Figures 2 to 8, and environmental characteristics of the sites are summarized in Table 1. Each EC tower was fenced to prevent cattle from damaging the instruments. The fenced exclosure at BLK100 was expanded in 2001 to include the vegetation transects because of observed grazing impacts adjacent to the tower exclosure late in the growing season and over winter. Cattle were not excluded from the vegetation transects at

Figure 2. Aerial photograph and ET, soil water, and LAI measurement locations at EC site BLK100.

Figure 3. Aerial photograph and EC, soil water and LAI measurement locations at EC site BLK009.

Figure 4. Aerial photograph and EC, soil water and LAI measurement locations at EC site PLC045.

Figure 5. Aerial photograph and EC, soil water and LAI measurement locations at EC site FSL138.

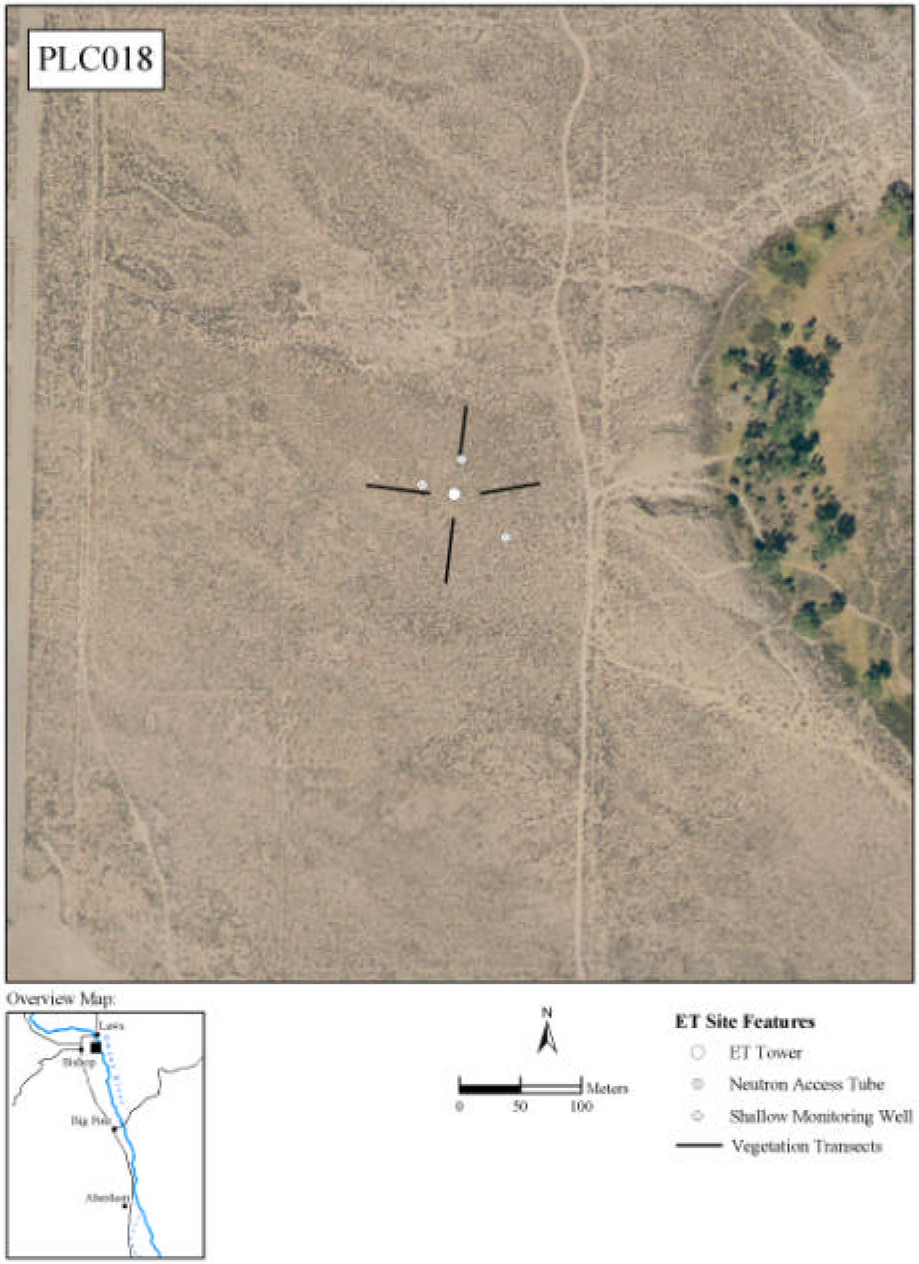

Figure 6. Aerial photograph and EC, soil water and LAI measurement locations at EC site PLC018.

Figure 7. Aerial photograph and EC, soil water and LAI measurement locations at EC site PLC074.

Figure 8. Aerial photograph and EC, soil water and LAI measurement locations at EC site PLC185.

Table 2. Dates of EC station operation.

Year	Site	Date established	Date removed
2000	BLK 100	April 21	January 8, 2001
2001	BLK 100	March 7	November 27
	BLK 9	April 11	November 27
	PLC 45	April 10	November 27
2002	BLK 100	March 12	October 2
	FSL 138	May 3	September 11
	PLC 18	May 2	October 8
	PLC 74	May 25	October 7
	PLC 185	May 24	October 7
2003	BLK 100	April 23	December 26
	PLC 74	April 24	November 17
	PLC 185	April 24	January 6, 2004

any other site. Three sites monitored in 2002, BLK100, PLC074 and PLC185,were also instrumented in 2003 partly to determine if ET and the soil water balance differed after a much wetter winter. Precipitation preceding the growing seasons each year 2000-2002 consisted of small events, and total precipitation was below normal (about 130 mm) in all years. Precipitation preceding the 2003 growing season was 3 to 5 times that in previous years (Table 1). In all years, EC measurements were collected during most of the growing season, approximately March 25 to October 15 (Table 2).

Eddy covariance theory and instrumentation

The EC method of measuring turbulent fluxes uses fast-response sensors to measure rapid changes in vertical wind speed and scalar quantities (e.g. water vapor density or heat content) to compute the flux of the scalar by means of the covariance of the vertical wind and the scalar (Arya, 2001). The latent heat flux is,

$$lE = l\,\overline{w' r_v'} \tag{1}$$

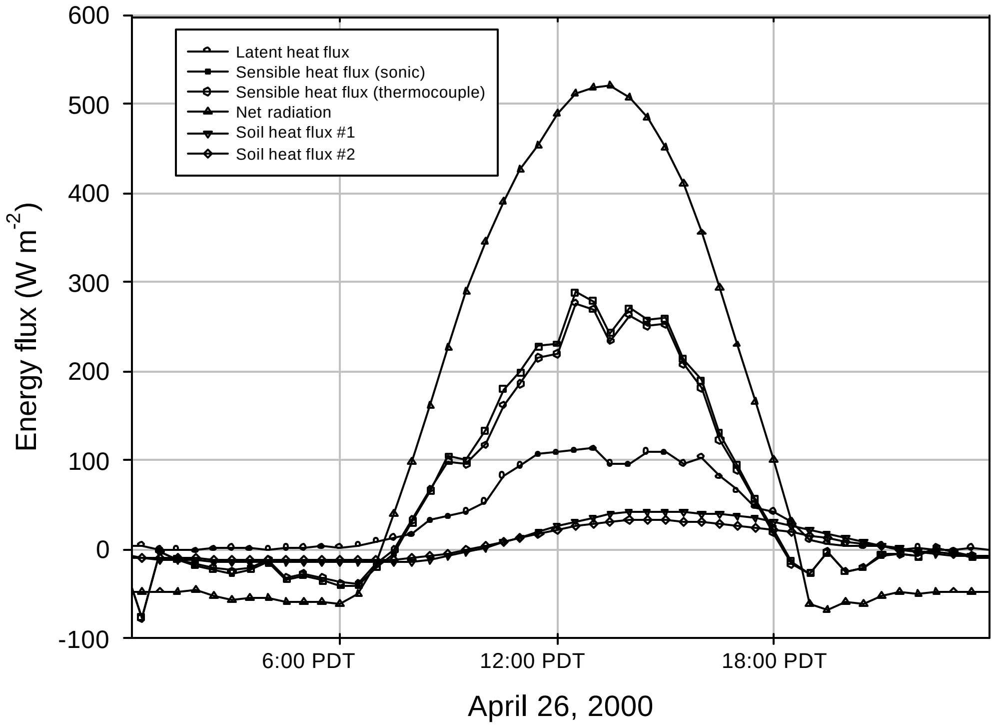

Figure 9. Energy balance components measured at BLK100. *H* calculated using air temperature measured with both fine wire thermocouple and sonic anemometer agreed well.

and the sensible heat flux is,

$$H = rC_p\overline{w'T'} \qquad (2)$$

where l is the latent heat of evaporation (J kg^{-1}), w is the vertical wind speed (m s^{-1}), r_v is the water vapor density (kg m^{-3}), r is the mean air density (kg m^{-3}), C_p is the specific heat of air (J kg^{-1} K^{-1}), T is the air temperature. Primes indicate deviations from the time-averaged mean, and the overbar indicates time averaging.

Vertical wind speed was measured with a Campbell CSAT sonic anemometer (Campbell Scientific Inc., 1998a), the water vapor density was measured with a Campbell KH20 krypton hygrometer (Campbell Scientific Inc., 1989), and air temperature was measured using a fine-wire thermocouple, all of which were mounted 2.5 m above the land surface. Sensible heat flux was calculated using both the temperature as calculated from the sonic anemometer and as measured by the fine wire thermocouple, and the two methods had close agreement at BLK100 (Figure 9). The fine wire thermocouples were replaced repeatedly due to breakage which resulted in an intermittent record; therefore, the sonic temperature was used in computing the sensible heat flux. The data were acquired and the covariance computed at 10 Hz, and fluxes were averaged over 30 minute intervals. The EC system has the advantage that the computed covariance theoretically provides a direct measure of the scalar flux at the point of measurement. Difficulties in the EC method arise in the demands made on the instrumentation to acquire data at the necessarily rapid sampling rate, and the fact that the measurements in practice are non-collocated volume averages rather than collocated at a point as assumed by Equations 1 and 2.

The EC measurements were corrected for absorption of the krypton hygrometer ultraviolet beam by oxygen (Campbell Scientific Inc., 1998b), and for the effect of fluctuating air density (Webb et al., 1980). These corrections were implemented as,

$$lE = l\left(\overline{w' r_v'} + \frac{r_v H}{r C_p T} + \frac{F k_0 H}{k_w T} \right) \tag{3}$$

where F is a factor to account for the fraction of oxygen in air (gm K J^{-1}), k_o is the oxygen absorption coefficient (0.0045 m^3 gm^{-1} cm^{-1}), and k_w is the water vapor absorption coefficient (0.154 m^3 gm^{-1} cm^{-1}). The first term in the parentheses is the uncorrected EC vapor flux, the second term corrects for fluctuations in air density, and the third term corrects for the effect of oxygen on the krypton hygrometer.

Though not necessary to make the EC measurement of turbulent fluxes, the EC systems were also equipped with a REBS Q-7.1 net radiometer (Campbell Scientific Inc., 1996), soil heat flux plates (Campbell Scientific Inc., 1999), soil temperature sensors, and a frequency domain reflectometer (Campbell Scientific Inc., 1996) for measuring soil wetness. These additional instruments allow the energy balance to be computed. Two soil heat flux plates were installed at a depth of 8 cm approximately 1 m apart, and soil temperature thermocouples were installed at depths of 2 and 6 cm between the flux plates. The soil heat flux at the soil surface was computed by correcting the heat flux measured at the flux plate for thermal storage in the soil above the flux plates,

$$G = G_z + \Delta z \frac{\Delta T}{\Delta t}\left(C_w q_v r_w + r_b C_s\right) \tag{4}$$

where G_z is the average of the two flux plates (W m^{-2}), Δz is the depth of the flux plates, ΔT is the average change in temperature of the two soil temperature thermocouples (C^o), Δt is the time interval over which the flux is averaged (s), C_w is the specific heat capacity of water (4.18 J g^{-1} K^{-1}), q_v is the volumetric soil water content, r_w is the density of water (1.00 gm cm^{-3}), r_b is the measured soil bulk density (1.11 gm cm^{-3}), and C_s is the specific heat capacity of dry soil material (0.87 J gm^{-1} K^{-1}). Soil bulk density was determined by oven drying soil samples, water content was measured by FDR, and the specific heat capacity of dry soil material was taken from Campbell and Norman, Table 8.2 (1998). The sign convention adopted throughout this report is: net radiation is positive when directed toward the land surface, sensible and latent heat fluxes are positive when directed away from the land surface, and soil heat flux is positive when directed into the soil.

Several quality control measures were implemented to ensure accurate data were collected. The towers were instrumented to measure all components of the energy balance (*EB*) to allow an independent check of the ET measured by the EC methods using,

$$EB = Rn - G - H - \lambda E \qquad (5)$$

where *Rn* is net radiation (W m-2), *H*, *G*, and λE as defined above. *EB* should equal zero if canopy heat storage, photosynthetic absorption of solar radiation, and advective energy transport processes are negligible. EC measurements collected during this study and others (Bidlake, 2000; Bidlake 2002; Norman and Baker, 2002; Berger et al., 2001; Sumner, 1996; Stannard, 1993) have found that EB does not equal zero, with the sum of the turbulent fluxes ($H + \lambda E$) measured by the EC instruments generally being less than the available energy (R_n - G). Results of the analysis of *EB* are described more fully in a separate section below.

Post processing of the EC data included inspection of the record for anomalies in all data streams and inspection of the turbulent flux data for sonic anemometer spikes or signal losses. If more than 5% of the 10 Hz signal from the eddy covariance sensors was lost over a thirty-minute sampling interval, that interval was discarded. Routine maintenance and data downloads were done during each site visit at roughly weekly intervals. Typically, the data were downloaded, the windows on the hygrometer were cleaned, the net radiometer domes were cleaned, the sonic anemometer and net radiometer were checked for level, the solar panel was cleaned, and sensor output was examined to make sure all sensors were recording correctly. Upon the completion of

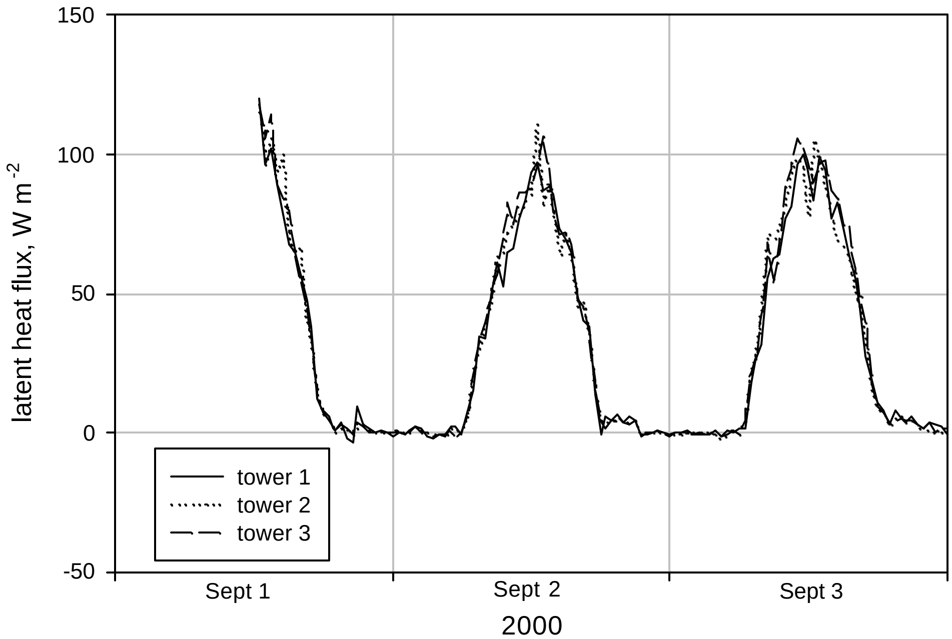

Figure 10. Latent heat flux from three collocated systems at BLK 100 for September 1-3, 2000.

measurements each year, the EC instruments were removed from the field for factory recalibration.

For 62 days during July to October, 2000, three EC systems were installed at BLK100 to collect concurrent ET, air temperature, and humidity measurements. For this comparison, the instrument towers were placed about 4 meters apart, arrayed roughly perpendicular to the mean wind direction. The most significant data gaps are in the net radiation record, which lost data during the interval from day of year (DOY) 119 to 130 due to a problem with the datalogger program, from DOY 177 to 180 due to rodents chewing through the instrument cable, and from DOY 284 though 294 due to a broken radiometer dome. All three systems were powered down

Table3. Statistics of EC tower comparison at BLK100.

	Tower 1	Tower 2	Tower 3
mean LE flux (W m^{-2})	32.87	34.26	33.89
standard deviation	47.03	48.61	48.36
% of mean of all towers (33.67 W m^{-2})	97.6%	101.7%	100.6%

and instruments removed from the field during the period DOY 242 through 245 due to inclement weather. Short intervals of data were lost when the transducer heads of the sonic anemometer were wet due to rain. Simultaneous operation of three collocated eddy covariance systems showed that latent heat fluxes measured by the three systems agreed within a few percent of with one another (Figure 10). Table 3 compares the statistics of the latent heat fluxes measured by each system.

The ET record at all sites contained gaps due to instrument failure, or the record was truncated before the end or after the beginning of the growing season. To provide uniform limits for integration and to permit site to site comparisons and year to year comparisons, the EC data were fit to a Fourier model like that used to predict reference ET (ETr, described below). This model was chosen because of its demonstrated ability to model the seasonal changes in evaporative demand represented by ETr (Or and Groeneveld, 1994). Occasionally the fitted model was poorly constrained during winter when EC data were lacking and gave negative values. When this occurred, daily ET was assumed to be 0.01 mm day^{-1} and the model was revised. This procedure was largely for graphical purposes, and the effect on the comparison with Kc and GB transpiration models was negligible because only the daily ET or T values during the growing season were summed.

Bowen ratio theory and instruments

Energy fluxes measured by the EC system were compared to fluxes measured with a Bowen ratio (BR) system to examine the EB closure problem and to develop recommendations for processing the EC data to estimate lE. A BR system was installed and operated by Dr. Jim Stroh of Evergreen State College from August 23 to September 3, 2002 at BLK100 adjacent to the EC tower. The instrument towers were located 5 m apart in an east-west alignment so wakes on the lee side of each tower would not interfere with the other tower during the prevailing afternoon southeasterly winds. The net radiometers were mounted 5 m apart and 3 m south of their respective instrument towers.

The BR method relies on different assumptions and instrumentation than EC to estimate fluxes. Agreement between the two methods would strongly corroborate the results, and disagreement between the methods can help determine likely sources of error. The BR method uses measurements of water vapor density and temperature at two heights to compute the average gradients near the surface, and then by equating the eddy diffusivity for sensible and latent heat, uses Equation 5 and the measured Bowen ratio ($b = H/lE$) to compute the turbulent fluxes. Beyond its use in the BR method, b is significant as a measure of the relative partitioning of available energy between sensible and latent heat. The BR system consisted of fine wire thermocouples mounted at 1.0 and 2.0 m above the surface, a chilled mirror hygrometer, an air pump and routing system that alternately directs an air stream from the upper and lower sensor arms to the hygrometer, a net radiometer, soil heat flux plates, and soil temperature sensors. Fluxes were averaged over 20 minute intervals. The BR method has the advantage that the instrumentation is relatively simple compared to the EC method, but has the disadvantage that energy balance is used to compute the fluxes. The energy balance cannot be used as a check on the internal consistency of the computed fluxes, and any errors in measuring available energy affect the computation of the turbulent fluxes. The chilled mirror hygrometer has a limited range of environmental conditions under which it will function properly. In very dry conditions, very warm conditions, or very cool conditions, formation of frost on the mirror surface confounds the dew point measurement. The early fall season was chosen for operation of the BR system at this site because it was expected that conditions would be within the applicable range of the chilled mirror hygrometer. Soil heat flux was computed as described for the EC systems.

Two sources of error that are common to both BR and EC measurements are the mismatch between the sampling areas ("footprints") of the various sensors used to compute fluxes and energy balances, and the variability of the landscape within the footprint. For example, the sonic anemometer and krypton hygrometer combine to sense water vapor flux integrated over a footprint with a radius on the order of 100 m, whereas the calculation of soil heat flux has a footprint of about a square meter. Similar mismatches of measurement areas or volumes are present in the BR instrumentation. Because the land surface properties that affect the energy balance are spatially heterogeneous, these footprint mismatches limit the precision with which the energy balance at a point can be estimated.

<u>Soil water, groundwater, and precipitation measurements</u>

Detailed measurements of soil water content were conducted using a combination of time domain reflectometry (TDR), neutron gauge , and gravimetric sampling. Soil depths 20 cm and below were monitored in 15 cm increments using a neutron gauge. Three or four access tubes were installed adjacent to the vegetation transects and usually to the water table. Only one

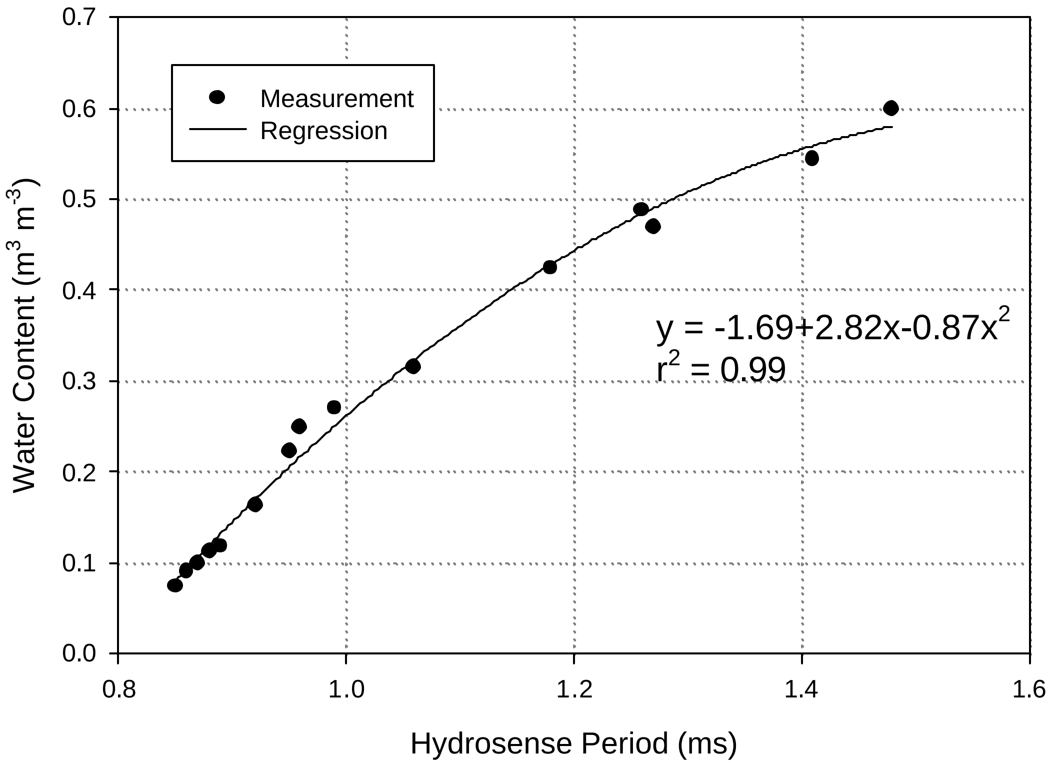

Figure 11. Hydrosense laboratory calibration for surface measurements at BLK100.

access tube extended to depths below one meter at PLC045 because augered holes in the dry, sandy soil collapsed repeatedly. Access tubes were constructed of PVC except at PLC018 where aluminum tubes were used. The neutron gauge was calibrated by regressing volumetric water content (2) of soil samples collected during access tube installation at each site against neutron gauge count ratio (count/field standard count) recorded at the sampling depths. Determination of 2 followed Blake and Hartage (1986). Soil cores of a known volume were collected, weighed, and dried at 105 ^{o}C for 24 hours to determine the gravimetric water content (g water/g soil) and bulk density (g soil cm^{-3} soil). Volumetric water content (cm^3 water/cm^3 soil) is the product of gravimetric water content and bulk density (assuming the density of water is 1 g cm^{-3}). Shallow

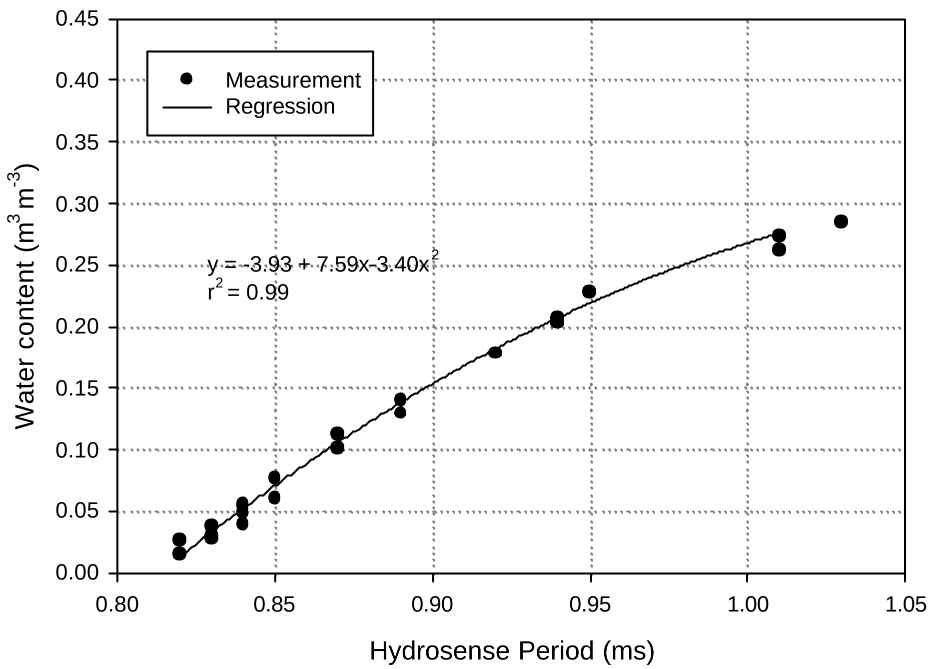

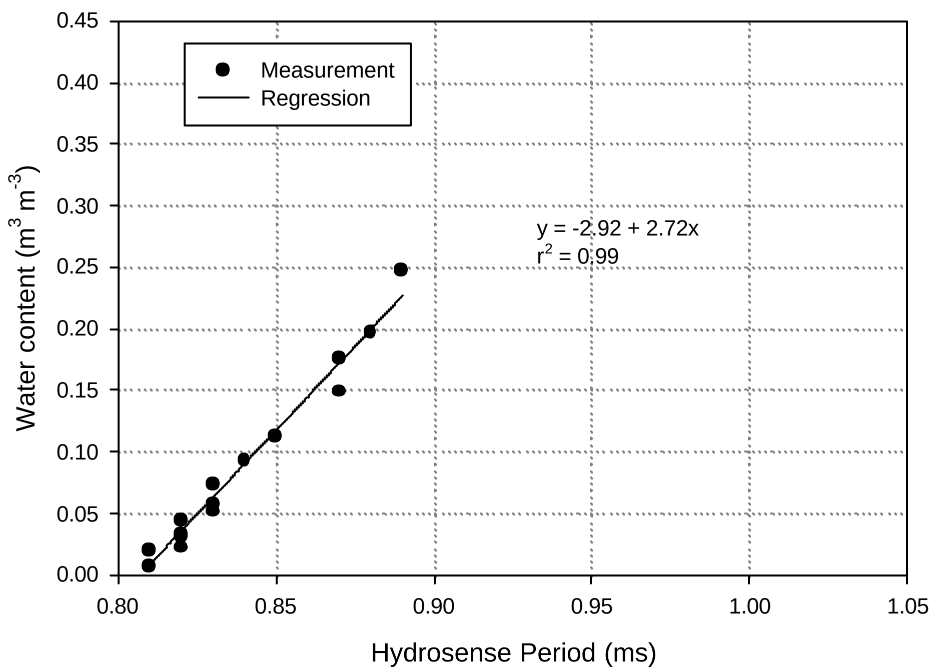

Figure 12. Hydrosense laboratory calibration for surface measurements at PLC074 (top) and PLC185 (bottom).

depths were monitored using gravimetric sampling (0-8 cm) or TDR. Surface TDR measurements are less destructive and quicker than gravimetric samples prompting the change in methods in 2003. Surface (0-12 cm) measurements were collected using a Hydrosense™ TDR system using site-specific calibrations prepared in the laboratory by gradual drying of soil with embedded TDR probes (Steinwand and Olsen, 2003). Linear or quadratic models were fit to data consisting of paired measurements of TDR period and volumetric soil water content (Figures 11 and 12). In the field, the instrument was most reliable at sites with dry sandy soils (PLC074, PLC185) and least reliable at BLK100 when the soil was moist probably due to soil salinity interference with the built in algorithm to interpret the TDR signal. Gravimetric samples were collected when the TDR failed. Soil water was measured biweekly during the growing season and approximately monthly in winter.

Soil water stored in the entire monitoring depth (cm H_2O/soil depth) was calculated according to,

$$Storage_{tube} = \sum q_i \Delta z_i \tag{6}$$

where 2_i is volumetric water content at depth i and $)z_i$ is the thickness of the soil interval represented by 2_i. Existing on-site test wells were monitored at FSL138, PLC074, BLK009, and BLK100 (beginning in February, 2001). Depth to water (DTW) in nearby test wells was monitored at PLC045, and BLK100 (before February, 2001). Sites PLC018 and PLC185 were not located near test wells. Water level loggers were installed in test wells at BLK100 and PLC074 in June and July, 2003 respectively, to replace manual measurements. Precipitation was measured after each event by Inyo County or daily by the National Oceanic and Atmospheric Administration (NOAA) (Table 1). Rain gauges assigned to the sites were: Inyo County RG-6:

BLK100, BLK009; Bishop Airport NOAA: PLC045, PLC018; Inyo County RG-3: PLC074, PLC185; Inyo County RG-1: FSL138.

Vegetation measurements

Four 50 m vegetation transects aligned approximately north, south, east, and west of the EC station exclosures were established at each site. Point frame measurements with 50 cm pin spacing were conducted approximately monthly during the growing season (approximately March through October), and first contacts and all contacts with green live, green leaves or stems were recorded by species to determine plant cover and leaf area index (LAI) (Goodall, 1952). Plant cover was calculated as the fraction of pins that contacted at least one green leaf or stem. Contact frequency (total contacts) total pins) was used to calculate LAI according to,

$$LAI = \frac{N}{K} \tag{7}$$

where N is contact frequency for a species and K is an extinction coefficient determined empirically for common Owens Valley species (Groeneveld, 1997). Extinction coefficients for species not examined by Groeneveld (1997) were assigned a value of 0.5 which was approximately the average value for common species.

Transpiration models

Two methods based on vegetation measurements were used to estimate transpiration to compare with the EC measurements. One method followed the procedures and models in the Green Book, section III. The second method utilized transpiration coefficients presented in Steinwand et al. (2001) and Steinwand (1999b). Both models were developed from porometric methods and assume soil water conditions are not limiting. Growing seasonal totals were daily values summed for the period March 25 to October 15.

Table 4. Date for maximum measured LAI for the dominant species and dates of maximum LAI in the Green Book and Kc models (LAI_j in the GB model is July 5 (DOY 186) for all species). LAI sampling dates used to for T_{Kc} and T_{GB} calculation are listed in the last column.

Year	Site	Dominant species^	Date of maximum LAI measured in this study	Kc LAI model maximum DOY	LAI Sampling dates for T_{GB} and T_{Kc} calculation
2000	BLK 100	SPAI, DISP2	July 7, Sept. 7	July 20, July 8	June 7 & July 7
2001	BLK 100	SPAI, DISP2	Sept. 9, Aug. 8	July 20, July 8	June 12 & July 9
	BLK 9	CHNA2, SPAI	May 15, June 14	July 3, July 20	June 14 & July 11
	PLC 45	ATTO	June 11	June 12	June 11 & July 9
2002	BLK 100	SPAI, DISP2	Aug. 5, June 3	July 20, July 8	June 3 & July 10
	FSL 138	DISP2, LETR5, JUBA	July 9 (DISP2)	July 8	June 3 & July 9
	PLC 18	CHNA2	June 3	July 3	June 3 & July 9
	PLC 74	SAVE4, ATTO, DISP2	June 5, June 5, July 5	June 23, June 12, July 8	June 5 & July 5
	PLC 185	SAVE4	May 8	June 23	June 5 & July 5
2003	BLK 100	SPAI, DISP2	Sept. 9	July 20, July 8	June 3 & July 14
	PLC 74	SAVE4, ATTO, DISP2	June 9	June 23, June 12, July 8	June 9 & July 15
	PLC 185	SAVE4	May 9	June 23	June 10 & July 14

^: grasses; SPAI, *Sporobolus airoides;* DISP2, *Distichlis spicata;* LETR5, *Leymus triticoides.* shrubs; JUBA, *Juncus balticus:* CHNA2, *Chysothamnus nauseosus;* ATTO *Atriplex lentiformis* ssp. *torreyi;* SAVE4, *Sarcobatus vermiculatus.*

The model contained in the Green Book to predict T is,

$$T_{GB} = \sum_{j=1}^{n} \sum_{i=1}^{m} (LAI_j \, e^{-\frac{(i-186)^2}{3000}})(b_{0j} + b_{1j} i + b_{2j} i^2) \tag{8}$$

where i is day of year, LAI_j is the LAI on July 5 for species j, n is number of species, $\$_0$, $\$_1$, and $\$_2$ are coefficients of a polynomial model fit to porometric measurements of transpiration per leaf area for each species (Green Book, Table III.D.1.c). Constants in the exponential model were based on the assumed progression of LAI during the year.

Transpiration coefficients are a dimensionless ratio of actual ET (in this case T) to a reference or potential ET typically determined over an irrigated grass or alfalfa reference crop. The general form of transpiration coefficients is,

$$Kc = \frac{actual\ ET}{reference\ ET} \quad (9)$$

Once the Kc for a plant species (usually a crop) is known, actual ET for another site or time can be derived from measurements of reference ET by rearranging Equation 9. The ratio in Equation 9 is a general concept, and transpiration coefficients take several forms including modifications for growing season weather, time-varying leaf area/canopy closure, or irrigation (Allen et al., 1998). The particular form of the Kc can be tailored to specific situations as long as its application is consistent with the definition and assumptions used to develop the coefficient. Transpiration coefficients from Steinwand (1999b) and Steinwand et al. (2001), measured LAI , and mean daily reference ET were used to calculate T_{Kc} as,

$$T_{Kc} = \sum_{j=1}^{n} \sum_{i=1}^{m} (Kc_{ij}\ \overline{ETr}_i\ LAI_j) \quad (10)$$

where i is DOY, ETr_i is mean daily reference ET, n is number of species, Kc_{ij} is the transpiration coefficient for species j, LAI_j is the midsummer LAI for species j. The Kc models were developed from a large database of porometric measurements of stomatal conductance, reference ET, and LAI for the five most common Owens Valley species.

Models of seasonal trends in LAI were included in T_{Kc} and T_{GB} to allow use of a single LAI measurement at the peak of the growing season to provide site-specific estimates of transpiration. Changes in LAI during the growing season were incorporated directly into T_{GB} by assuming the seasonal trend follows the Gaussian model in Equation 8. In contrast, seasonal LAI trends were incorporated during the construction of Kc_{ij} in Equation 10 by relying on

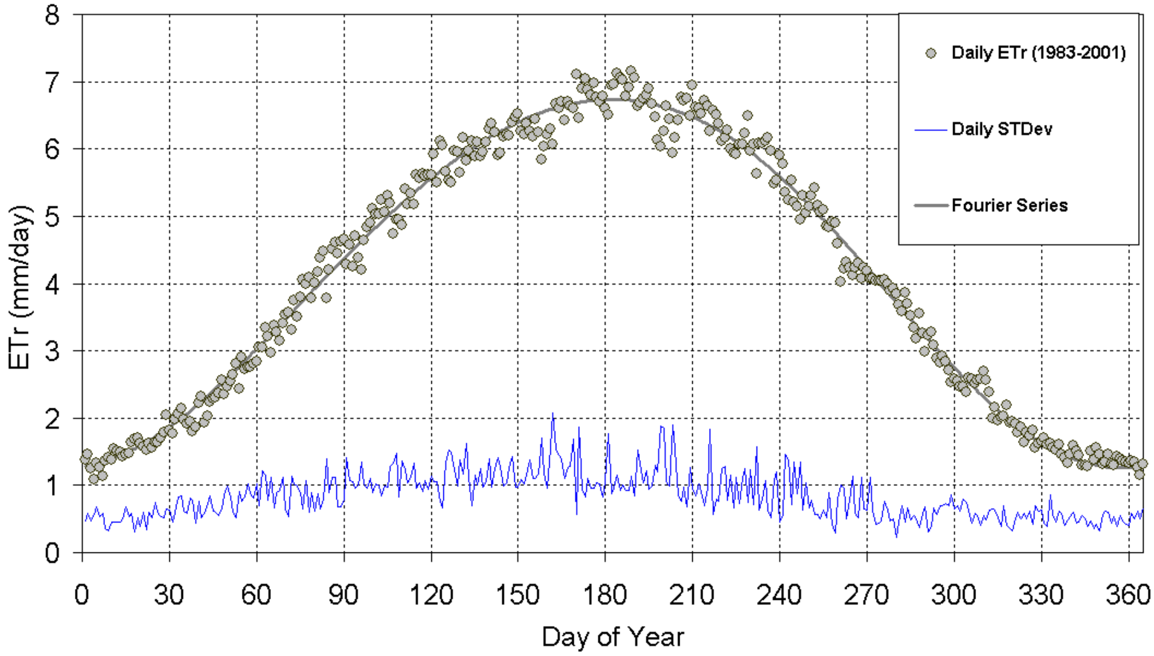

Figure 13. Mean daily ETr and its standard deviation (STD) estimated by the modified Penman equation from climatic data collected at Bishop, California (CIMIS, 2003, station #35).

models of daily LAI fit to existing data and normalized to a maximum LAI of 1.0. The Green Book model fixes the peak LAI at day of year DOY 186 (July 5). The peak LAI in the Kc models varies by species but is in June or July (Table 4). LAI measurements in this study typically were collected in early June and early July bracketing the maximum LAI in T_{Kc} and T_{GB} models. Calculations using both June and July field data were prepared in this study, but the comparison of transpiration totals relied on the LAI data collected nearest the date of maximum LAI in the models (Table 4). LAI of minor species for which no Kc or Green Book polynomial models were available was apportioned among the known species based on their relative proportion of total LAI.

T_{Kc} can be used to estimate transpiration for a preceding period by utilizing actual ETr_i measurements (look back mode), but to predict transpiration as required by current procedures to manage pumping requires a model of daily *ETr* (prediction mode) to apply Equation 10. As part of a related study conducted by Inyo County, a stochastic model for generating mean ETr_i sequences for the Owens Valley was estimated from a 19 year (1983-2001) sequence of observations collected at Bishop (CIMIS 2003). The procedure was identical to that of a previous cooperative study (Or and Groeneveld, 1994) except a longer data record was used. CIMIS uses a modified Penman equation to compute ETr_i, from which mean ETr_i and a corresponding standard deviation were obtained. A clear seasonal trend existed in the ETr_i time series which was removed prior to fitting a stochastic model (Figure 13). A Fourier series was fitted to ETr_i using procedures described by Salas et al., (1980). The first two harmonics of the Fourier series are,

$$\overline{ETr}_i = < ETr > + \sum_{j=1}^{2} \left[A(j)\mathrm{COS}\left(\frac{2pij}{365}\right) + B(j)\mathrm{SIN}\left(\frac{2pij}{365}\right) \right] \tag{11}$$

where i is the day of year, $<ETr>$ is mean daily ETr for the entire year (4.12 mm/day), A(1)=-2.73; A(2)=-0.112; B(1)=0.187; and B(2)=0.097. We used the first harmonic only because it was capable of explaining more than 98% of the variation in average ETr_i indicating a strong seasonal (periodical) trend as evident from the data.

An approach based on classical time-series analysis was adopted for fitting a stochastic model to the residuals of mean ETr_i series, i.e., after removing the deterministic trend. Several possible ARMA(p,q) stochastic models were tested based on criteria of best fit and parsimony. Estimated parameters by the maximum likelihood method, statistics, and tests of the residuals are given in Table 5. An ARMA(1,1) model was selected as the best model for the ETr_i data based

Table 5**.** Estimated model parameters for standardized mean daily ETr series for 1983-2001 in Bishop, California. Data are from CIMIS Station #35).

ARMA(p,q) Model Order				
Parameters		AR(1)	AR(2)	ARMA(1,1)
$?_1$		0.438	0.421	0.506
$?_2$			0.031	
$?_1$				0.085
Goodness-of-Fit and Parsimony Tests				
Residuals variance s^2_e		0.050	0.055	0.050
Porte Manteau Test - $Q_{L=90}$		98.8	97.0	97.2
AIC		-1088	-1086	-1087

on goodness-of-fit test results (Table 5), and capability to be reduced into a predictive model for *ETr*. The ARMA(1,1) model is given by:

$$ETr_i = f_1\, ETr_{i-1} - q_1 e_{i-1} + e_i \tag{12}$$

where f_1 is an autoregression parameter, 2_1 is a moving average parameter, and g_i is a normally distributed zero mean term with variance equal to s^2_e. The adequacy of the ARMA(1,1) was also confirmed by its best-fit to the autocorrelation of ETr residuals.

We adopted a method proposed by Graupe and Krause (1973) for improving the ETr_i model by transforming the ARMA(1,1) of ETr_i estimates which are based on measurements that contain error into a first order autoregressive model, AR(1), of the unobservable "true" state:

$$\tilde{E}Tr_{i+1} = j_1\, \tilde{E}Tr_i + u_i \tag{13}$$

where $ETr_i = ETr_i + v_i$, and $s^2_u = s^2_e[1+2^2_1-2_1/f_1-2_1 f_1]$ (s^2_u=0.06) An estimate of the measurement variance is given by: $s^2_v = s^2_e[2_1/f_1]$ (with s^2_v=0.0084).

Results and Discussion

Site characteristics

Depth to water measured at the EC sites is presented in Figures 14 to 18. Typically, the shallowest DTW occurred in the spring (March or April) and declined to a maximum depth at end of the growing season (October). FSL138 was an exception where maximum depth to water in 746T occurred in late July. Water tables at all sites increased during the winter when the vegetation was senescent. Test well 850T was installed in at BLK100 in 2001, but based on the comparison with nearby test well 454T, DTW fluctuations were similar in all four years EC measurements were collected. The general declining trend superimposed on the annual cycle at BLK100 (Figure 14) was due to persistent below normal runoff conditions during this study. Additionally, on August 11, 2003 two LADWP production wells sealed below a confining layer and located 2015 meters from 850T were activated as part of a test to determine impacts of pumping the deep confined aquifer on the shallow water table in the region. Because the pumping effects must propagate through the confining layer, the drawdown at the EC site was gradual and relatively small; approximately 15 cm by May, 2004. The water level at PLC074 declined during the growing season, but small fluctuations observed in July through September probably corresponded with irrigation releases on pastures located west of the site. There was no apparent affect on measured ET during periods of irrigation suggesting the fetch was acceptable. No piezometer was located near PLC018 and PLC185. Soil water content at

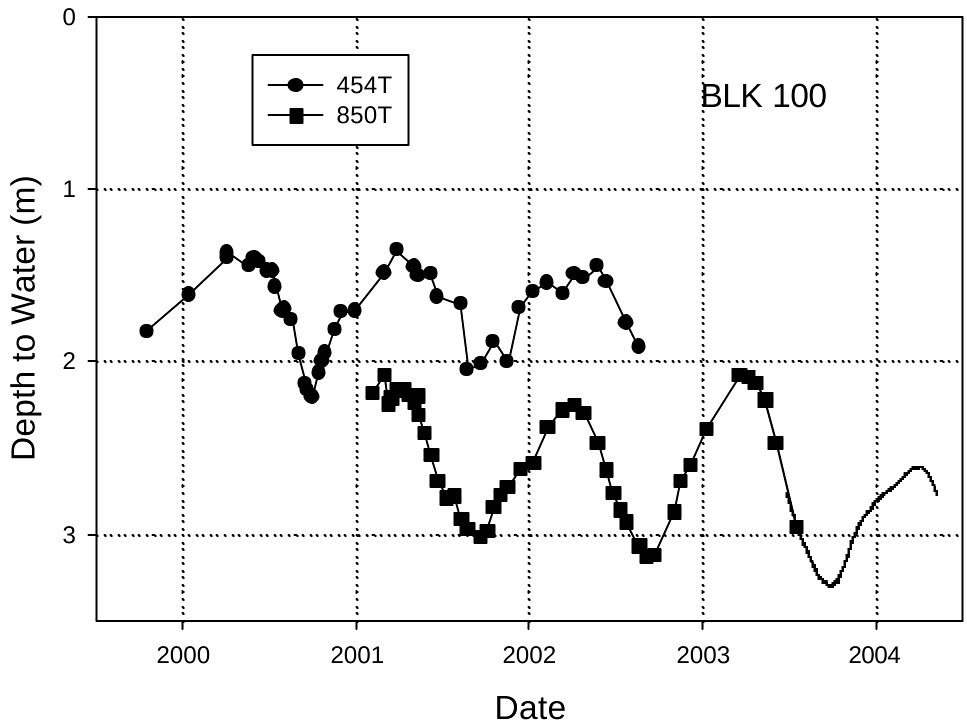

Figure 14. Depth to water in two test wells located near BLK100. Test well 850T is adjacent to the EC station; 454T is located southeast of the site, adjacent to the LA Aqueduct.

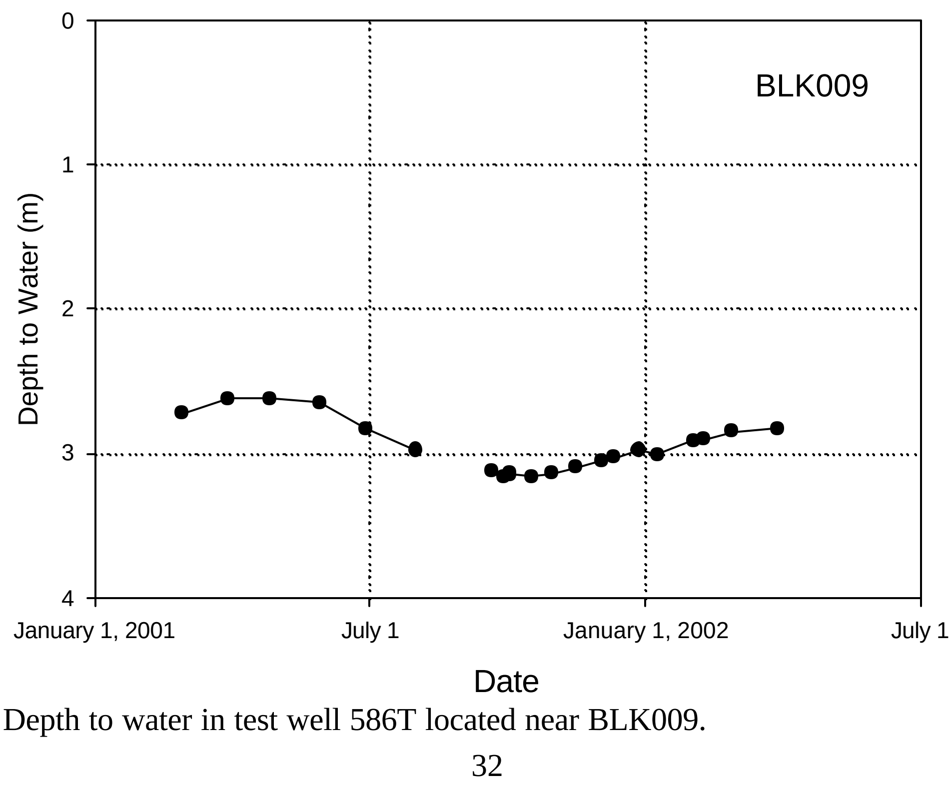

Figure 15. Depth to water in test well 586T located near BLK009.

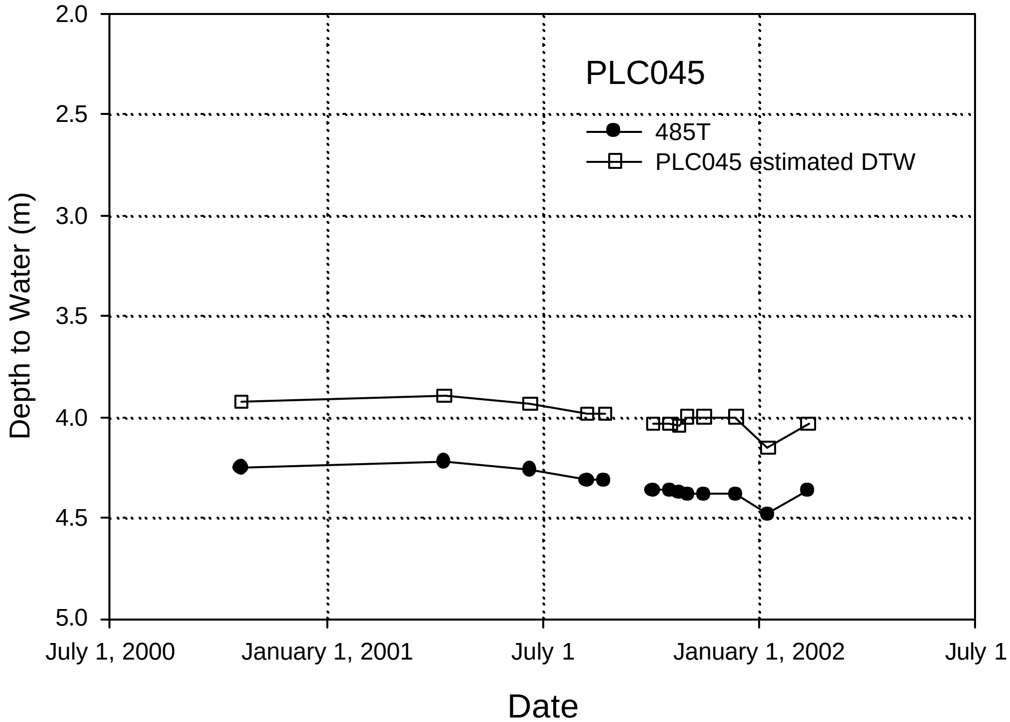

Figure 16. Depth to water in test well 485T located south of PLC045 and estimated DTW at PLC 045 by assuming the fluctuations at the two locations were similar.

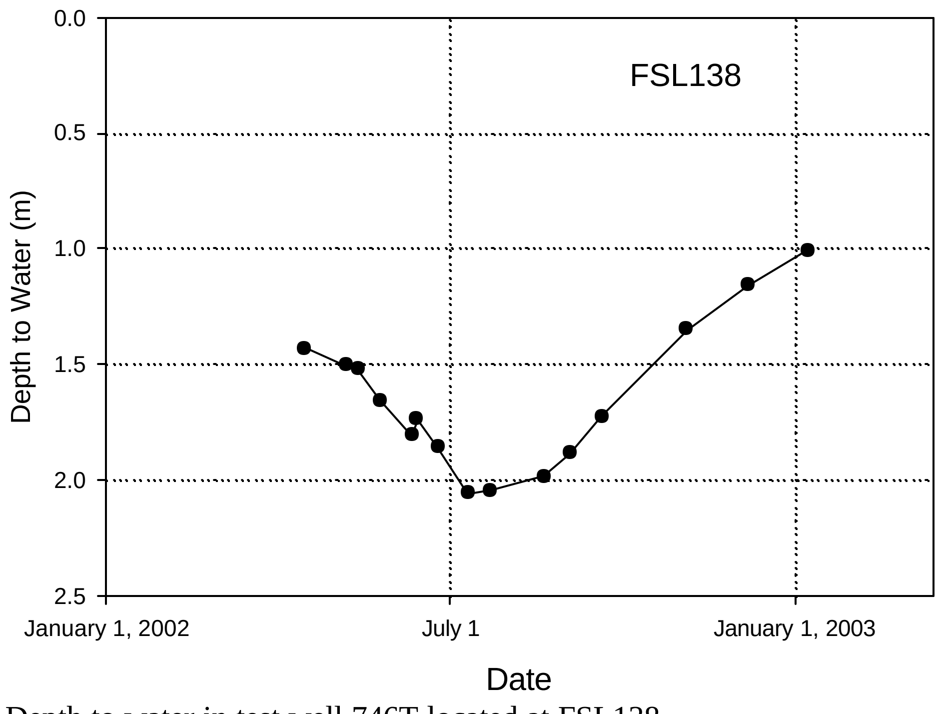

Figure 17. Depth to water in test well 746T located at FSL138.

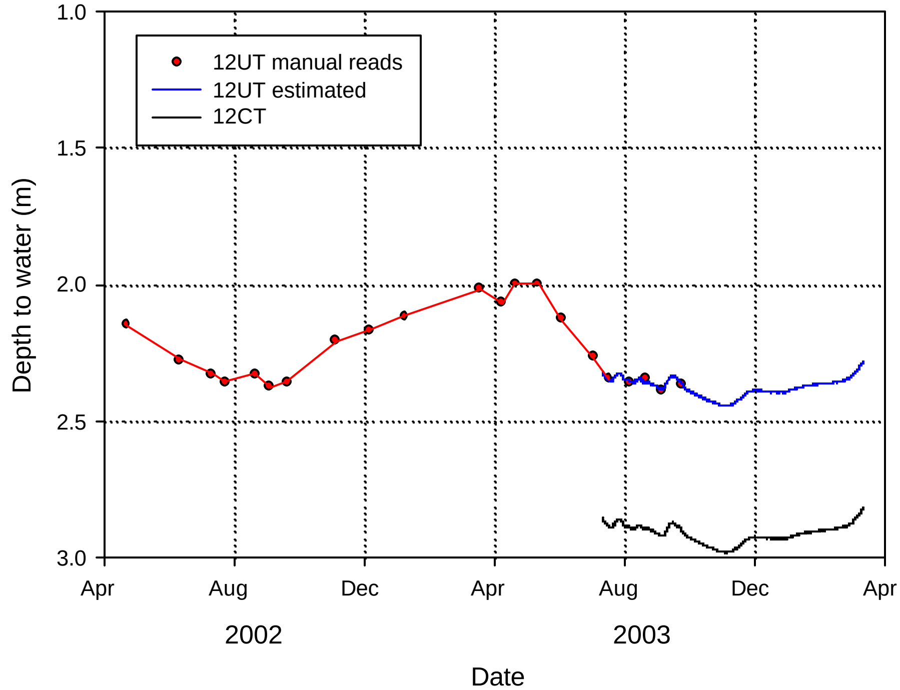

Figure 18. Depth to water from land surface in test well 12UT located at PLC074 and adjacent well 12CT measured from reference point with water level logger.

PLC018 at depth did not change and was approximately at the limiting water content for sandy soil (2-3% *2)* showing that depth to water was deeper than 5 m. The water table was 4 m (mean of three observations) at PLC185 during access tube installation in the May 2002. This was probably a month after and the water table was probably slightly lower than the annual high stand based on inspection of hydrographs of test wells in the area. Water levels regionally and soil water monitoring suggest conditions at PLC185 were similar in 2002 and 2003. Piezometers in the area (T842, T480, T479, and V002G) all had equal or slightly shallower (0.06m) DTW in April 2003 than in 2002, and soil water measurements did not indicate the water table rose above 4m. Depth to water at PLC045 was estimated from the initial water table depth (3.9 m)

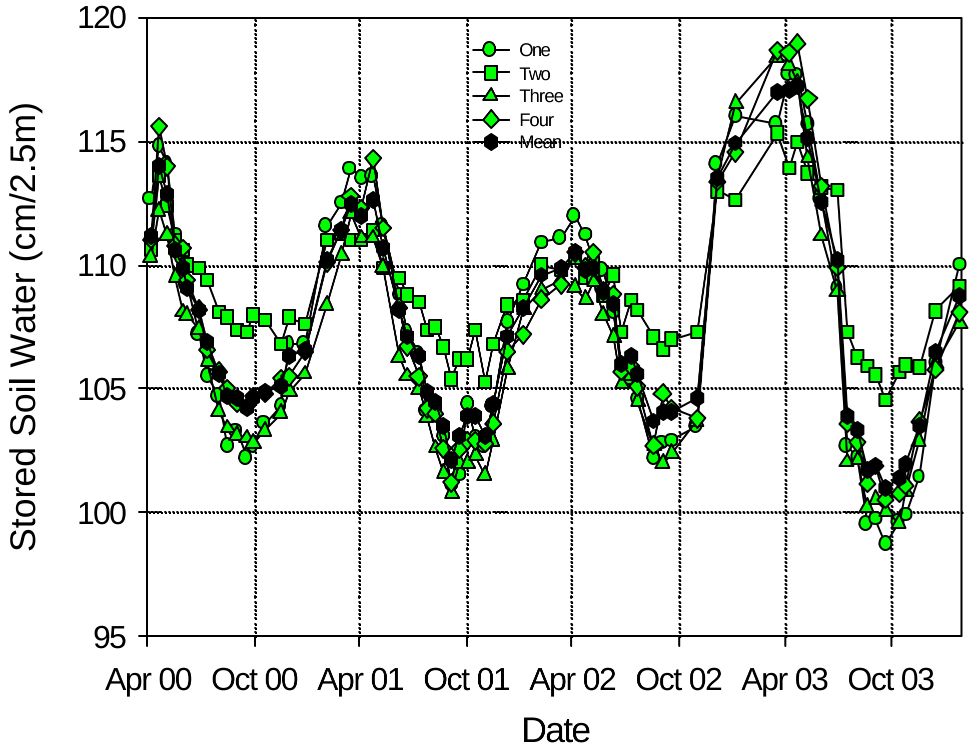

Figure 19. Stored soil water at BLK100.

observed during access tube installation and fluctuations observed at a test well 485T in similar vegetation 0.5 km southeast of the site.

Precipitation preceding the growing season each year during 2000-2002 consisted of small events, and total precipitation was below average in all years (Table 1). Only two summer storms in July 2001 were of significant size to affect either ET or LAI measurements, and only at PLC045. Precipitation preceding the 2003 growing season was 3 to 5 times that in previous years (Table 1). Summer precipitation was slightly greater in 2003 than in previous years, but was still a small (<40mm) component of the water balance.

Soil water accumulated during winter from precipitation and groundwater recharge was progressively depleted through the summer at all sites reflecting ET and water table decline (Figures 19 to 25). Seasonal fluctuations were greater at sites clearly coupled to the

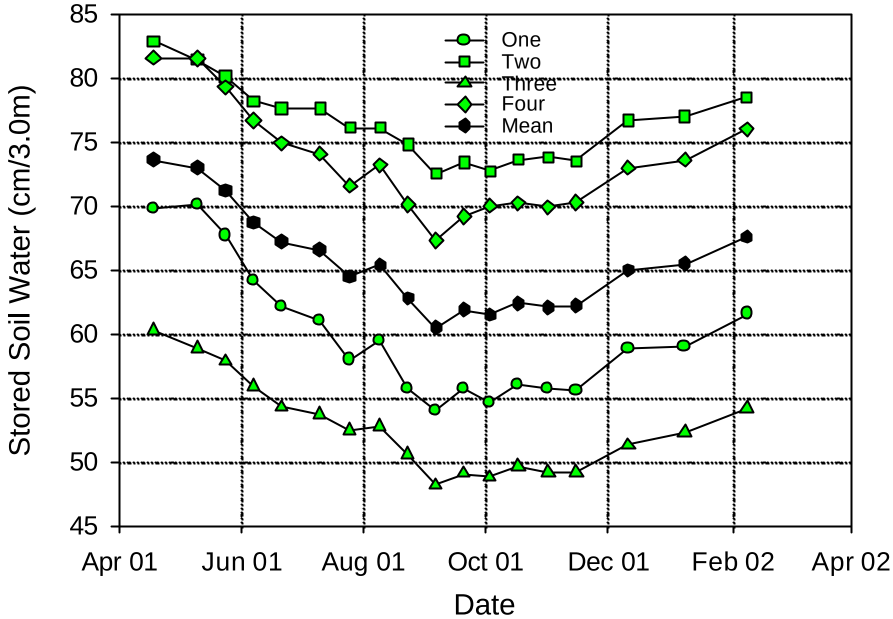

Figure 20. Stored soil water at BLK009.

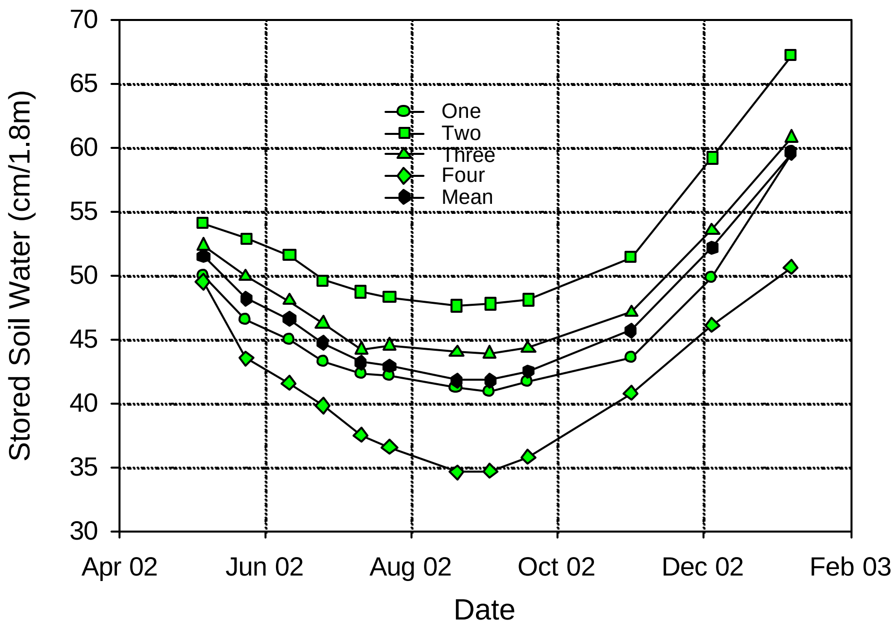

Figure 21. Stored soil water at FSL138.

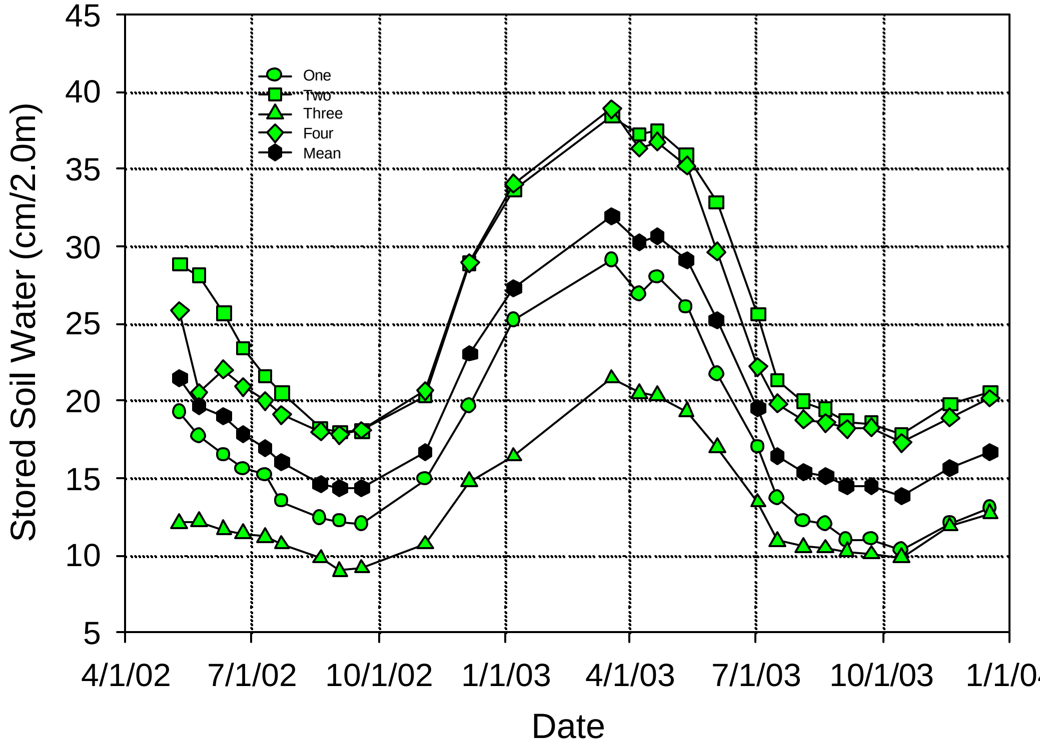

Figure 22. Stored soil water at PLC074.

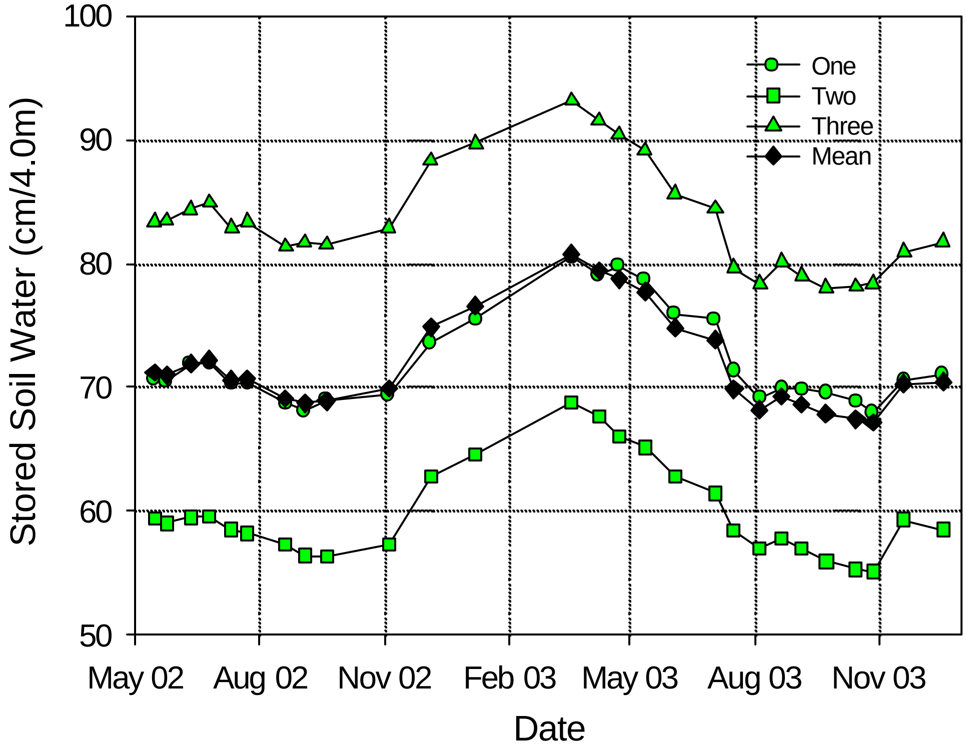

Figure 23. Stored soil water at PLC185.

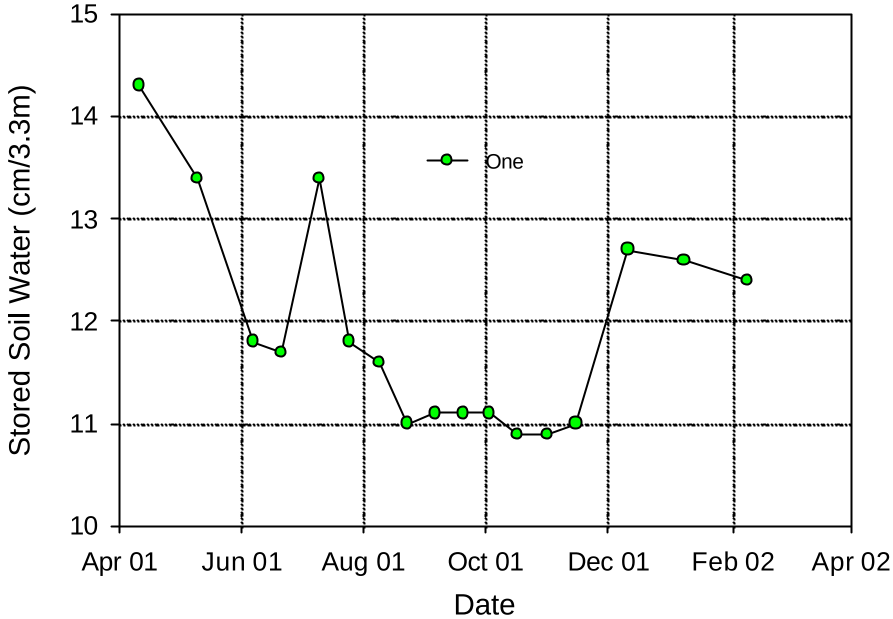

Figure 24. Stored soil water at PLC045. Approximately 11 cm represents a profile at limiting water content.

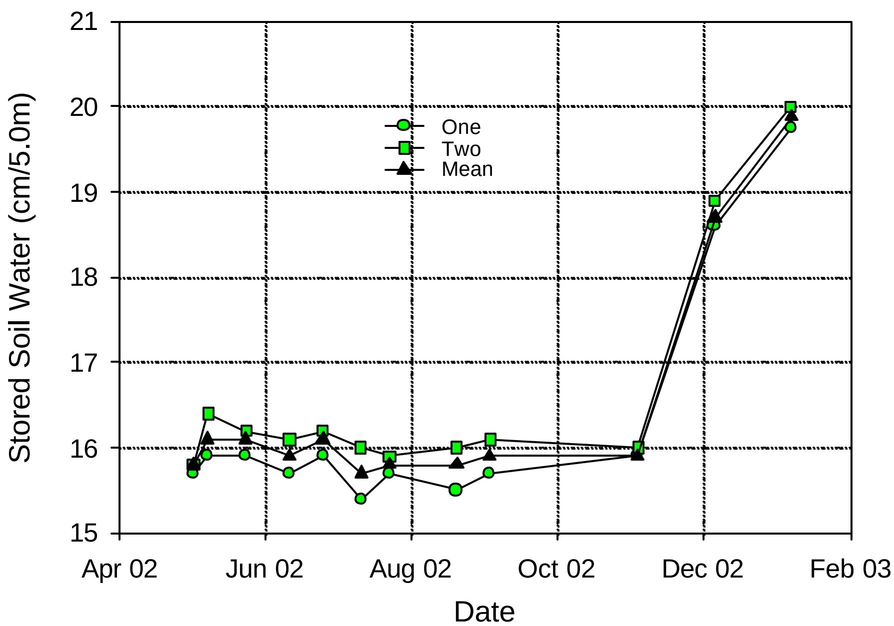

Figure 25. Stored soil water at PLC018.

water table and with higher vegetation cover (BLK100, BLK009, FSL138, PLC074). Soil water declines during summer, 2002, were minimal at PLC045, PLC018 and PLC185 because the small amount of winter precipitation was largely exhausted when monitoring began and because of the weak influence of groundwater within the depth monitored. Coupling of the soil and groundwater is discussed more fully below. Soil water storage changes at access tubes within a site over the growing season were generally parallel suggesting that uptake/drainage was similar and that differences in storage between tubes represented differences in soil properties, vegetation density, or microtopography (i.e. DTW).

Soil water profiles collected at each access tube were examined to assess the coupling of soil water with water table fluctuations. Examples of spring, midsummer, and fall conditions are presented for each access tube in Figures 26-36. Even though estimates of limiting water content were not available, it was evident from the high *2* that ample soil water was available for plant uptake at sites BLK100 (all years), BLK009, PLC185 and FSL138.

Soil water contents at BLK100 fluctuated throughout the profile reflecting the coupling with the water table fluctuations (i.e. capillarity and drainage) and plant uptake (Figures 26-30). Tube 1002 at BLK100 was located in a small 2m^2 bare spot nearly devoid of vegetation, and *2* was relatively constant except for precipitation infiltration in the upper 1.1 m suggesting plant uptake largely controlled soil water decline at depth at vegetated locations. In 2003, water content at depths greater than approximately one meter was comparable to past years, but shallower depths were wetter due to greater winter precipitation. Winter precipitation was exhausted by fall each year as evidenced by similar water contents above 1.1 m.

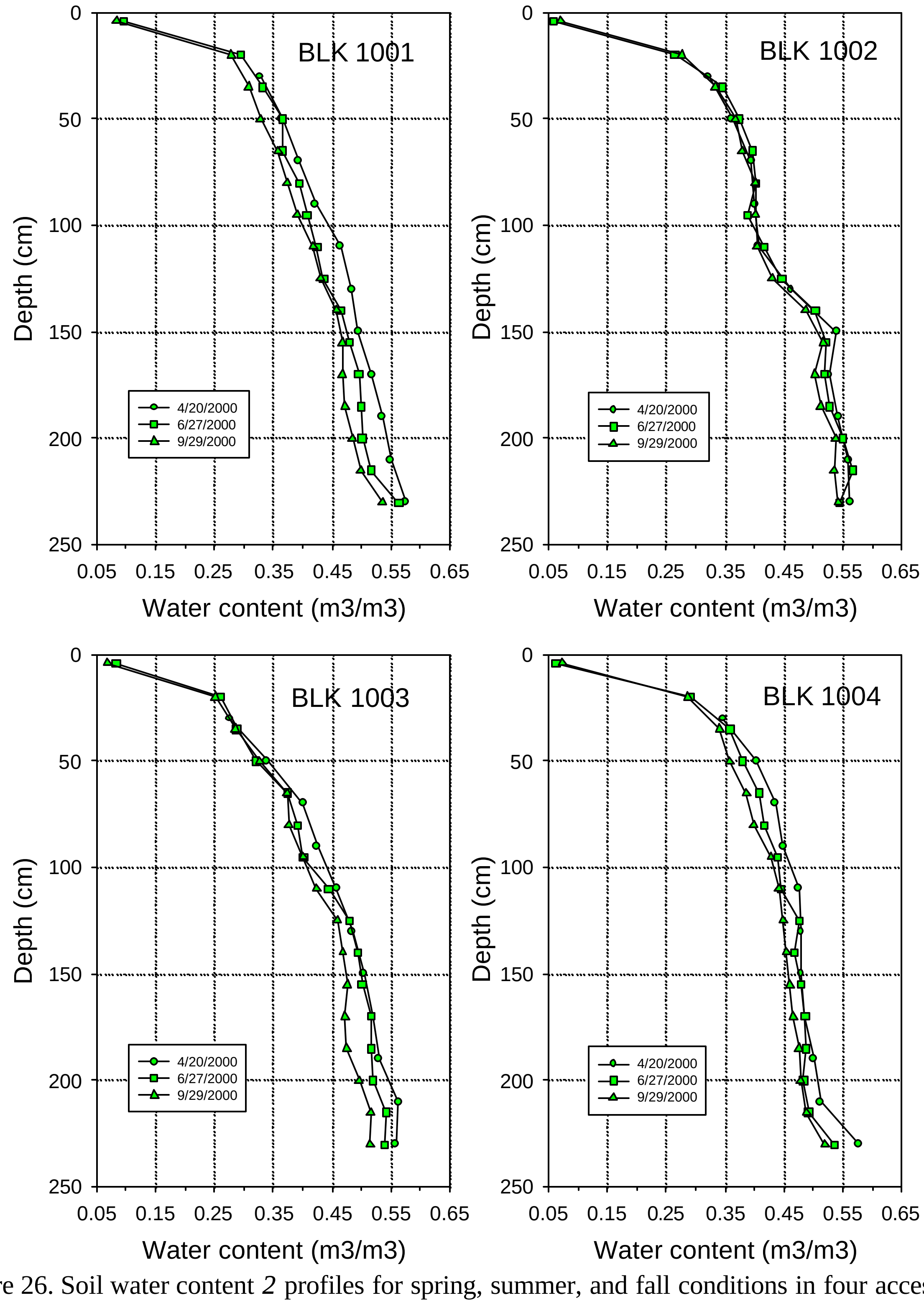

Figure 26. Soil water content *2* profiles for spring, summer, and fall conditions in four access tubes at BLK100 in 2000.

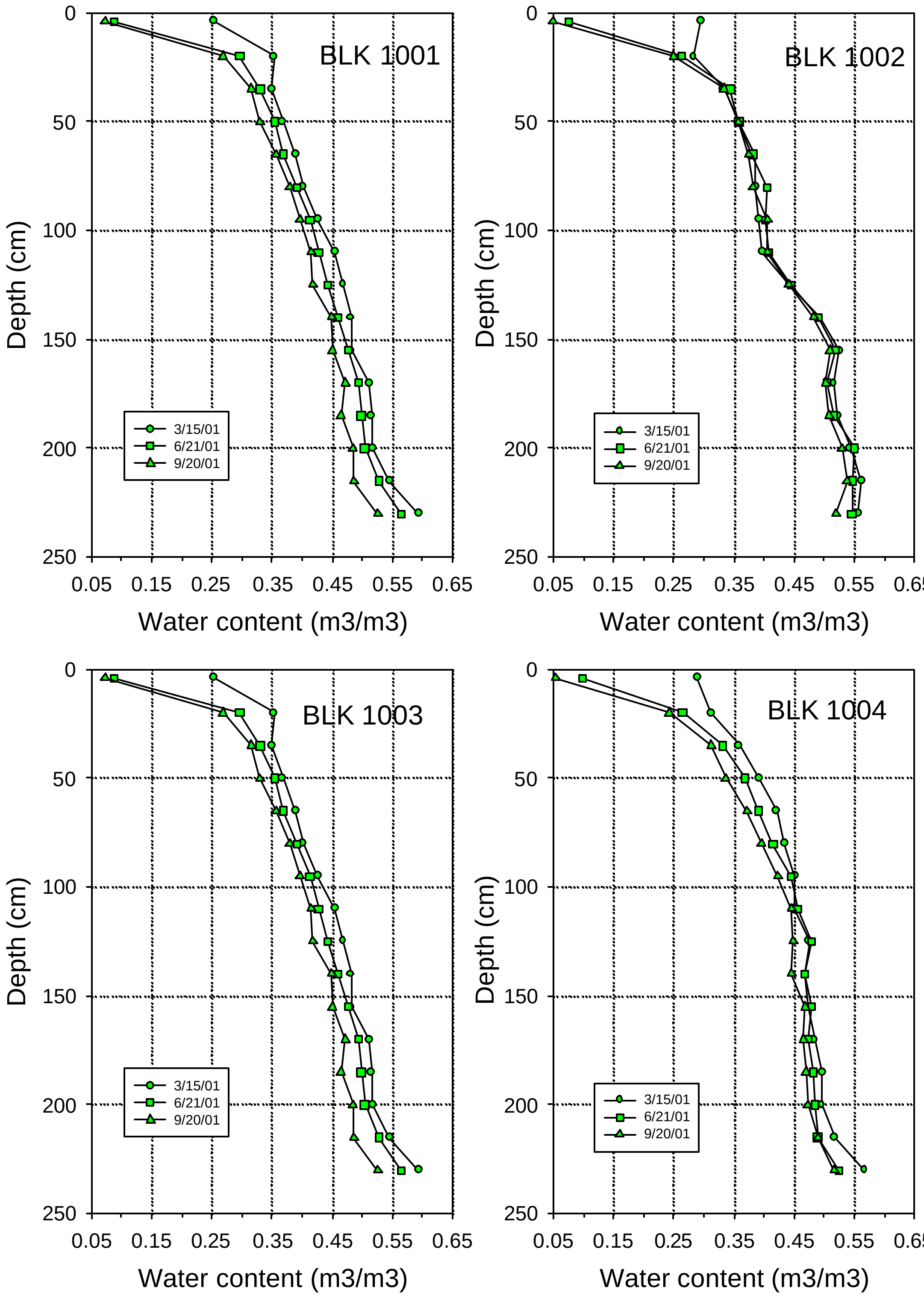

Figure 27. Soil water content *2* profiles for spring, summer, and fall conditions in four access tubes at BLK100 in 2001.

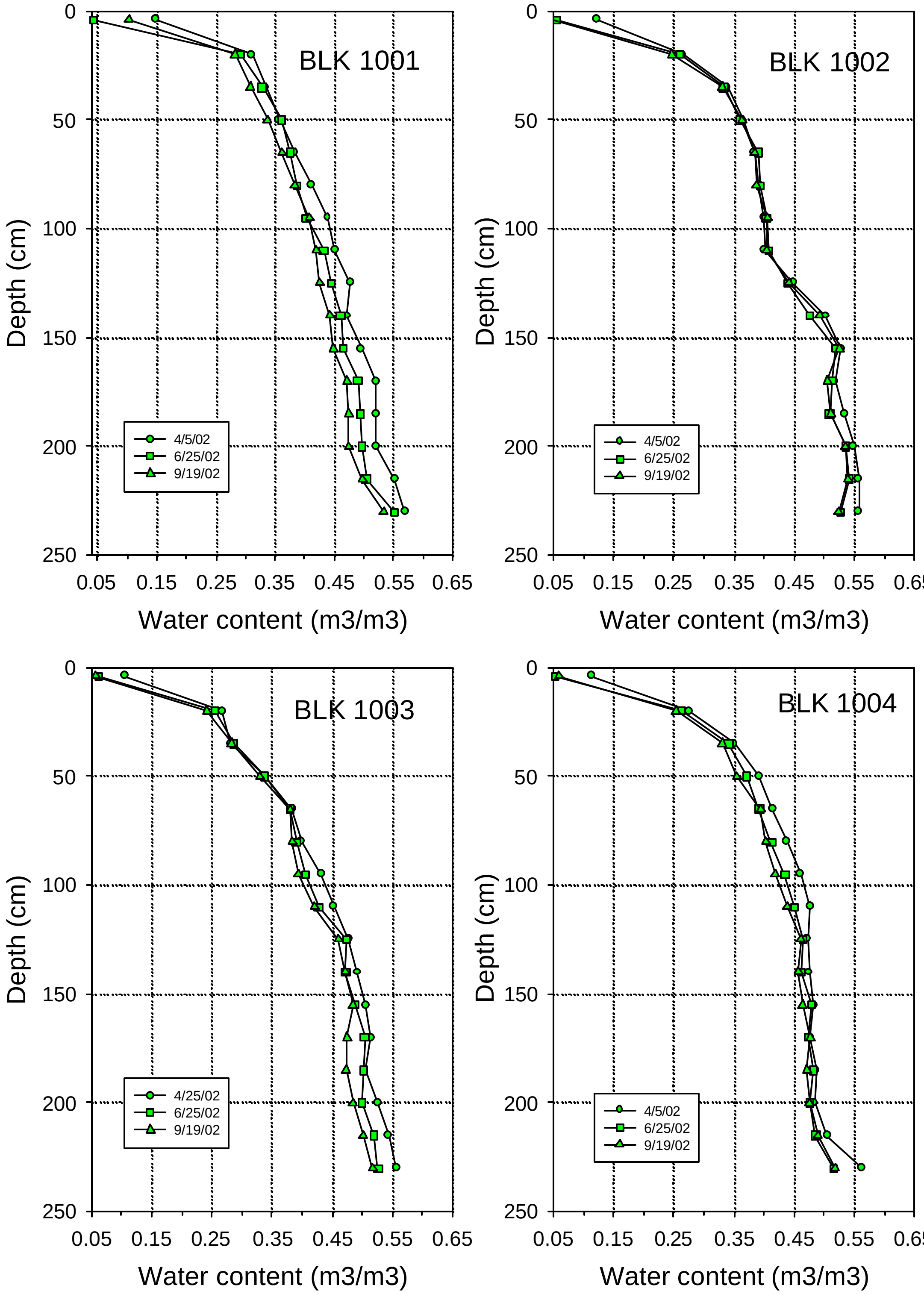

Figure 28. Soil water content *2* profiles for spring, summer, and fall conditions in four access tubes at BLK100 in 2002.

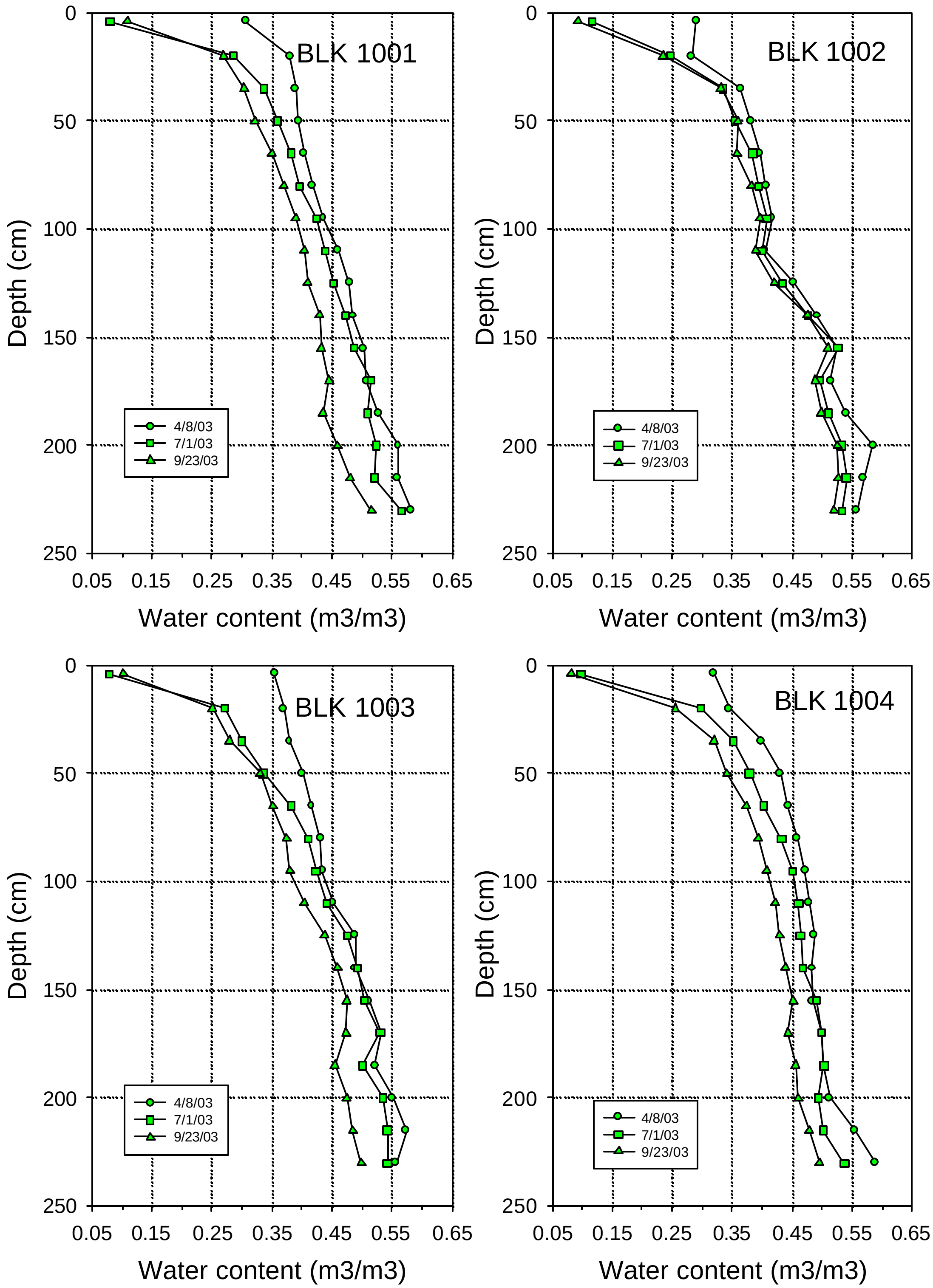

Figure 29. Soil water content 2 profiles for spring, summer, and fall conditions in four access tubes at BLK100 in 2003.

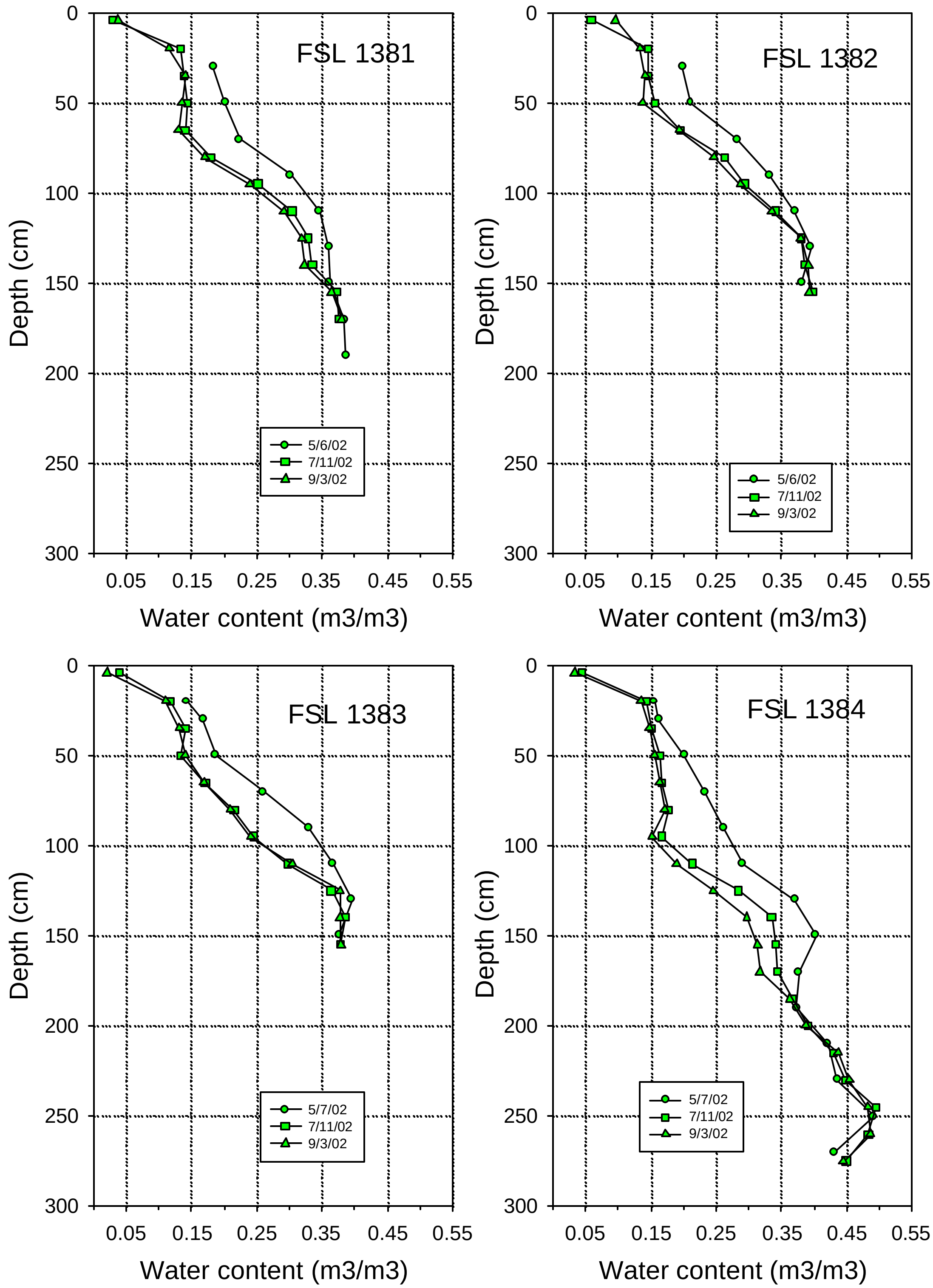

Figure 30. Soil water content *2* profiles for spring, summer, and fall conditions in four access tubes at FSL138 in 2002.

Like BLK100, FSL138 showed uptake throughout the profile above the water table (Figure 30). Except for one location, soil water uptake largely ceased after July 11, corresponding with reduced ET and stable or rising water table.

Vertical variation in soil water fluctuations was more complex at moist shrub dominated sites. The soil at BLK009 can be divided into three zones based on observed soil water fluctuations (Figure 31). Above 0.9 m, the soil was affected by infiltrating rain. Soil water content was relatively static at intermediate depths (0.90 to 1.50-2.00 m). Below the intermediate zone, soil water was coupled to water table fluctuations. Like BLK009, the soil at PLC185 can be divided into three zones (Figures 32 and 33). Soil at PLC185 was dry in the upper 1.0 m except for precipitation inputs. Intermediate depths from 1.0 m to approximately 2.7 to 3.0 m , depending on location, had nearly constant water content corresponding with changes in soil texture. Under the drought conditions of 2002, water in this zone evidently was not available for uptake or uptake at these depths was negligible due to low plant cover (low rooting density). At greater depths, soil water fluctuations were coupled to water table fluctuations, although the coupling was weak for two of the three locations. The primary plant uptake occurred in soil above 1m and below 3.5m with a small amount of plant uptake observed in the intermediate zone only in 2003 (e.g. tube 1853, Figure 33). PLC074 had sandy and sandy loam soils, but the water table was relatively shallow (<3 m) and probably accessible to plant roots. Following the dry winter in 2002, at two locations, 741 and 743, the upper 1 m was relatively dry and decoupled from water table changes (Figure 34). At two other locations, 742 and 744, soil water content in the upper and lower profile was above limiting water content, and it was difficult to distinguish whether the upper 1 m was coupled with the water table or whether

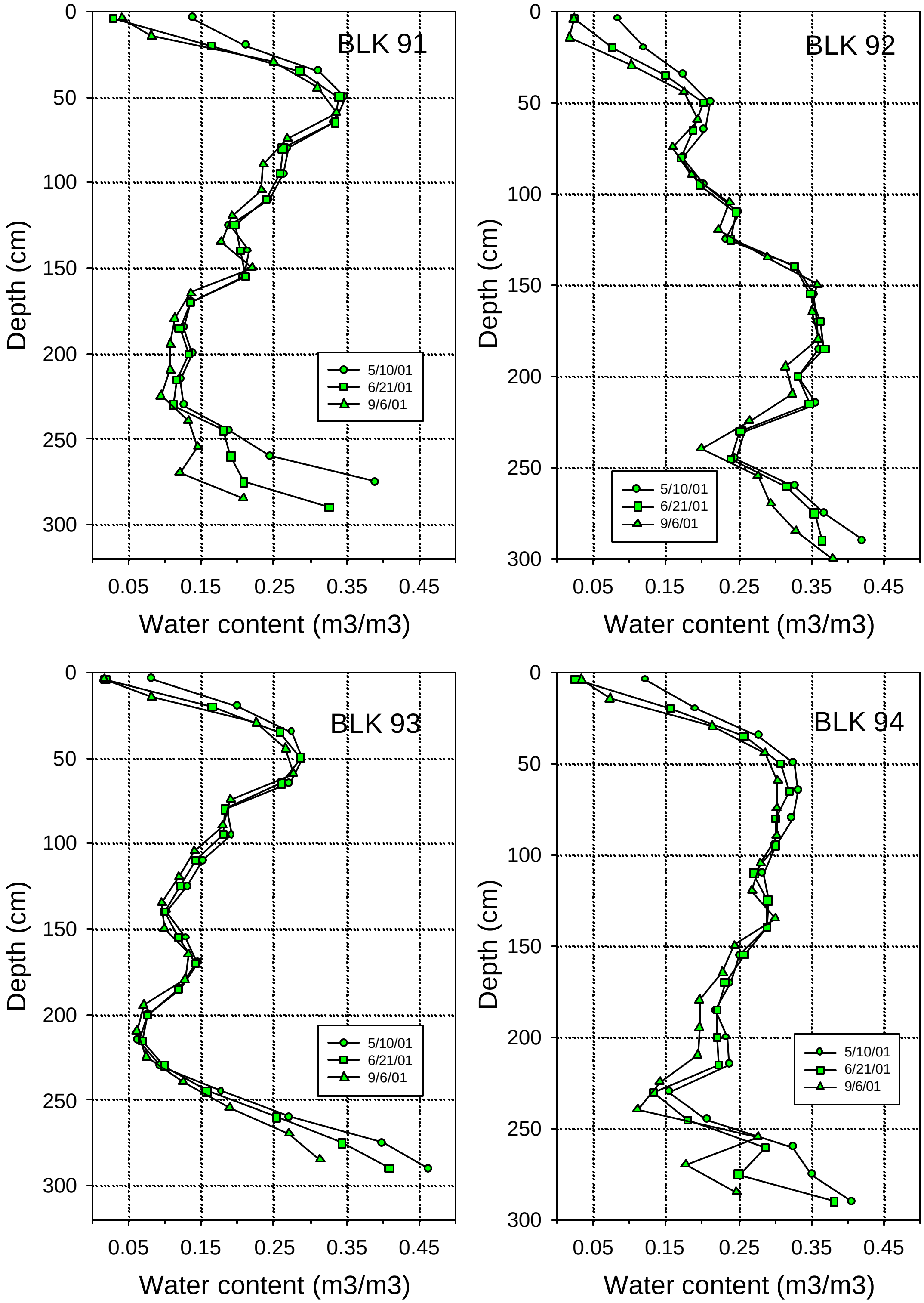

Figure 31. Soil water content *2* profiles for spring, summer, and fall conditions in four access tubes at BLK009 in 2001.

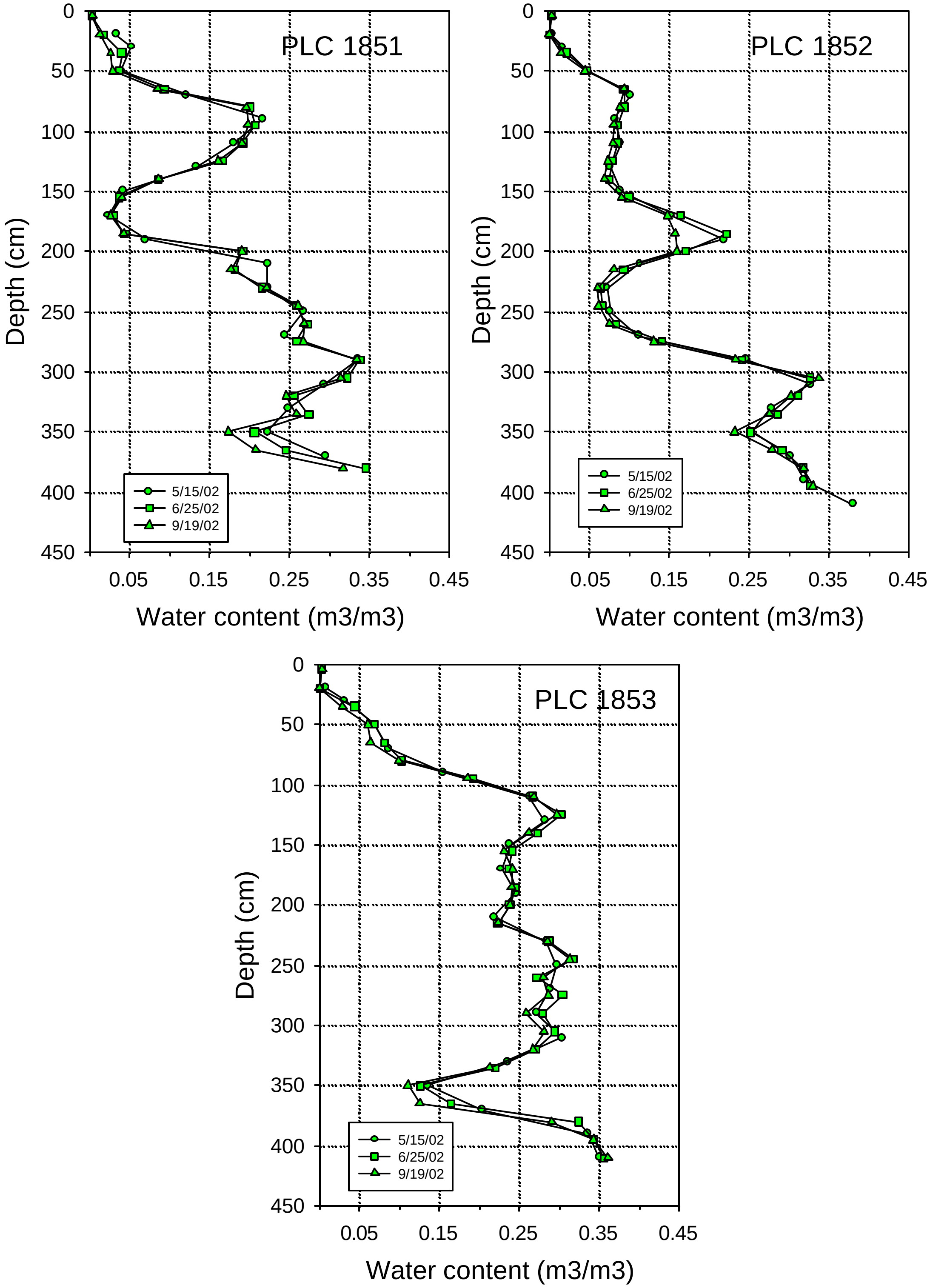

Figure 32. Soil water content *2* profiles for spring, summer, and fall conditions in three access tubes at PLC185 in 2002.

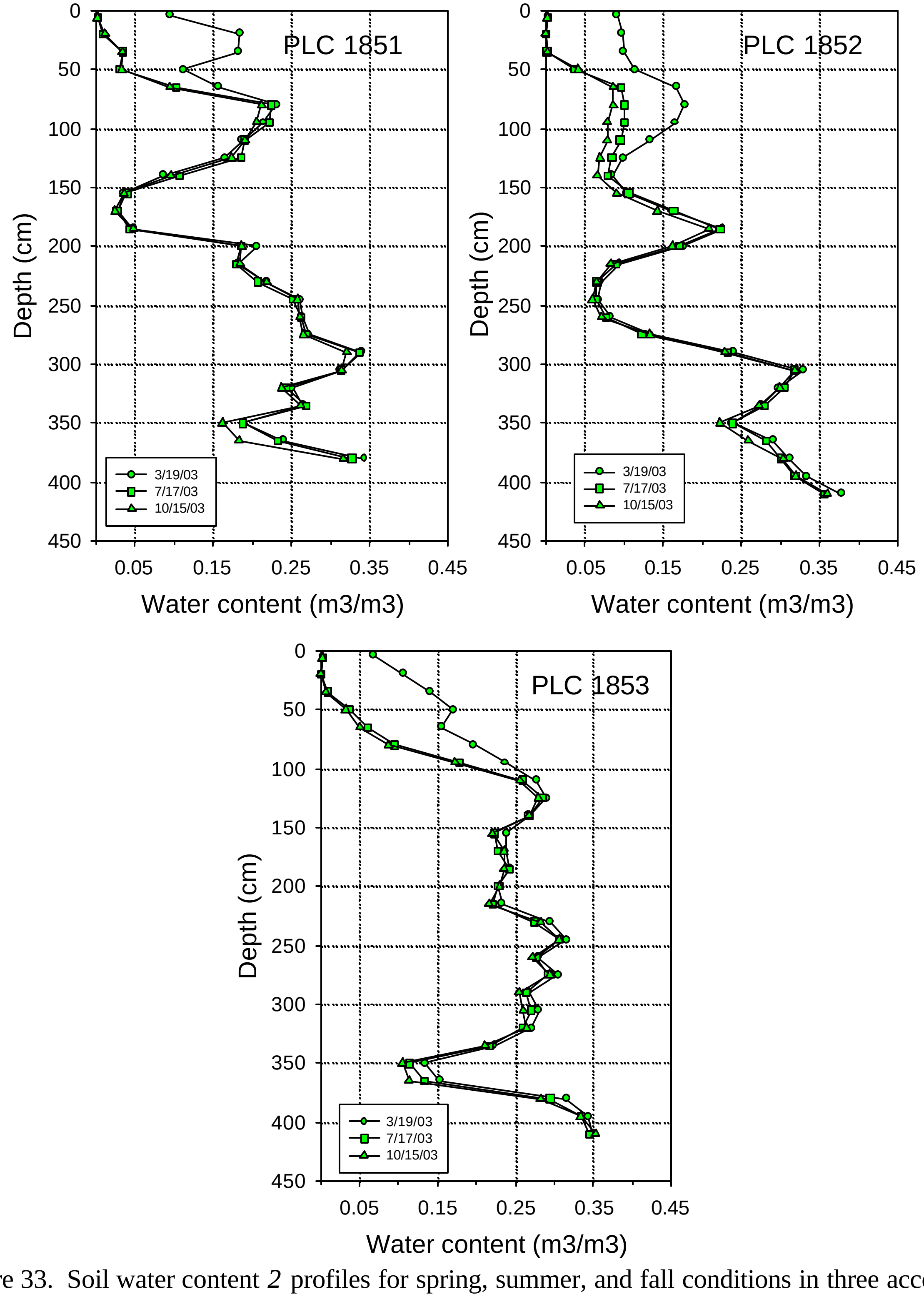

Figure 33. Soil water content *2* profiles for spring, summer, and fall conditions in three access tubes at PLC185 in 2003.

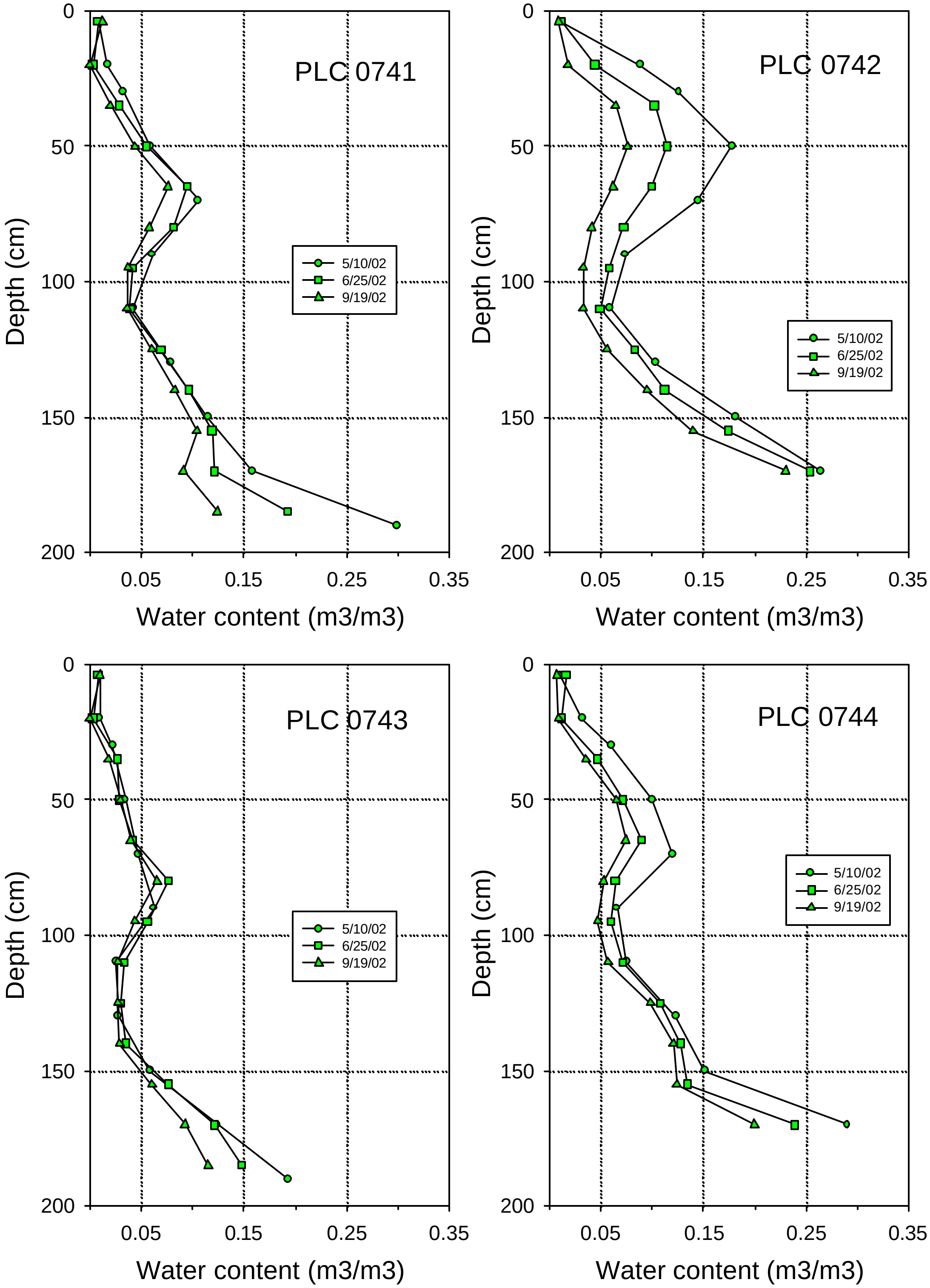

Figure 34. Soil water content *2* profiles for spring, summer, and fall conditions in four access tubes at PLC074 in 2002.

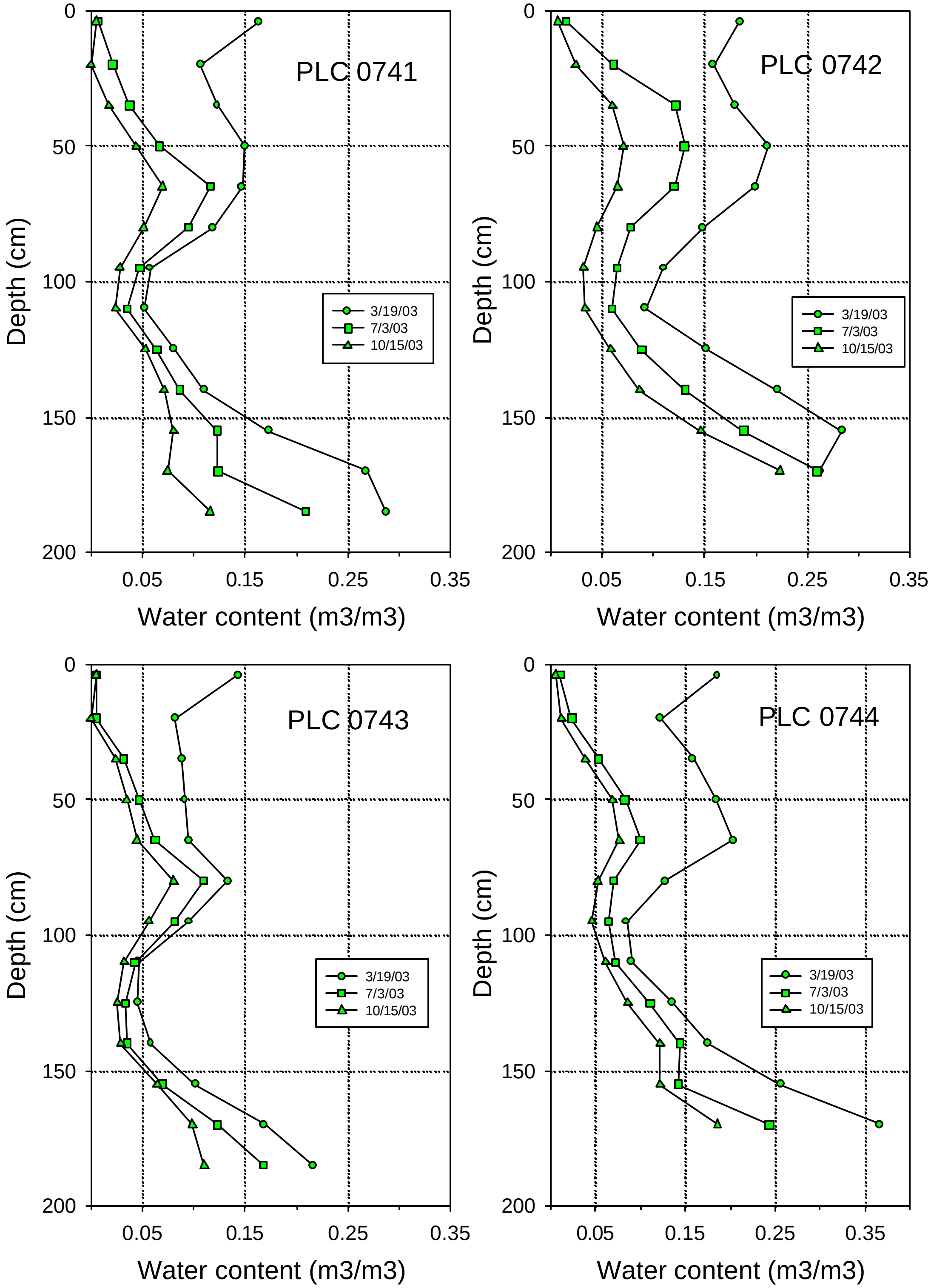

Figure 35. Soil water content *2* profiles for spring, summer, and fall conditions in four access tubes at PLC074 in 2003.

the declines in *2* reflected uptake of precipitation-derived soil water (see below). Given the low precipitation the preceding winter, most of the shallow soil water was probably derived from groundwater. All access tube locations were coupled to water table fluctuations at depths below 1 to 1.5 m. In 2003, the soil at PLC074 was moist throughout the 2.0 m profile due to recharge from the water table and deeper infiltration of winter precipitation (Figure 35). Infiltration reached 1m in all tubes. Depths greater than 1.1m (tubes 742 and 744) to 1.4m (tubes 741 and 743) received recharge during the winter from capillarity above the water table suggesting that the water observed above 1m in 2002 was probably derived from precipitation.

Two sites had predominately dry soils several meters thick above the water table. At PLC045, *2* increased at depths less than 0.5-0.9 m due to winter and summer rains, but below 0.9 m, *2* was less than 0.05 m^3m^{-3} which is approximately the limiting value for sandy loam and sandy soils (McCuen et al., 1981). The extreme limit of capillarity above the water table (3.8 m deep) noted during access tube installation in early spring was at 3.2 m (Figure 36). Soil at PLC018 was dry and sandy similar to PLC045 except the limit of capillarity was below the bottom of the access tubes, 4.7 m (Figure 37). Conditions at these sites probably violate assumptions of sufficient soil water in the Kc and Green Book transpiration models.

LAI generally conformed to the expected seasonal trend with peak LAI occurring in early to mid summer (Figure 38). LAI at meadow sites usually peaked in early July, approximately one month later than shrub-dominated sites which on average exhibited maximum LAI in June. The earlier peak leaf area of shrubs is consistent with LAI models in Steinwand (1998). The seasonal trend at PLC045 began to decline precipitously in mid June but rebounded following

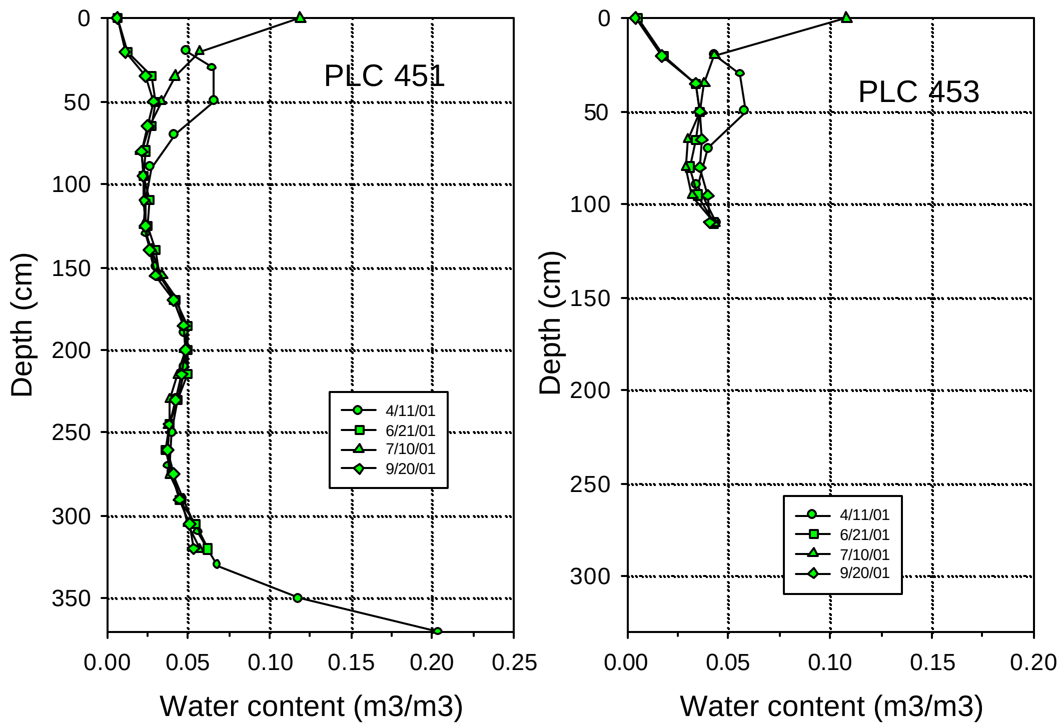

Figure 36. Soil water content *2* profiles for spring, summer, and fall conditions in two access tubes at PLC045 in 2001.

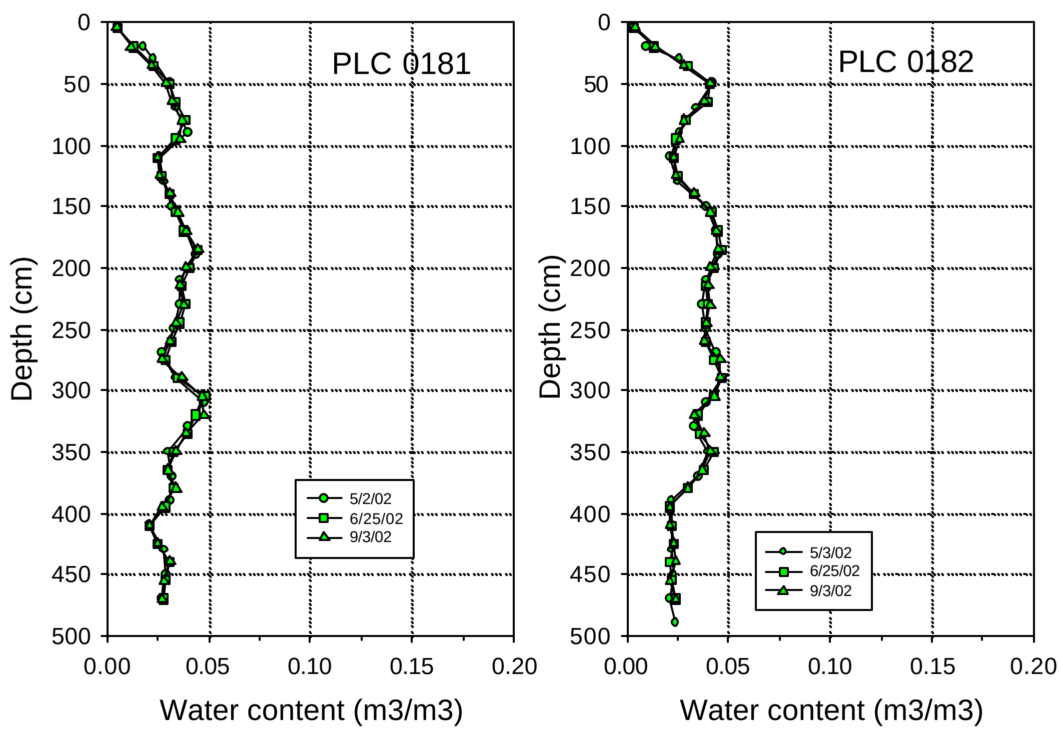

Figure 37. Soil water content *2* profiles for spring, summer, and fall conditions in two access tubes at PLC018 in 2002.

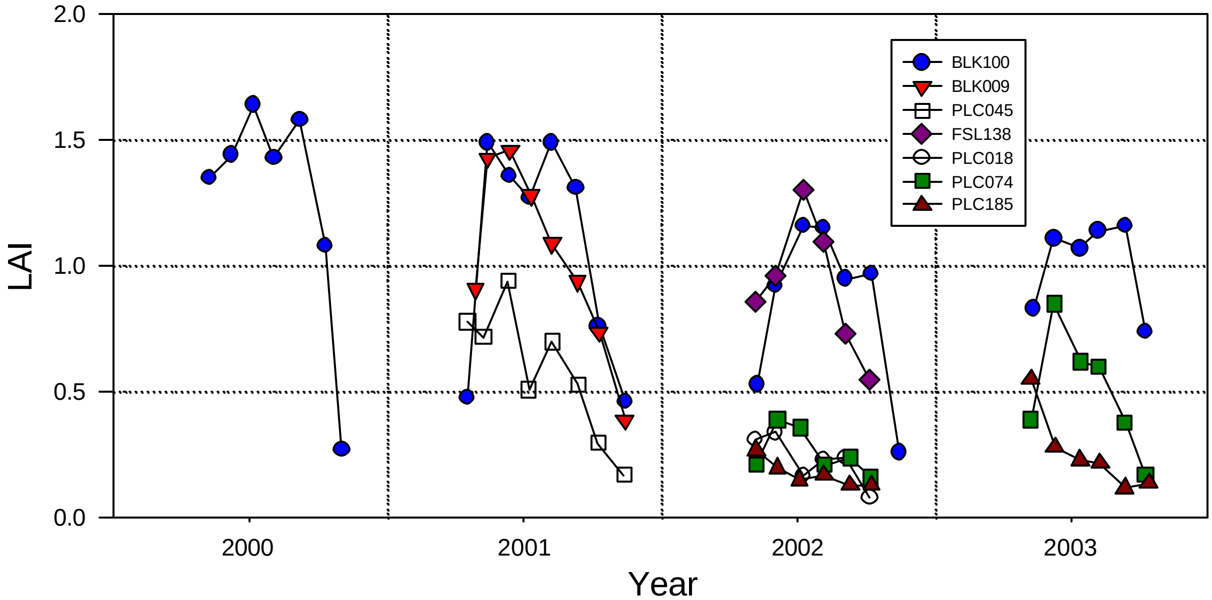

Figure 38. LAI of all species for all sites. Values are the mean of four transects.

with PLC074 in 2002 most divergent from the overall trend (Figure 39). Total plant cover and LAI were linearly related (Figure 40) which was expected given the linear relationship between LAI and cover for individual species (Steinwand, 1999a and b).

Three sites were monitored multiple years. Typically, BLK100 maintained a high leaf area through June, July, and August before declining in September (2000 and 2001) or October (2002 and 2003). The lower in LAI in 2002 and 2003 did not correspond to construction of the exclosure, or changes in precipitation or DTW. Leaf area trends were similar in 2002 and 2003 at PLC185 reaching a maximum in May and maintaining relatively low cover throughout the summer. The increased LAI in May 2003 compared to 2002 was largely due to greater numbers of short-lived annuals although SAVE4 and ATCO LAI were slightly greater as well. LAI all species except SAVE4 increased markedly at PLC074 in 2003 probably responding to increased winter precipitation.

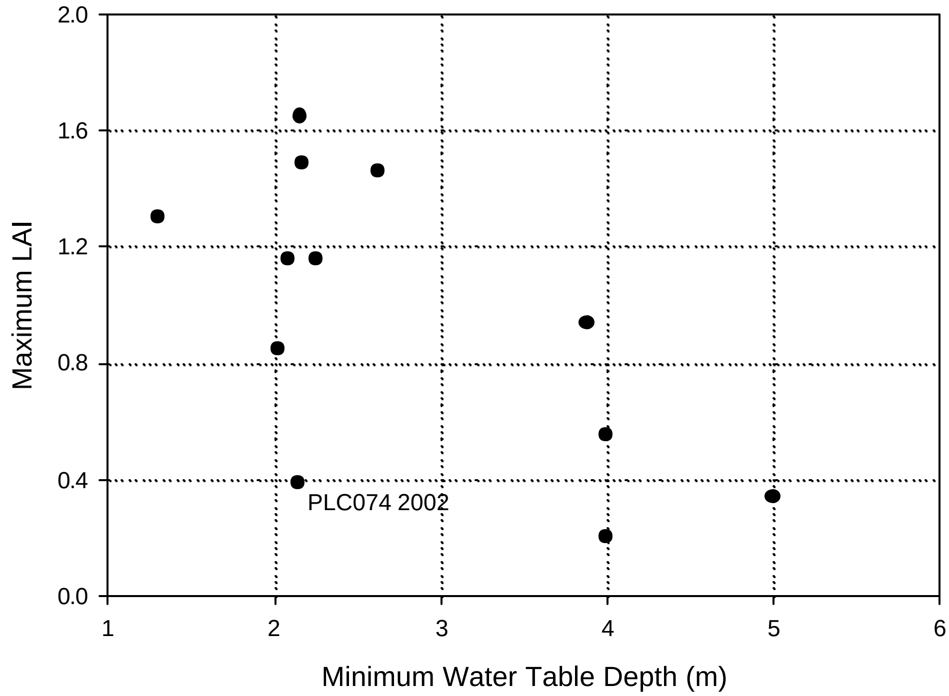

Figure 39. LAI and DTW measured at ET sites.

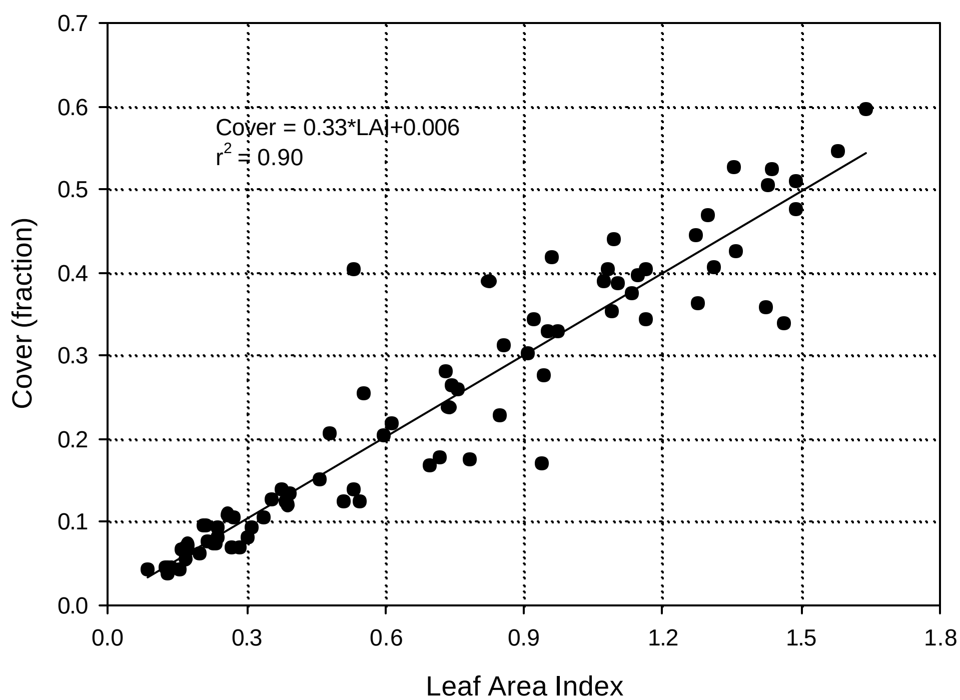

Figure 40. Relationship between plant cover (fraction) and LAI measured at the ET sites.

approximately 10mm of rain creating a bimodal pattern in LAI and ET. This was the only site to exhibit a noticeable response to summer precipitation. LAI was only weakly related to DTW

EC energy balance components and closure

An example of the half-hourly *EB* for the EC system at BLK 100 for several days in 2002 is given in Figure 41. *EB* ranged from (rarely) near zero to over 100 W m^{-2} with a mean *EB* closure error over the period of 43.9 W m^{-2}. Mean available energy during this period was 124.0 W m^{-2}, thus the turbulent fluxes did not account for over one-third of the available energy. During DOY 238, 2002, the energy balance closure error was greater than 150 W m^{-2}. The closure error tended to be highest during the afternoon, but persisted throughout the day.

Comparison of Figures 41 and 42 shows that the *EB* error tended to be largest during periods of relatively higher wind speeds in the afternoon. The linear correlation coefficient between the horizontal wind speed and the EB error was $r = 0.46$. Except for DOY 238, winds were from the southeast during the afternoon, which should be the most favorable wind direction for the EC instruments; therefore, the EB error maxima did not appear to be attributable to disruption of the flow by the sensors and mounting structure. The peak *EB* closure error occurred on DOY 238, and flow distortion may have contributed to the error that day.

For all sites, the mean *EB* calculated on a daily basis ranged from 47 to 94% (Figures 43 to 47). Highly erratic values of *EB* occurred before and after the growing season (84>DOY >288) when all the fluxes were relatively small. Generally, the closure error was repeatable between years at the same site and least early in the growing season and increased approximately 20% by the end of the season. The increase in closure error usually began about midsummer

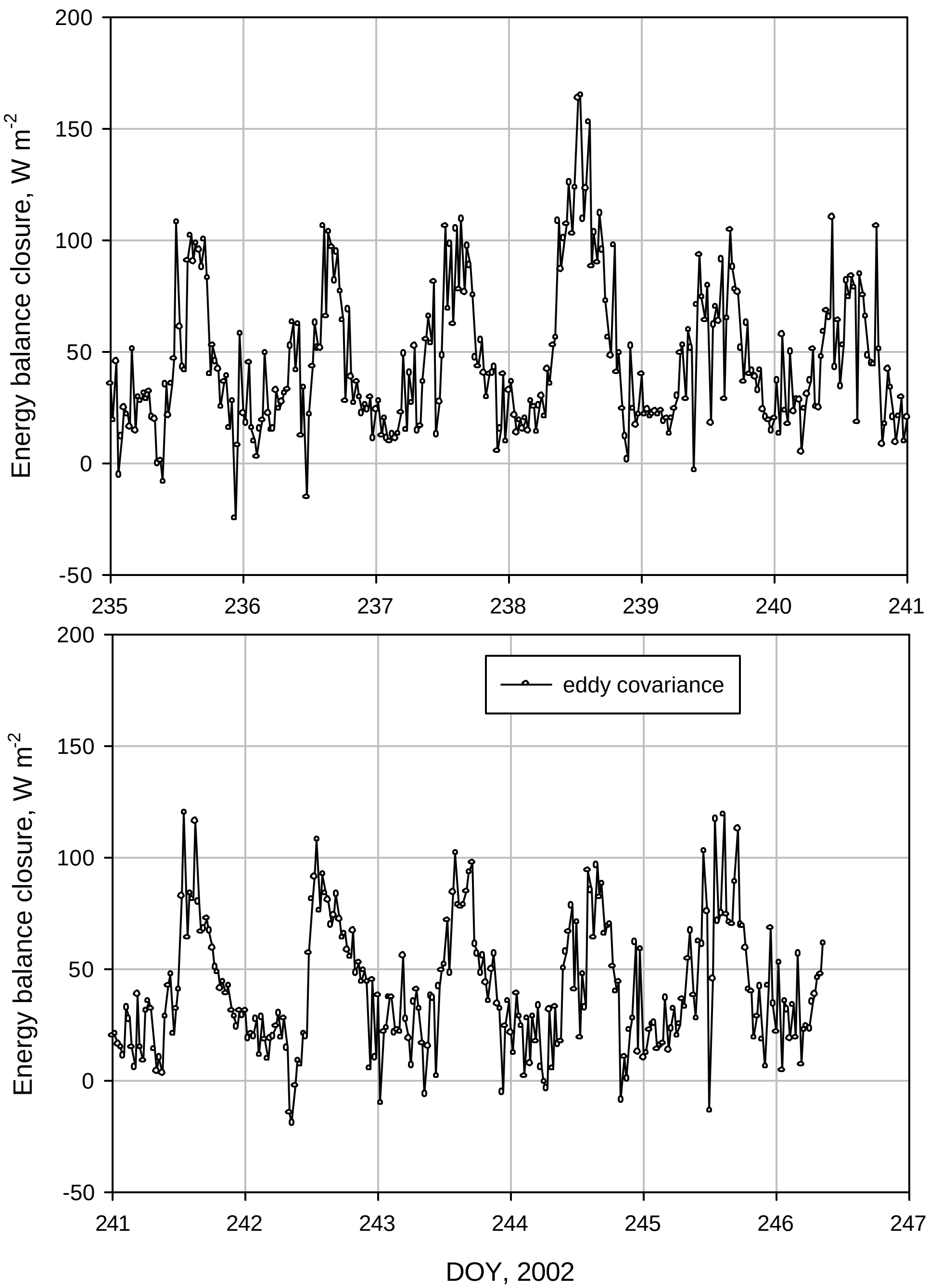

Figure 41. Example of the energy balance closure error for EC system on half hourly basis at BLK 100 during the period of BR system operation.

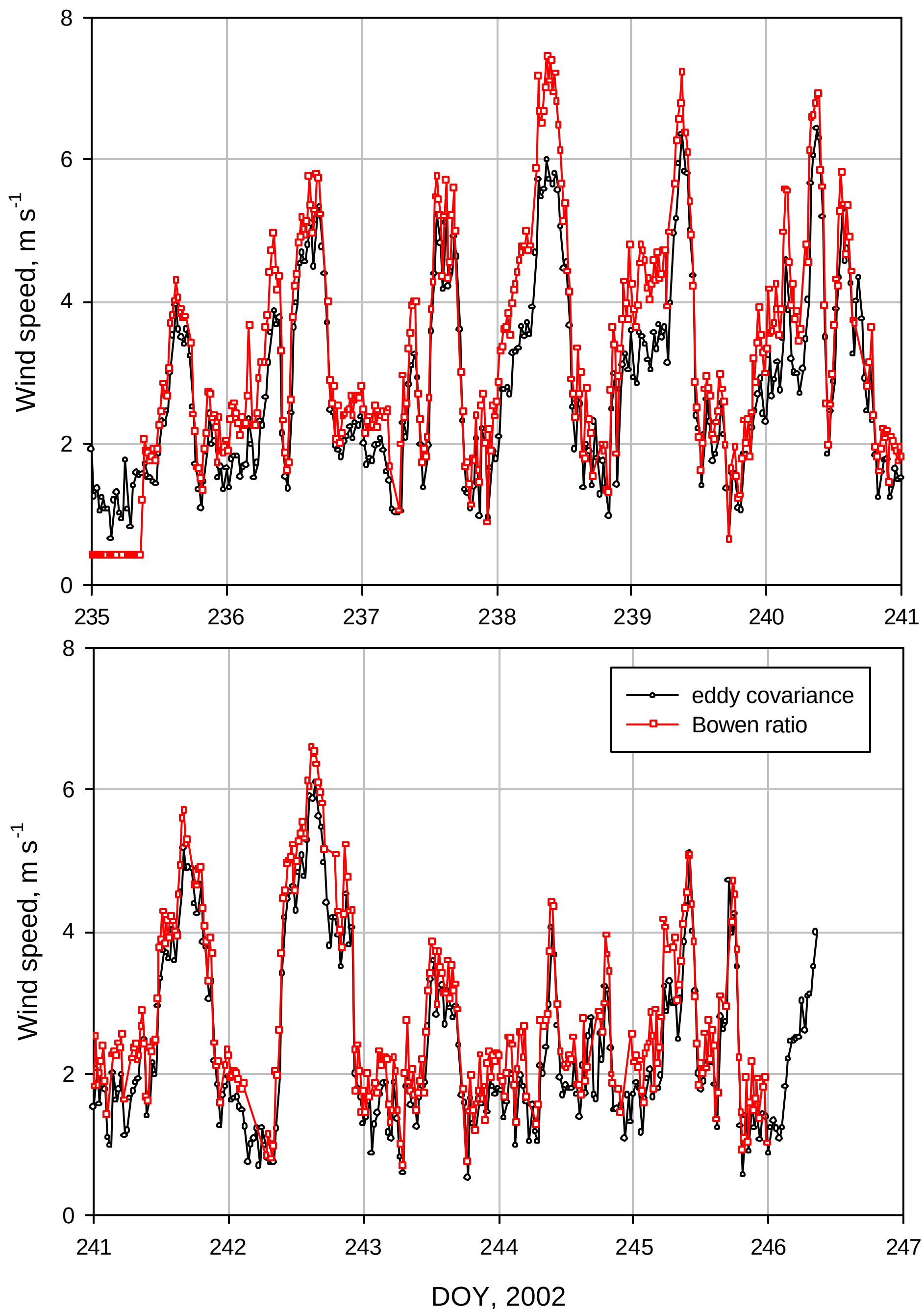

Figure 42. Wind speed at BLK 100 measured with eddy covariance and Bowen Ratio instruments in 2002.

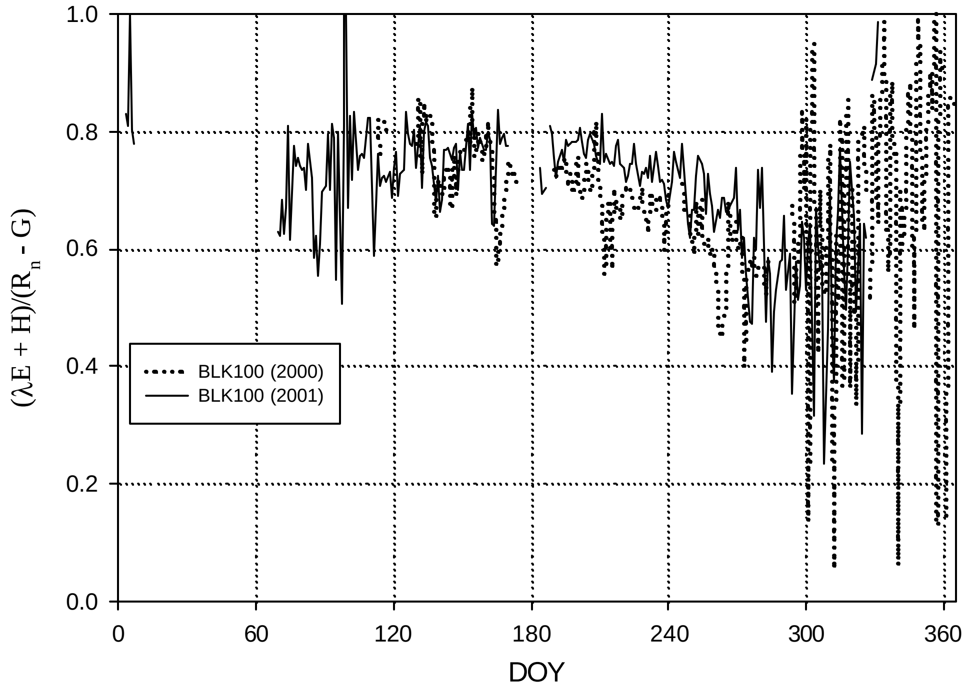

Figure 43. *EB* for BLK100 in 2000 and 2001.

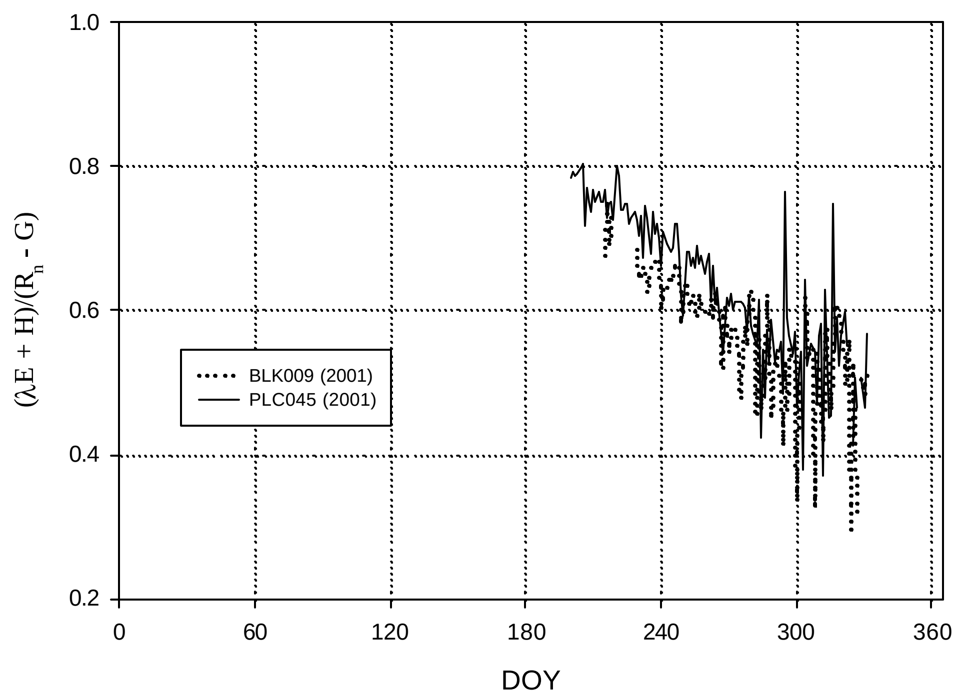

Figure 44. *EB* for BLK009 and BLK045 in 2001.

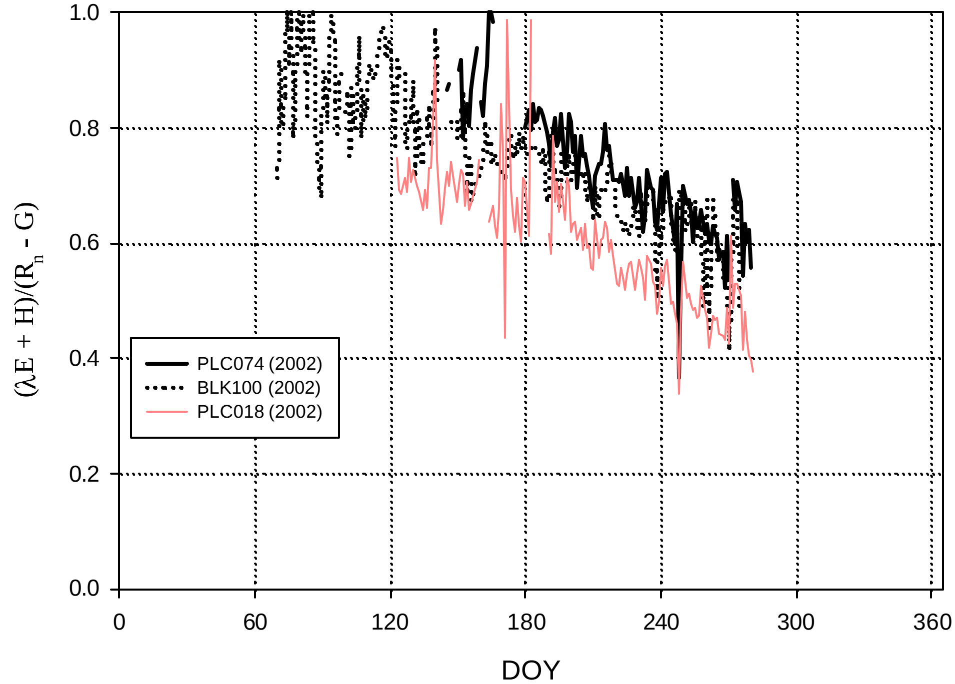

Figure 45. *EB* for PLC018, PLC074 and BLK100 in 2002.

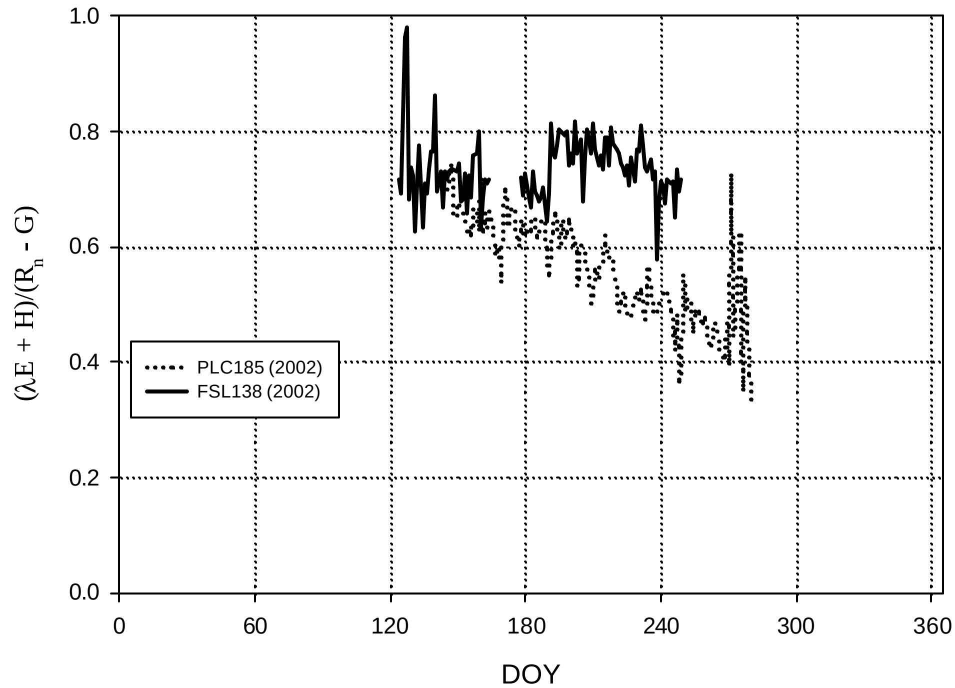

Figure 46. *EB* for PLC185 and FSL138 in 2002.

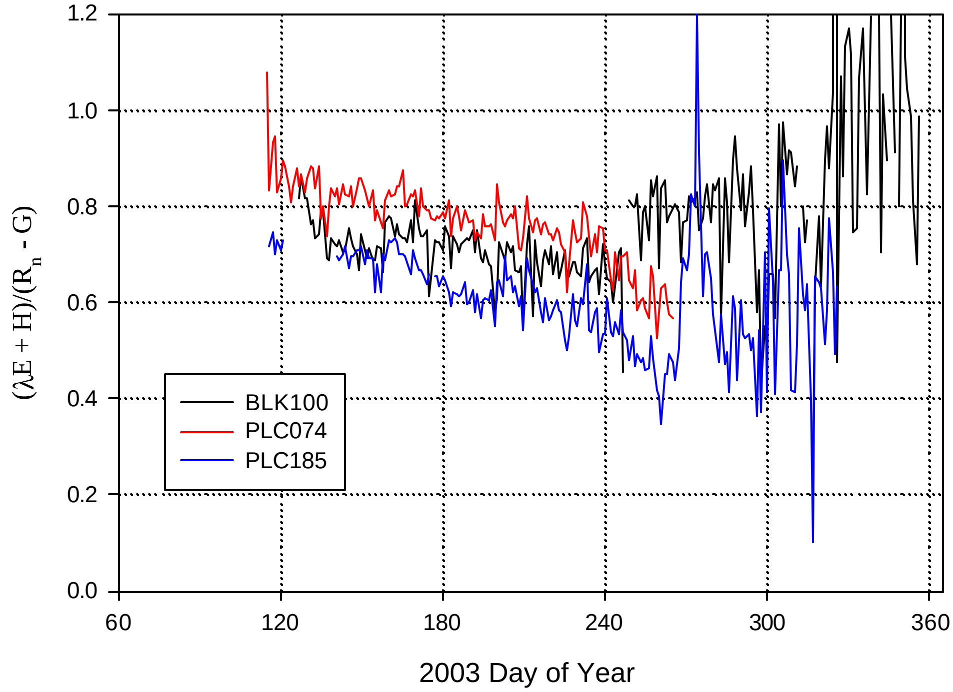

Figure 47. EB for PLC185, PLC074 and BLK100 in 2003.

(DOY 186) and was not evident before or after the growing season. Changes in EB seem related to H or lE individually or in combination rather than calibration drift, but the relationship is not understood. Interestingly, the EB trend at FSL138 was not similar to trends evident at other sites. The closure error at FSL138 was relatively stable except for a sharp decrease about DOY 191 that corresponded with a sudden decrease in lE suggesting the closure error was related to lE. At other sites, however, the late summer increase in the closure error was more gradual and increased as lE decreased. The step change in closure error in BLK100 in 2003 was an instrumentation artifact (Figure 47).

Failure of EC systems to achieve EB closure has been observed in other studies, and various instrumental or theoretical explanations have been put forth to address the problem.

Zeller et al. (1989) and Massman et al. (1990) examined sources of error in EC turbulent flux measurements due to mismatches in sensor response times, sensor volume or line averaging effects, flow distortion around sensors and mounting structures, spatial separation of sensors, and sampling rate (aliasing) effects. Each source of error tends to reduce the covariance measured by the EC system, thereby causing the turbulent fluxes to be underestimated. After implementing corrections for each of these sources of error, their energy balance still failed to achieve closure, which they attributed to inaccuracy of the measurement of R_n and G.

In the event of non-closure of the energy balance, there are various strategies to correct the EC fluxes. Besides the formal frequency domain transfer function corrections used by Zeller et al. (1989) and Massman et al. (1990), several simple ad hoc corrections based on the Equation 5 can be made, the choice of which depends on the suspected source of error. If the error is due to the hygrometer, energy balance can be achieved by assuming all the error is in the latent heat term. If the error is due to the sonic anemometer or due to a loss of covariance that affects H and lE in similar proportions, the turbulent fluxes can be corrected by assuming that b is measured correctly and adjusting the magnitude of the turbulent fluxes such that energy balance is achieved.

Examination of the EB from EC systems operated as part of this study revealed that closure errors of similar magnitude occurred at sites with minimal ET (e.g. PLC018, Figure 45) suggesting that both turbulent fluxes are underestimated. Also, lE measured by the EC system at all sites was near 0 W m^{-2} during nighttime, as would be expected for the dry soil surface present at the sites. Therefore, though the error may have been partly due to the hygrometer, ascribing the EB error solely to the lE term was unwarranted. BR system b measured with the

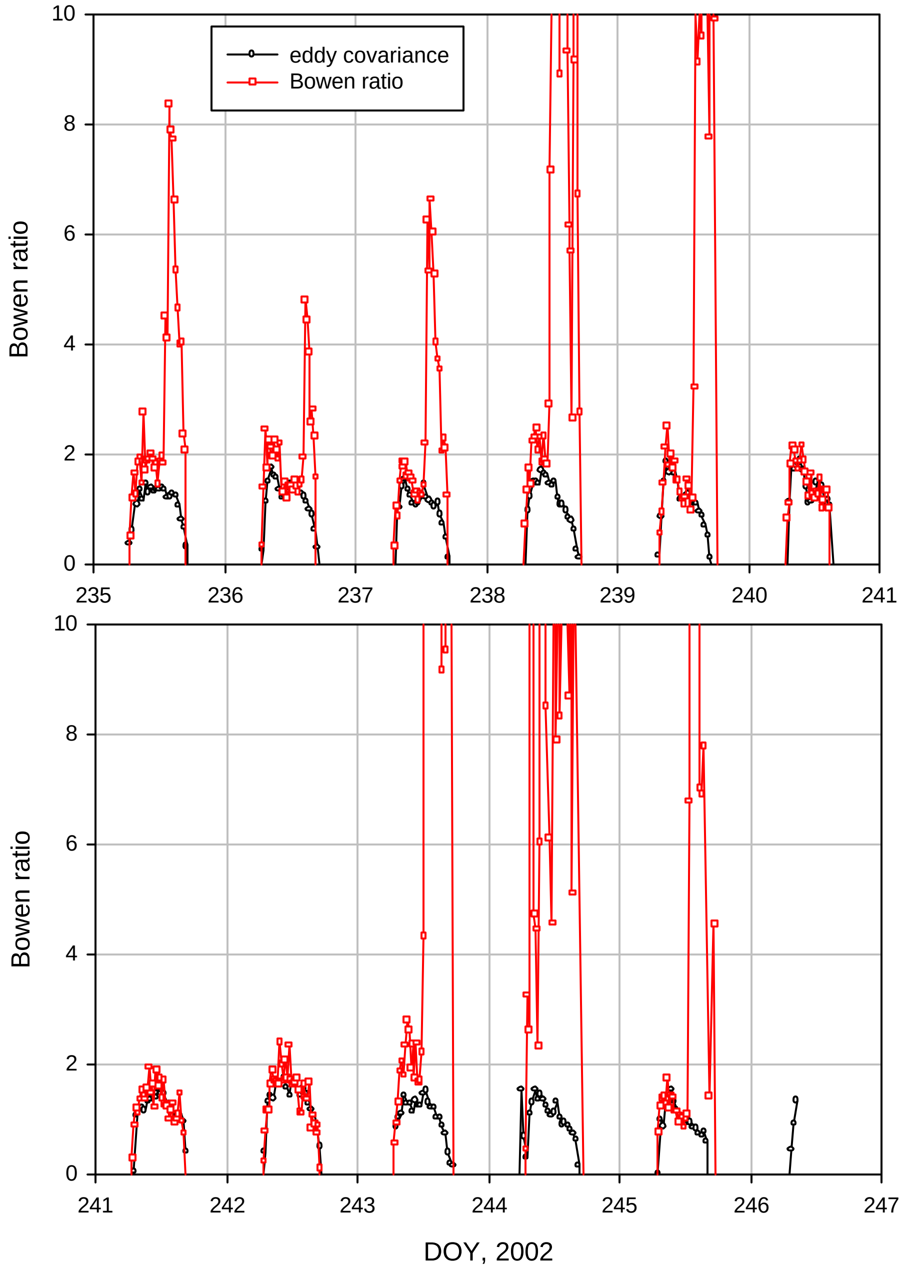

Figure 48. Daytime Bowen ratio (H/lE) at BLK 100 measured with eddy covariance and Bowen Ratio instruments in 2002. Only daytime b are shown because nighttime b for both systems tended to be highly erratic due to the small magnitude and variable sign of lE.

BR and EC systems agreed during daylight hours, except at times when the produced large erratic values (Figure 48). The b values were comparable between the two systems during the morning hours, climbing to a midday peak of ~1.7, then during the afternoon hours BR b often grow very large while the EC b smoothly decline from their midday peak. The large afternoon b sometimes measured by the BR system are considered erroneous, because the clear dry conditions during the measurement period should produce smoothly varying b during daylight hours. The cause of these erroneous measurements is unknown. During periods of afternoon winds, the BR system often yielded unstable large Bowen ratios. Additionally, values of b produced by the EC system followed a smoothly varying pattern repeated each day of increase from negative values in the early morning to a midday maxima followed by decrease to negative values in the evening. Thus, use of b measured by the EC system is probably the most reliable way to correct the EC turbulent fluxes. The correction applied was,

$$lE_{corr} = \frac{R_n - G}{b + 1} \tag{14}$$

Of course, when Equation 13 is used to correct the EC measurements, the computed flux is no longer independent of the energy balance measurements. Additionally, measurements at dawn and dusk when b is near -1 must either be discarded, similar to the processing of BR measurements, or not be corrected. Periods when b is near -1 have little influence on daily or seasonal ET estimates, because ET is usually low during the time of day when this condition prevails. Prior to the application of Equation 14, the only corrections applied to the EC lE measurement were the oxygen and air density corrections. Using b as the correction factor thus

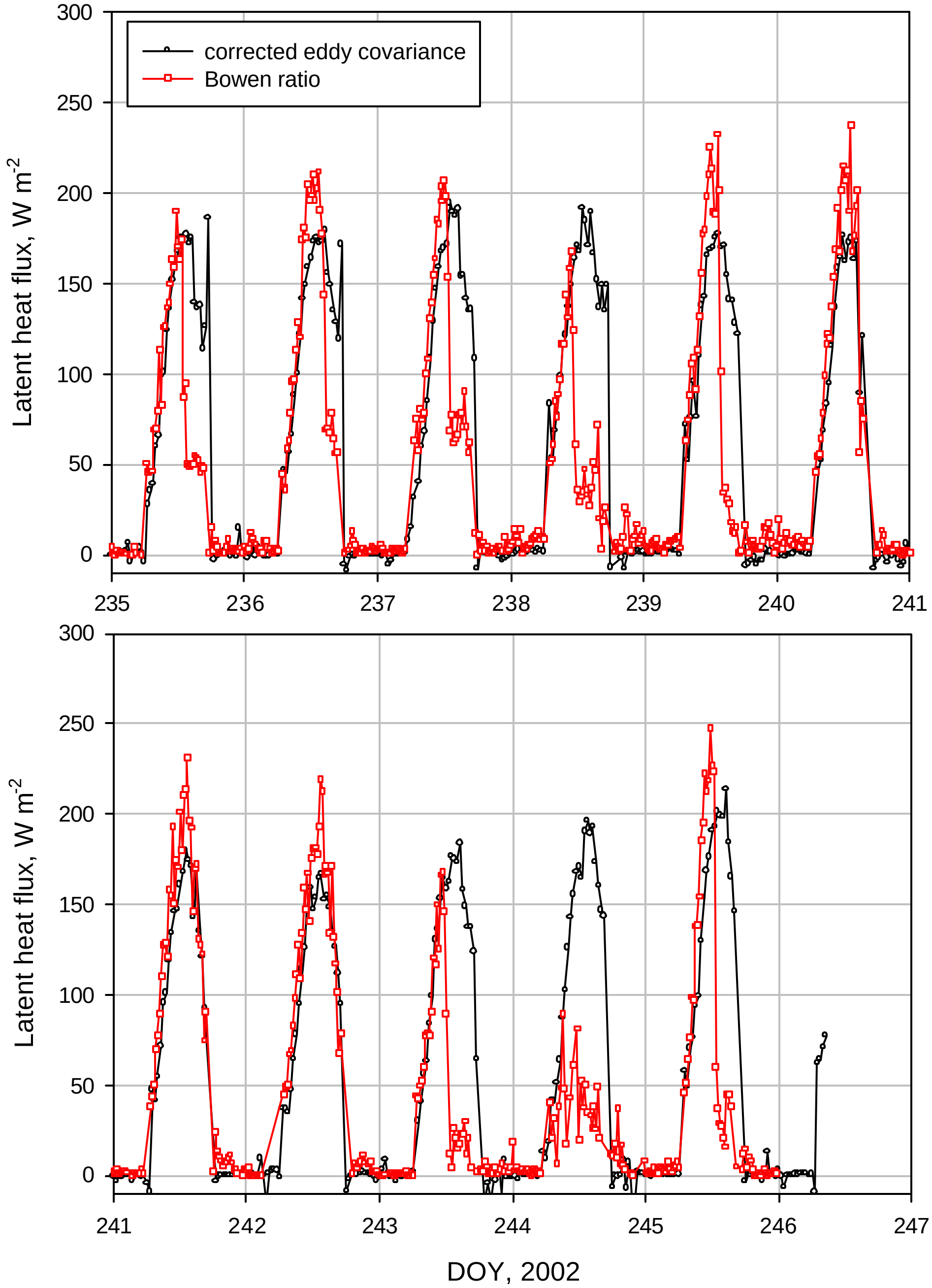

Figure 49. Latent heat flux at BLK 100 measured with eddy covariance and Bowen Ratio instruments in 2002. EC latent heat flux has been corrected using Equation 14.

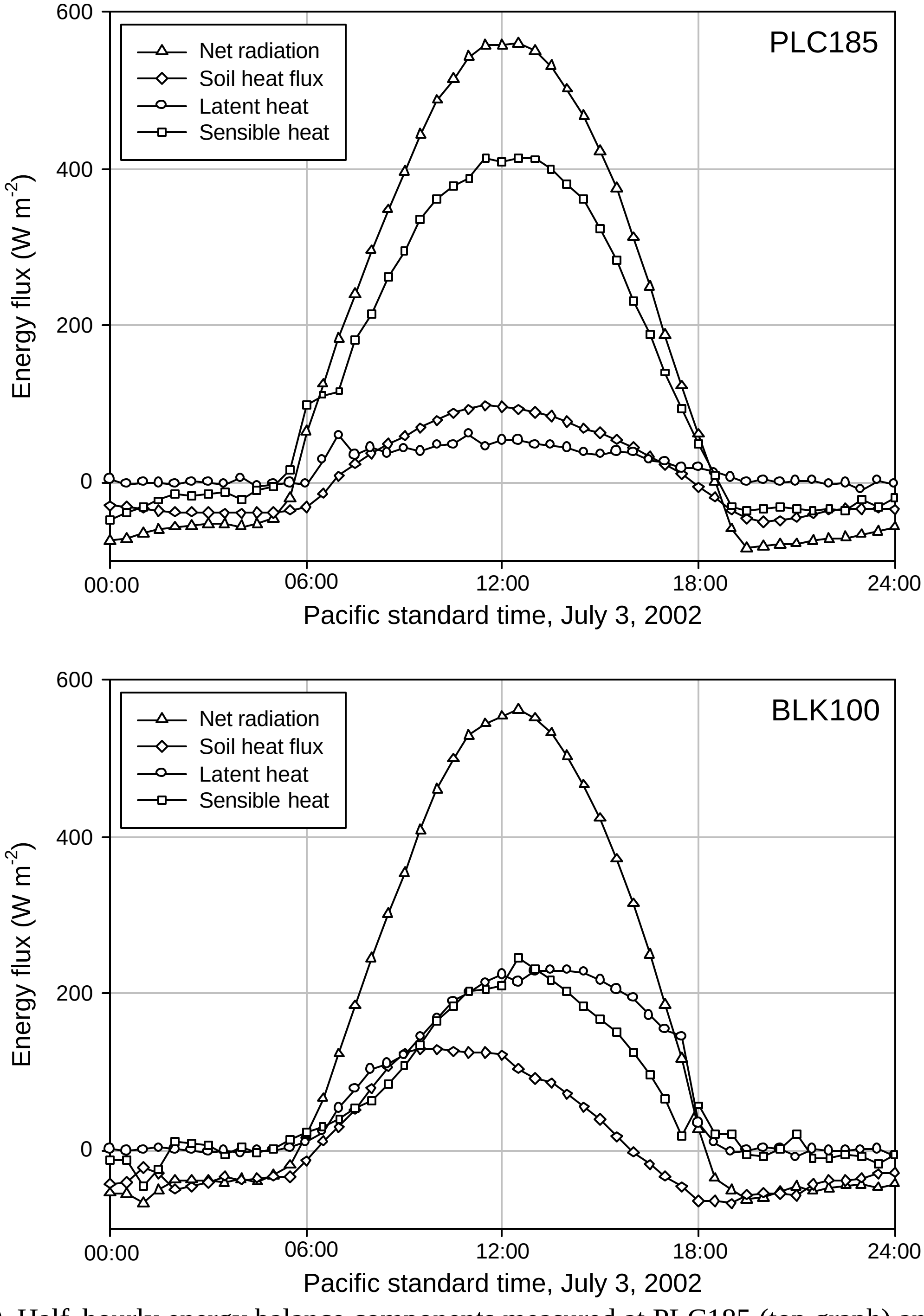

Figure 50. Half-hourly energy balance components measured at PLC185 (top graph) and BLK100 (bottom graph).

assumes that other sources of error affect the turbulent fluxes in equal proportion (i.e., multiplicatively). When lE measured with the EC system is corrected using Equation 14, it produces similar results to lE measured with the BR system during periods when b produced by both system was similar (Figure 49). During periods when b measured with the BR system was erroneously large (e.g. at night), lE_{corr} was greater than that measured with the BR system.

Eddy covariance results

Two examples of the diurnal fluxes typical of summer conditions at a dry and wet site of the Owens Valley are shown in Figure 50 where daytime surface heating due to solar radiation is partitioned into positive daytime sensible and latent heat fluxes. Soil heat flux was a relatively small component of the energy balance and changed sign from negative to positive in mid-morning and from positive to negative in late evening. At night, net radiation was negative due to thermal emission from the land surface, latent heat flux was near zero due to the cessation of plant transpiration, and sensible heat flux was small and negative.

The lE_{corr} was usually, but not exclusively, greater than the uncorrected EC measurement (Figures 51 and 52). The correction increased ET estimates a few tenths of mm day $^{-1}$ up to 1 mm day^{-1} depending on the site. One disadvantage of adopting this correction was the shorter record of corrected ET because there were fewer days when all instruments were functioning. The disadvantage was particularly acute at BLK009 and PLC045 where datalogger problems prevented collection of *Rn* and *G* for the first half of the growing season.

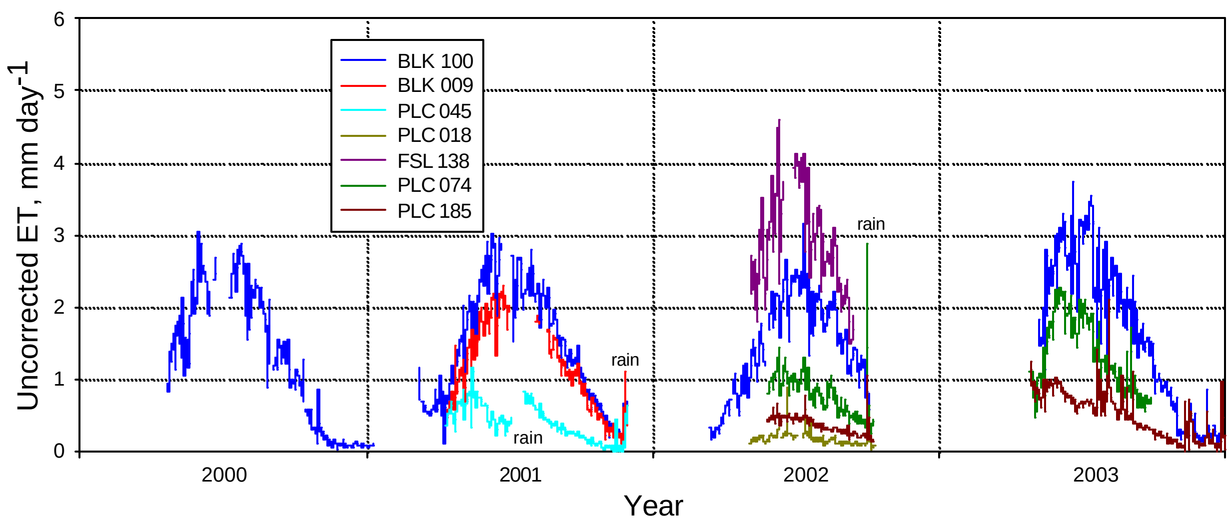

Figure 51. All uncorrected ET measured by EC systems.

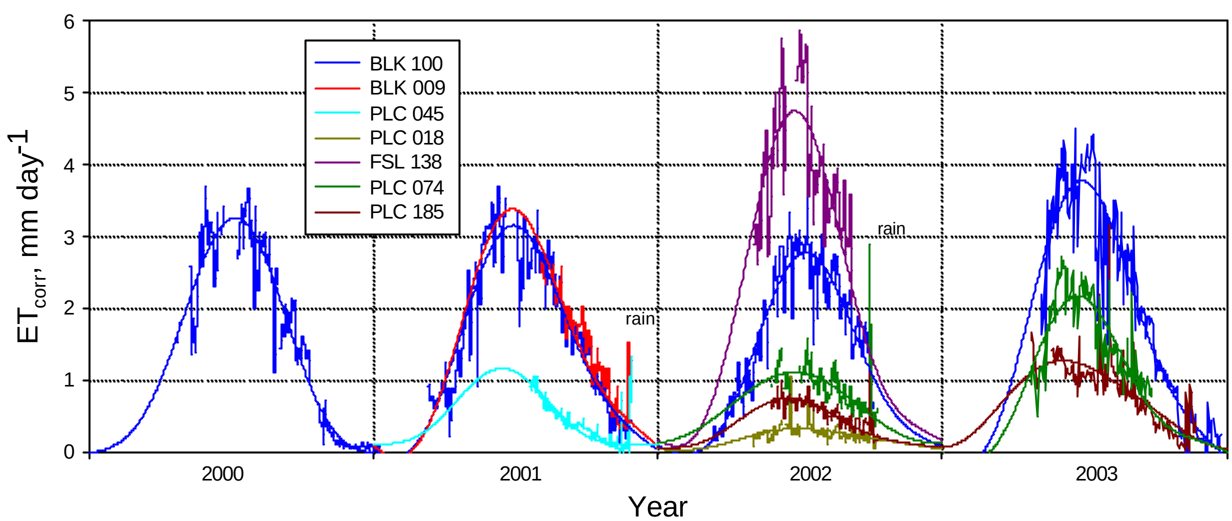

Figure 52. All ET corrected for energy imbalance and fitted Fourier models used for integration.

Table 6. ET_{corr} Fourier model coefficients and r^2 for each site-year.

Year	Site	mean	A(1)	A(2)	B(1)	B(2)	r^2
		mm day^{-1}					
2000	BLK 100	1.37	-1.62	0.26	-0.12	0.06	0.93
2001	BLK 100	1.33	-1.56	0.27	-0.13	-0.12	0.90
	BLK 9	1.43	-1.65	0.31	-0.14	-0.17	0.95
	PLC 45	0.50	-0.50	0.12	0.15	-0.08	0.85
2002	BLK 100	1.12	-1.33	0.30	-0.27	0.03	0.98
	FSL 138	1.94	-2.28	0.50	0.10	-0.20	0.70
	PLC 18	0.18	-0.14	0.01	-0.03	-0.02	0.54
	PLC 74	0.60	-0.49	0.02	0.06	-0.004	0.63
	PLC 185	0.35	-0.33	0.05	0.05	-0.05	0.57
2003	BLK 100	1.53	-1.92	0.33	-0.14	-0.17	0.91
	PLC 74	0.81	-1.07	0.27	0.01	-0.16	0.91
	PLC 185	0.68	-0.57	-0.04	0.14	-0.05	0.76

The Fourier models also are shown in Figure 52, and coefficients and fitting statistics are given in Table 6. The relatively low r^2 for PLC018 and PLC185 (Table 6) was due in large part to the low and relatively flat seasonal ET trend (small variance). Visual inspection, however, suggests the agreement between the data and Fourier model was acceptable for the purpose of integration.. ET at each site is described further in the next section.

Comparison of lE_{corr}, T_{Kc}, and T_{GB}

Performance of the Kc and Green Book models was evaluated three ways: 1) correspondence of T_{Kc} and T_{GB} with trends in lE_{corr}, i.e. shape of the models 2) comparison of seasonal transpiration totals estimated by T_{Kc} and T_{GB} with lE_{corr} Fourier model totals, and 3) comparison field measurements with models for individual species LAI and ETr components of T_{Kc} and T_{GB} (LAI only).

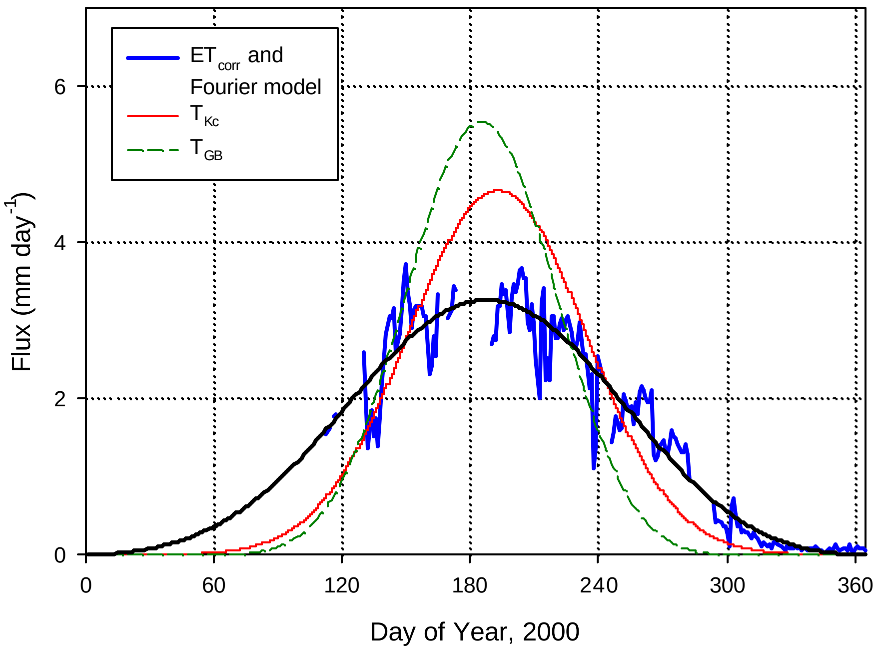

Figure 53. λE_{corr} at BLK100 in 2000 measured with the EC system and T_{GB} and T_{Kc} estimated using measured LAI Equations 7 and 9. Fourier model fitted to λE_{corr} also shown.

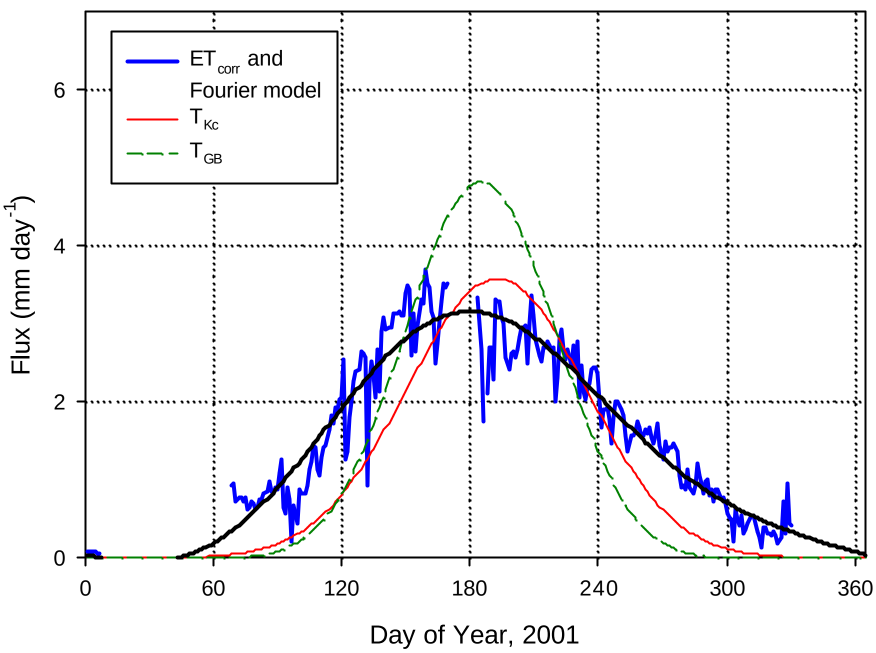

Figure 54. λE_{corr} at BLK100 in 2001 measured with the EC system and T_{GB} and T_{Kc}. Fourier model fitted to λE_{corr} also shown.

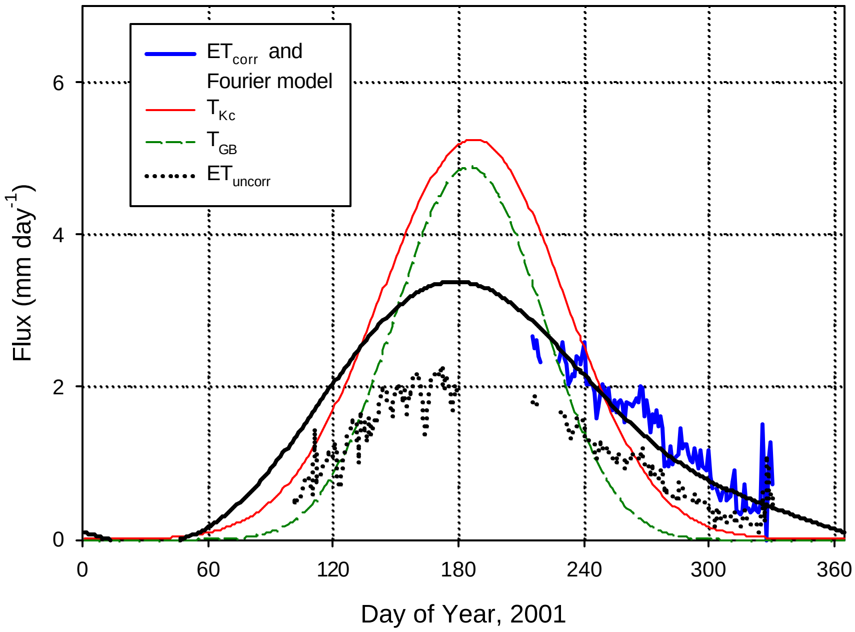

Figure 55. lE_{corr} at BLK009 in 2001 measured with the EC system and T_{GB} and T_{Kc}. EC measurements corrected and uncorrected for energy balance closure error are presented. Fourier model fitted to lE_{corr} also shown.

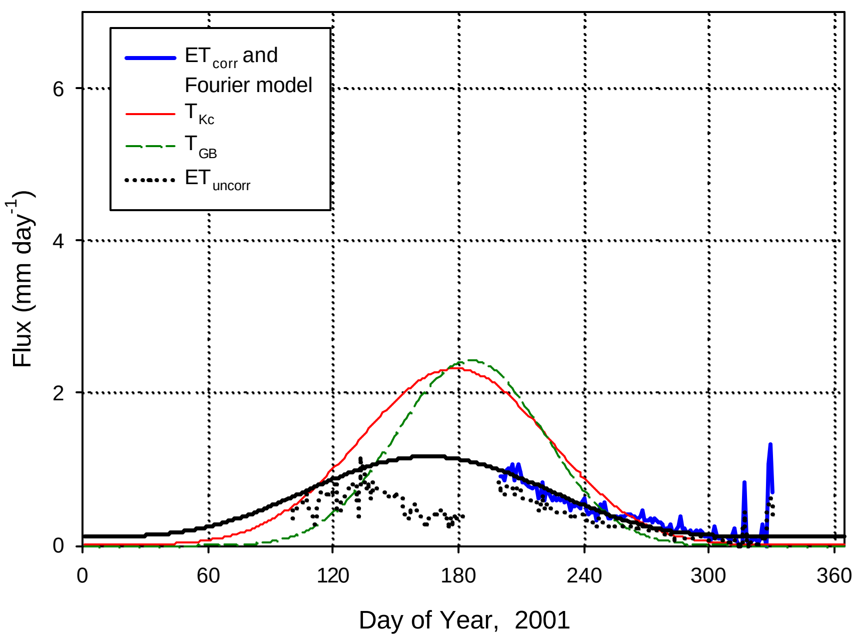

Figure 56. lE_{corr} at PLC045 in 2001 measured with the EC system and T_{GB} and $T_{Kc.}$ EC measurements corrected and uncorrected for energy balance closure error are presented. Fourier model fitted to lE_{corr} also shown.

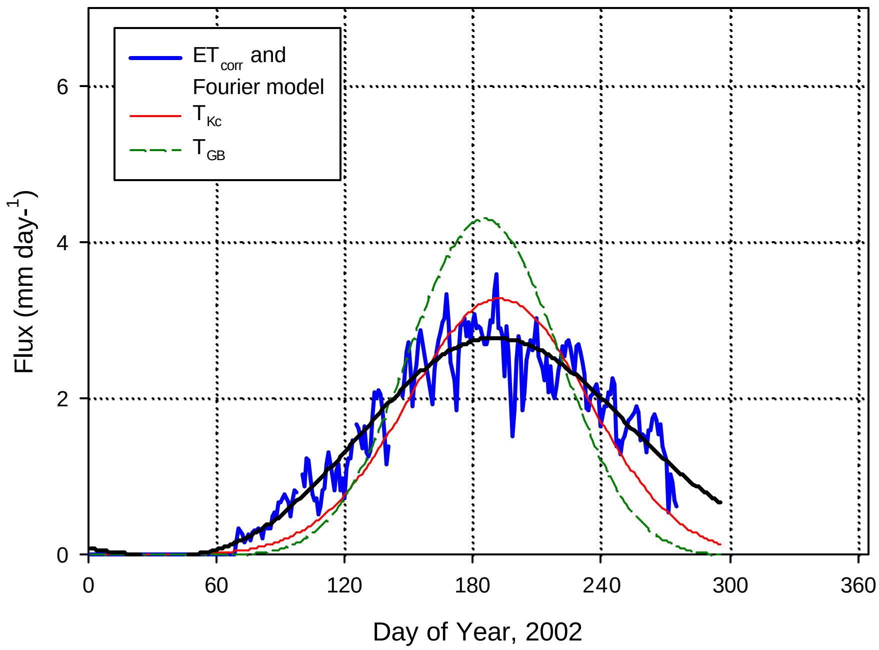

Figure 57. lE_{corr} at BLK100 in 2002 measured with the EC system and T_{GB} and T_{Kc}. Fourier model fitted to lE_{corr} also shown.

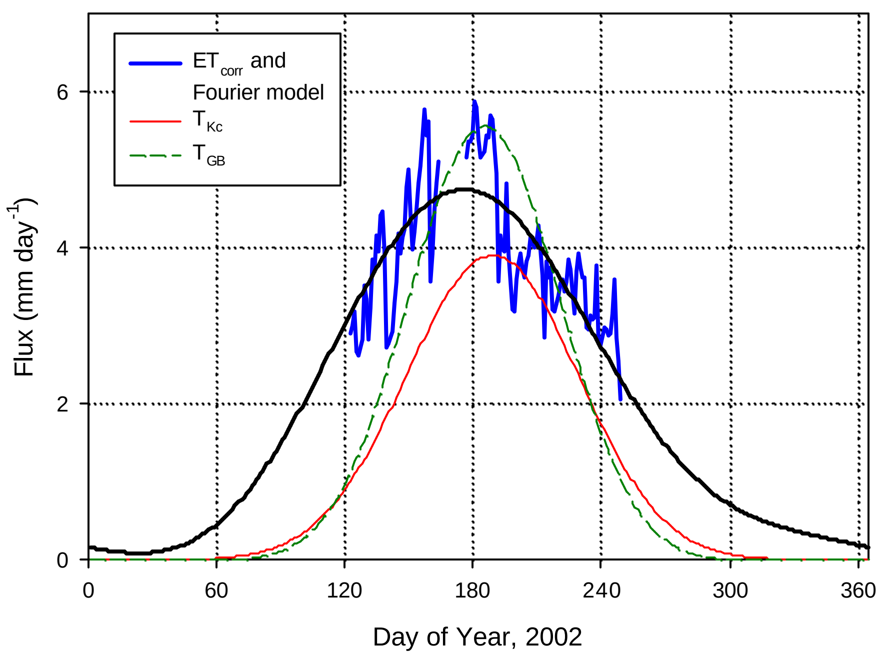

Figure 58. lE_{corr} at FSL138 in 2002 measured with the EC system and T_{GB} and T_{Kc}. Fourier model fitted to lE_{corr} also shown.

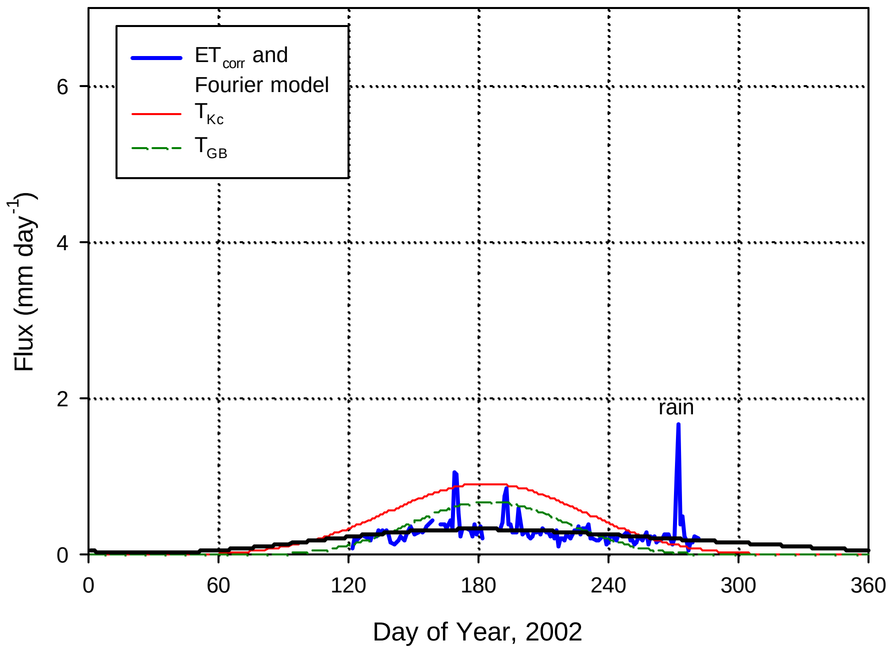

Figure 59. lE_{corr} at PLC018 in 2002 measured with the EC system and T_{GB} and T_{Kc}. Fourier model fitted to lE_{corr} also shown.

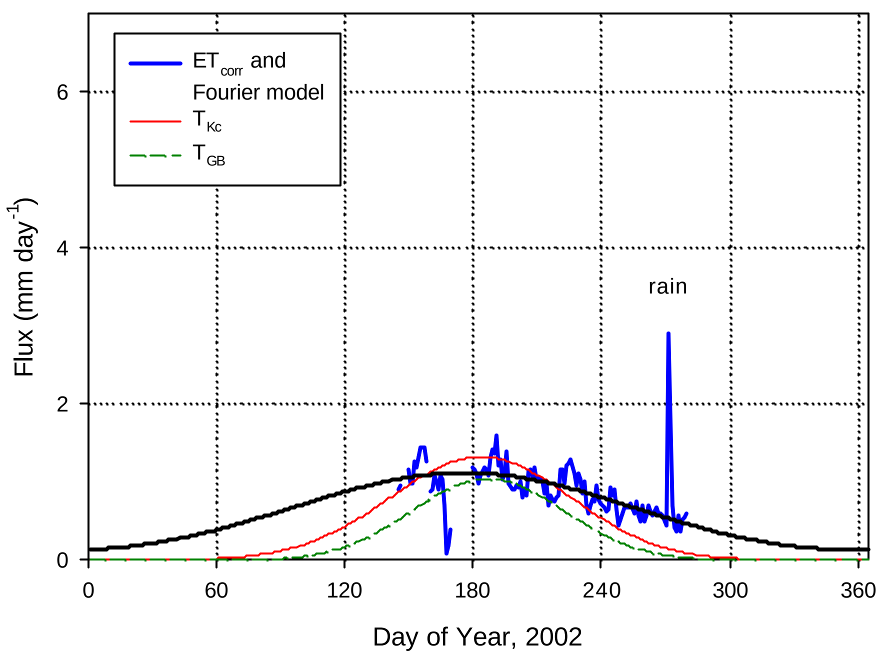

Figure 60. lE_{corr} at PLC074 in 2002 measured with the EC system and T_{GB} and T_{Kc}. Fourier model fitted to lE_{corr} also shown.

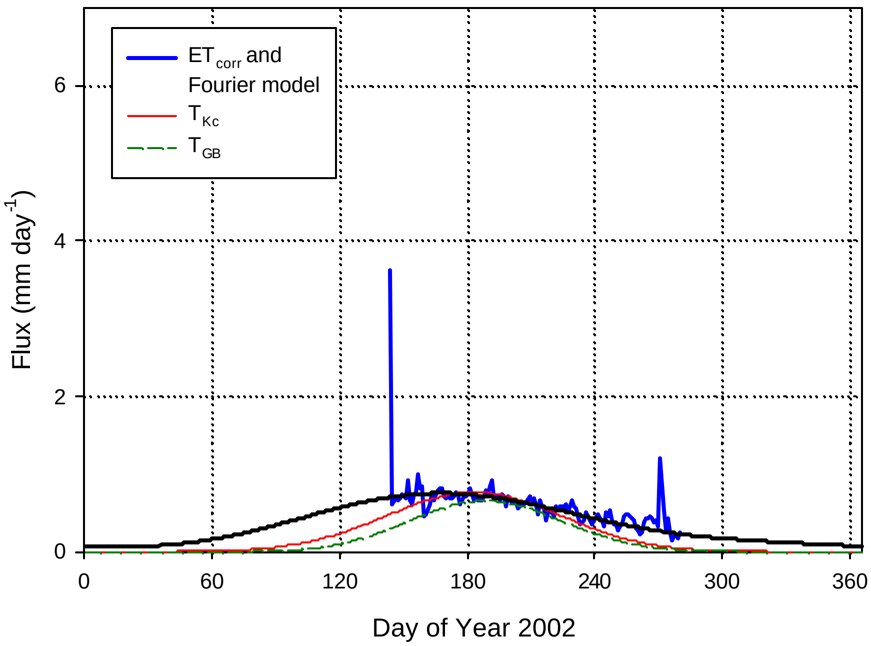

Figure 61. λE_{corr} at PLC185 in 2002 measured with the EC system and T_{GB} and T_{Kc}. Fourier model fitted to λE_{corr} also shown.

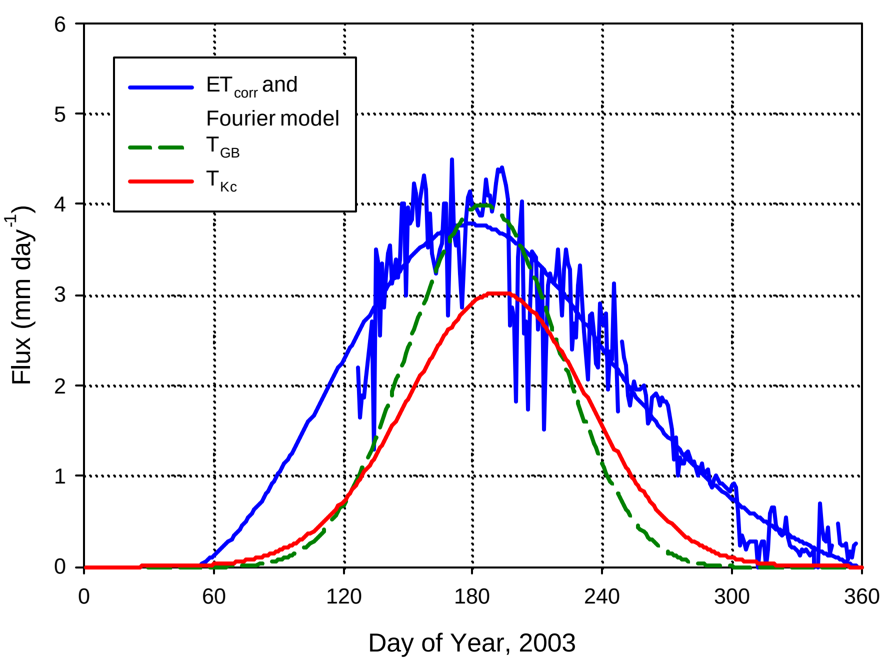

Figure 62. λE_{corr} at BLK100 in 2003 measured with the EC system and T_{GB} and T_{Kc}. Fourier model fitted to λE_{corr} also shown.

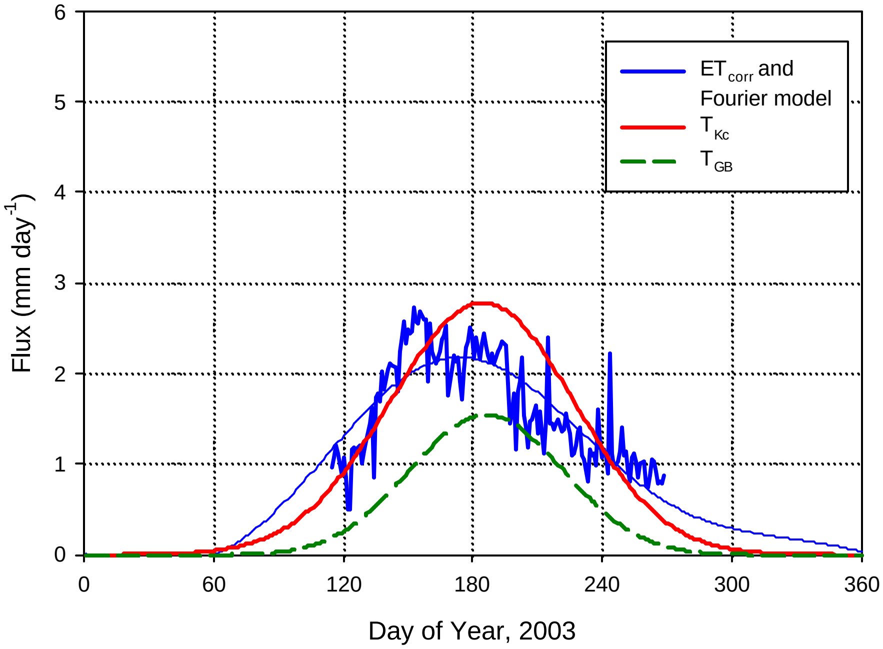

Figure 63. lE_{corr} at PLC074 in 2003 measured with the EC system and T_{GB} and T_{Kc}. Fourier model fitted to lE_{corr} also shown.

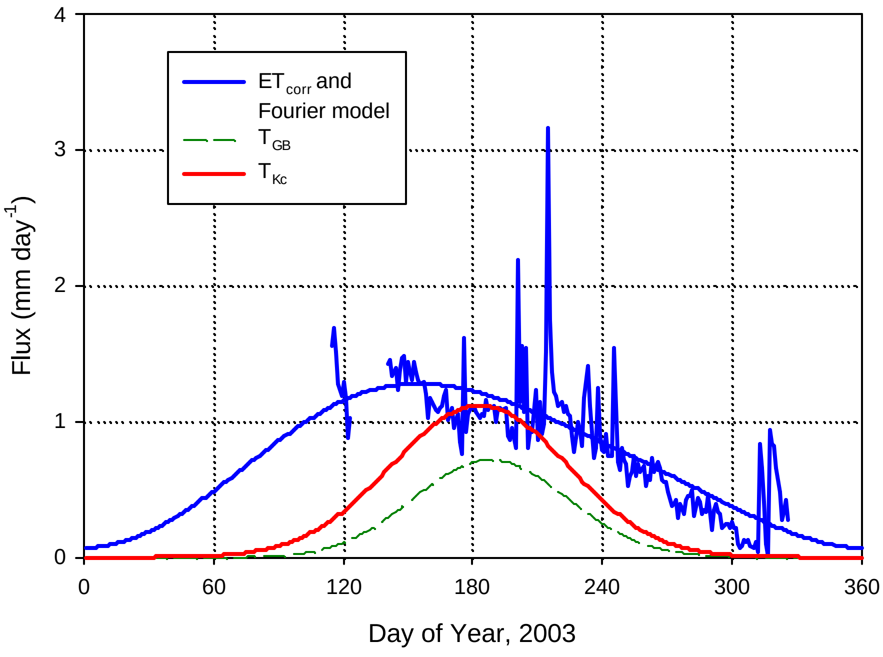

Figure 64. lE_{corr} at PLC185 in 2003 measured with the EC system and T_{GB} and T_{Kc}. Fourier model fitted to lE_{corr} also shown.

Seasonal trends in ET corresponded with the expected trends in evaporative demand throughout the summer. ET peaked in midsummer and was greater at sites with higher LAI. Daily values of λE_{corr} and fitted Fourier models are presented in Figures 53 to 64 along with T_{Kc} and T_{GB}. At grass-dominated sites, T_{GB} exceeded T_{Kc}, but relative magnitudes were reversed at shrub-dominated sites consistent with the comparison by Steinwand (2000b). At most sites, T_{Kc} and T_{GB} usually underestimated early and late season λE_{corr}, but overestimated midsummer λE_{corr}. Seasonal T_{Kc} and T_{GB} loosely tracked λE_{corr} at BLK100 (all years), PLC074, and PLC185 (2002). Seasonal trends in T_{Kc} and T_{GB} compared less favorably with field measurements at BLK009, FSL138, PLC045, and PLC018. At PLC045, and PLC018, the poor agreement was likely due to failure of site conditions to meet model assumptions. At PLC045 and PLC018, the water table was at or below the maximum rooting depth for saltbush and rabbitbrush, respectively, and the upper 4 to 5 meters of soil was near the limiting water content. Both models assume soil water is sufficient, and therefore, it was not surprising that T_{Kc} and T_{GB} overestimated the observed ET. The decline in LAI and ET (inferred from decline in uncorrected λE) during June at PLC045 corresponded with the exhaustion of available soil water within the monitored soil depth (3.3m) by June 21 (Figure 56) suggesting that the uptake rate of groundwater alone was insufficient to support early season leaf area. Subsequently, leaf area and ET at this site responded to approximately 35 mm of rain in early July (Figure 38). The T_{Kc} and T_{GB} models cannot accommodate the bimodal response exhibited at this site, and the seasonal ET total based on the Fourier model integration is overestimated. At FSL138, T_{GB} tracked λE_{corr} better than T_{Kc}, but neither model estimated the seasonal total well or tracked the early (April and May) and late (August and Sept.) season ET. The sharp decline in λE_{corr} at FSL138 on July 11 corresponded

Table 7. RMSE between eddy covariance ET corrected for energy balance closure and T estimated from Kc and GB models.

Year	Site	T_{Kc} RMSE ^ June Meas.	T_{Kc} RMSE July Meas.	T_{GB} RMSE June Meas.	T_{GB} RMSE July Meas.
		mm day^{-1}			
2000	BLK 100	0.58	0.71	0.98	1.13
2001	BLK 100	0.71	0.72	1.02	0.94
	BLK 9	0.85	0.74	0.97	1.00
	PLC 45	0.49	0.49	0.52	0.26
2002	BLK 100	0.61	0.51	0.75	0.92
	FSL 138	2.10	1.48	1.65	1.16
	PLC 18	0.60	0.25	0.56	0.25
	PLC 74	0.40	0.42	0.49	0.54
	PLC 185	0.19	0.23	0.24	0.29
2003	BLK 100	0.95	0.98	0.94	0.97
	PLC 74	0.48	0.50	0.63	0.86
	PLC 185	0.48	0.52	0.63	0.65

^: RMSE = $[\Sigma(ET_{corr}\text{-model})^2/n]^{0.5}$

with termination of soil water uptake at depths above 1 m and with the deepest water table depth (2.05 m). This site had the shallowest water table of all sites, and the λE_{corr} decline may reflect a decrease in surface E as the soil dried and/or decrease in T as the water table approached the bottom of the saltgrass root zone of approximately 2 m (Groeneveld, 1990). Total LAI began to decline steadily after the July 9 measurement suggesting that curtailed transpiration constituted some fraction of the observed reduction in λE_{corr}. Most of the change in LAI was due to decline in DISP2. Vegetation at this site also had a significant component of beardless wildrye, *Leymus triticoides* and minor amounts of *Juncus sp*. The LAI of species without known Kc was approximately 40% of the total LAI at the peak of the summer. It is not known if differing physiology of these species contributed to the observed ET step change. Failure of the models at BLK009 was not easily attributable to substantial E or plant water stress, and the large difference from measured ET may reflect an inherent inability of both

Table 8. Eddy covariance ET corrected for energy balance closure and T model predictions. LAI data collected in early June and July (before and after the solstice) were used to bracket the Kc and GB model predictions of T. T_{Kc} relied on mean daily ETr. Measured and predicted fluxes are the sum of daily totals extrapolated for the growing season (March 25 to October 15).

Year	Site	ET_{corr}	$T_{Kc\ June}$	$T_{Kc\ July}$	$T_{GB\ June}$	$T_{GB\ July}$
		mm				
2000	BLK 100	460	450^	478	479	521
2001	BLK 100	446	399	369	450	415
	BLK 9	471	652	569	487	405
	PLC 45	165^^	254	245	166	90
2002	BLK 100	377	273	340	311	376
	FSL 138	646	284	388	347	484
	PLC 18	53	195	100	116	60
	PLC 74	177	133	120	94	80
	PLC 185	108	77	62	59	46
2003	BLK 100	527	330	314	367	346
	PLC 74	282	292	207	193	135
	PLC 185	205	112	97	60	56

^: Shaded values represent measurement date nearest the solstice (T_{GB}) or the maximum LAI in the T_{Kc} model for the dominant species.
^^: This value is exaggerated because of the poor correspondence of the shape of the Fourier model with the bimodal ET trend.

models for the dominant species, CHNA2. Although there were no obvious signs of water deficit in the LAI or appearance of the grasses, overestimation of the grass ET component cannot be ruled out with certainty because the water table was near the typical maximum rooting depth for SPAI, the second most abundant species at the site.

The model agreement with daily lE_{corr} was evaluated by calculating the root mean squared error (RMSE) between T_{Kc} or T_{GB} and measured daily lE_{corr}. Usually, RMSE of T_{Kc} was smaller than the corresponding T_{GB} (Table 7) suggesting the former model better approximates the overall progression of ET through the season. Performance for both models was poorest at FSL138, but the low RMSE for BLK009 and PLC045 were deceptive because the period with available lE_{corr} was limited to late July and after. Large suspected differences between the

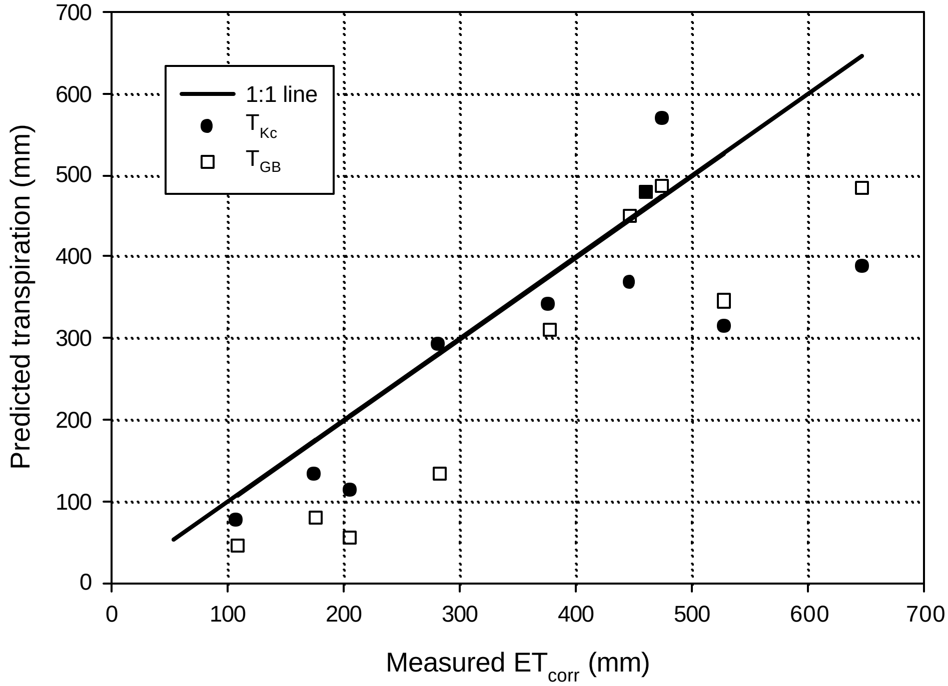

Figure 65. Predicted growing season transpiration from the Kc and GB models (shaded cells in Table 8) plotted against measured ET. PLC045 and PLC018 not plotted.

models and ET earlier in the growing season when lE_{corr} could not be calculated (Figures 55 and 56) and were not included in the RMSE calculation.

ET_{corr} summed for the growing season the growing season ranged between 53 and 646 mm (Table 8). Measured ET agreed best with T_{Kc} predictions of transpiration for five site-years: BLK100, 2002; PLC074, 2002; PLC074, 2003; PLC185, 2002; and PLC185, 2003. T_{GB} performed better for four site-years: BLK100, 2001; BLK100, 2003; BLK009; and FSL138. The model estimated totals were essentially equal for one site-year, BLK100 in 2000. Comparisons for PLC018 and PLC045 were not informative because conditions at those sites clearly violated assumptions of sufficient soil water present in both models. Better agreement with the seasonal totals at these sites should be considered a failure in the models. Mean difference between predicted and measured ET (n=10) was virtually identical; 88mm for T_{Kc} and 90mm for T_{GB}. Considering forecasted water requirements at monitoring sites using the Green Book method typically are less than 300 to 400mm, an average error of this magnitude is of considerable concern. T_{Kc} and T_{GB} varied several centimeters depending on which LAI measurements bracketing the midsummer solstice were used. In four instances the difference between seasonal totals using June and July LAI measurements in the same model was larger than the difference between the T_{Kc} and T_{GB} models. In those cases, reliance on a single midsummer measurement date determined a priori to represent the maximum LAI was as large a source of error as model selection. Based on a simple tabulation of the sites, the Kc performed marginally better (five to four) but given the relatively large error and variation caused by matching measured and modeled peak LAI, the appropriate conclusion is that the models performed equally.

Overall, both models usually underestimated measured ET (Figure 65). Underestimation by the transpiration models could have been caused by bare soil E and direct evaporation of precipitation sensed by the EC instruments but not accounted for by the transpiration models. Summer precipitation was small, less than 15 mm except for PLC045 (35mm), BLK100 in 2003 (38mm), and PLC185 in 2003 (17mm), so the impact of direct evaporation on measured ET was negligible. The primary method to minimize bare soil evaporation in this study was to avoid sites with water tables near the surface. Bare soil evaporation is a two stage process. Evaporation of the first stage with wet soil at the surface is limited by available energy; second stage evaporation is limited by the rate of unsaturated water transport through a dry surface layer. The surface layers (0-12 cm or deeper) were near the limiting water content for most of the growing season suggesting the flux through the bare surface was small (Hillel, 1980), yet the contribution of evaporation from winter precipitation held in the shallow soil layers early in the growing season cannot be easily discounted. Jacobs et al. (2002) found that the transition to second stage evaporation in Florida wetlands was marked by an increase in sensible heat and decrease in latent heat flux. No such transition was evident in this study except at PLC045 from DOY 130 to DOY 183. Also, the models often overestimated midsummer ET and underestimated late summer ET, long after winter precipitation was exhausted. Underestimation by the transpiration models in this study was apparently the due to a deficiency in the shape of the models and not failure to account for a significant flux measured by the EC towers.

The GB and Kc models contain submodels for LAI and mean ETr_i (Kc only), that can be compared with field measurements to lend insight into factors affecting the overall model performance. As before, LAI measured nearest the summer solstice was used in the GB model, and LAI measured nearest the date of maximum LAI for the dominant species was used in the Kc model (Table 4). The GB LAI models underestimated LAI for nearly all species and sites except possibly for SAVE at PLC074 (Figures 65 to 79). The Kc LAI models nearly always modeled LAI better than the GB models but still underestimated LAI for species at BLK100, BLK009 and PLC018. Performance of both models could have been improved by choosing an alternate measurement date(s) instead of relying on a fixed LAI measurement date to fix the maximum LAI in the model. The maximum LAI for individual species was often a month or more shifted from the Kc and GB model peak LAI. The agreement between the timing of observed and modeled peak LAI, however, was slightly better for the Kc model.

Mean daily ETr tracked measured ETr well except for short periods in midsummer all four years (Figure 80). The disagreement was most evident in June and July, 2001 and 2002 and

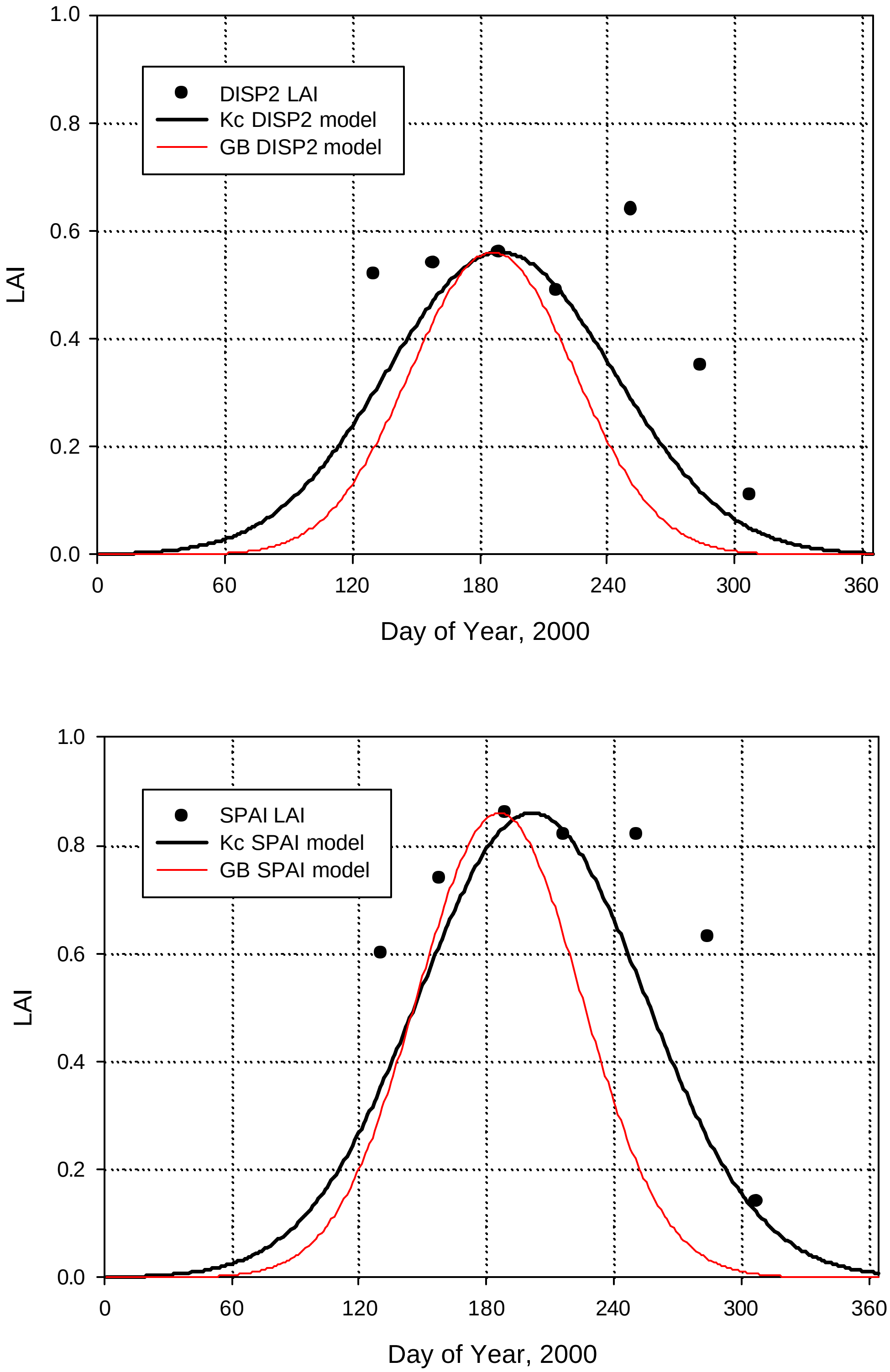

Figure 66. Measured LAI for dominant species, SPAI and DISP2, at BLK100 in 2000 and LAI models in T_{Kc} (Steinwand, 1998) and T_{GB}. Measured LAI is the mean of the four transects. Measurements taken on July 7 were used to set the maximum of the LAI models.

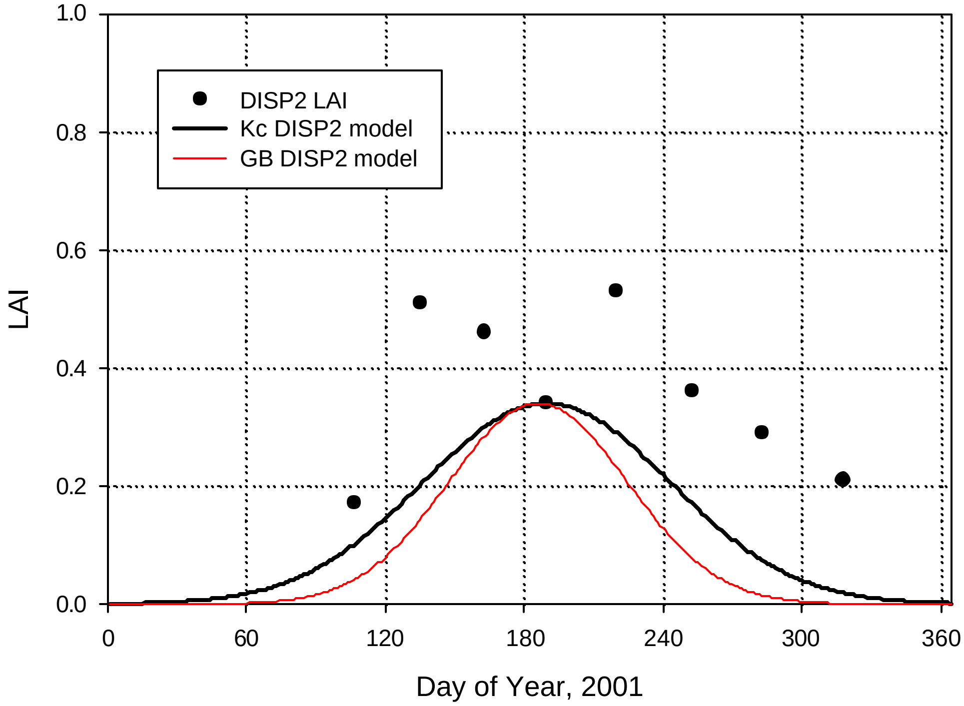

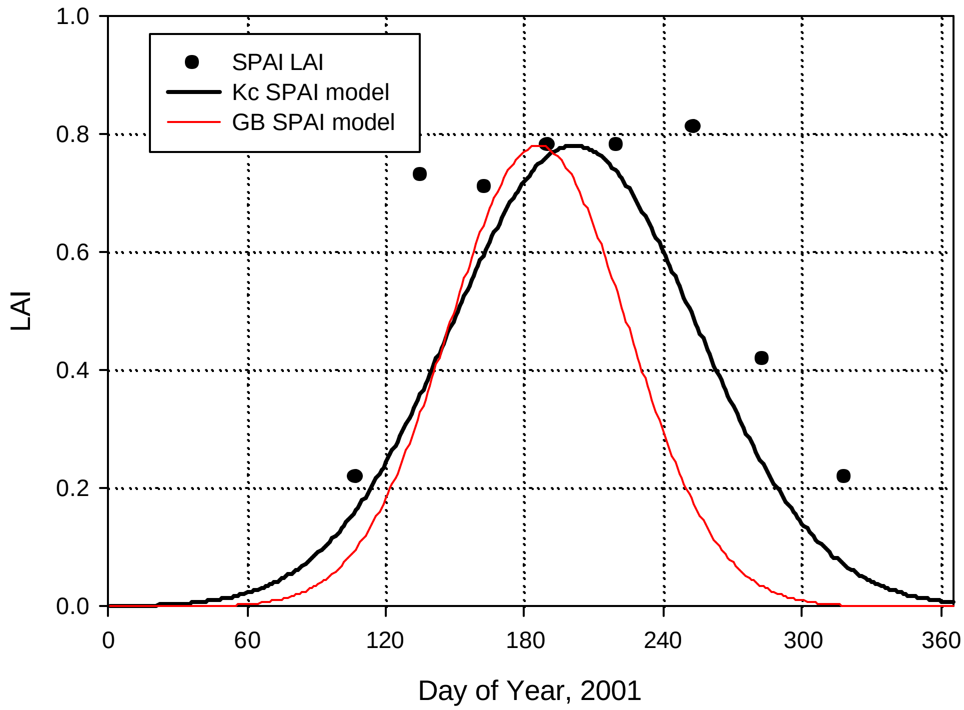

Figure 67. Measured LAI for dominant species, SPAI and DISP2, at BLK100 in 2001 and LAI models in T_{Kc} (Steinwand, 1998) and T_{GB}. Measured LAI is the mean of the four transects. Measurements taken on July 9 were used to set the maximum of the LAI models.

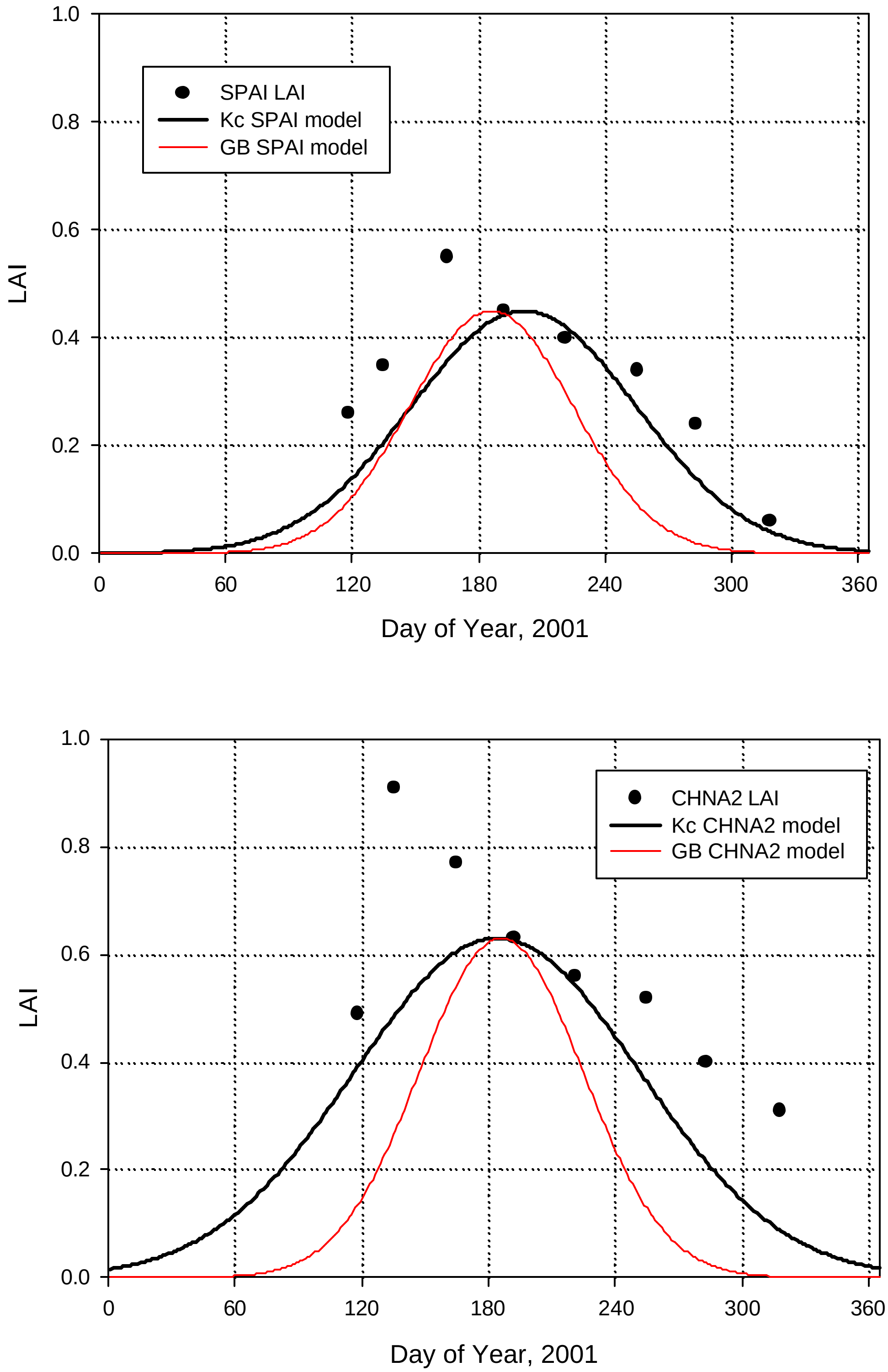

Figure 68. Measured LAI for dominant species, SPAI and CHNA2, at BLK009 in 2001 and LAI models in T_{Kc} (Steinwand, 1998) and T_{GB}. Measured LAI is the mean of the four transects. Measurements taken on July 11 were used to set the maximum of the LAI models.

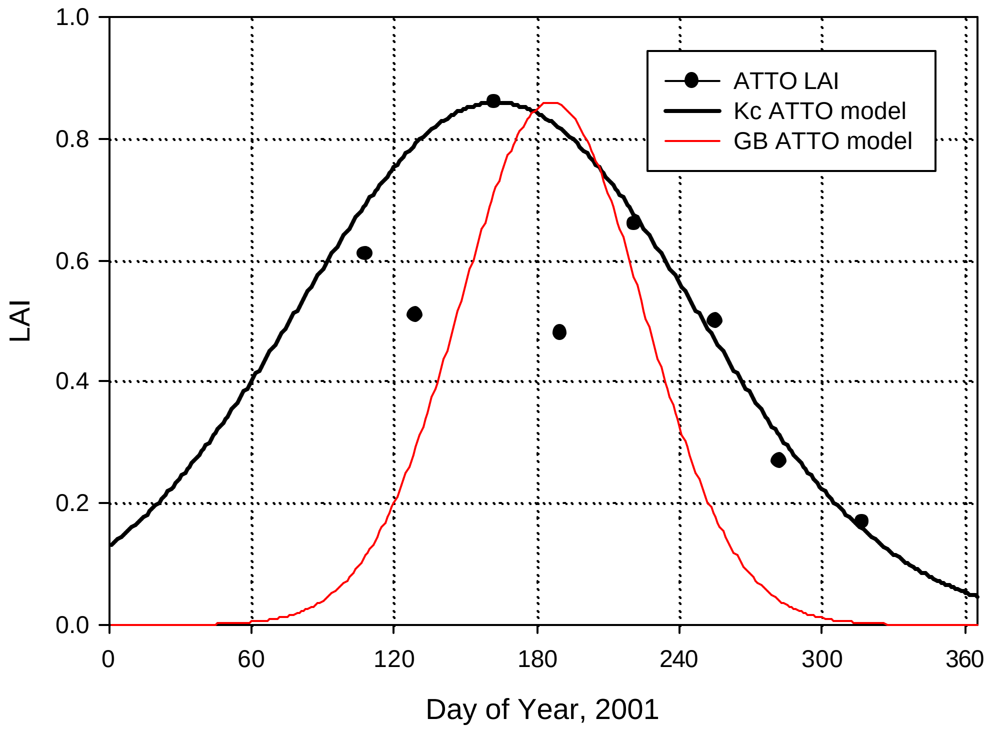

Figure 69. Measured LAI for dominant species, ATTO, at PLC045 in 2001 and LAI models in T_{Kc} (Steinwand, 1998) and T_{GB}. Measured LAI is the mean of the four transects. Measurements taken on July 9 were used to set the maximum of the LAI models. Neither model was designed to accommodate the bimodal pattern exhibited at this site.

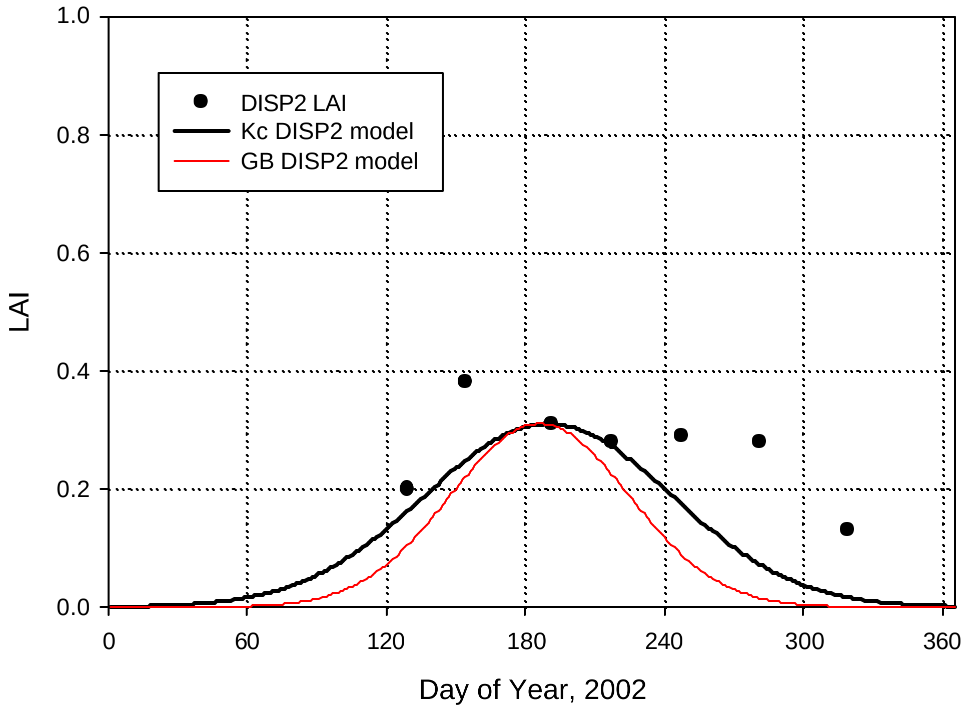

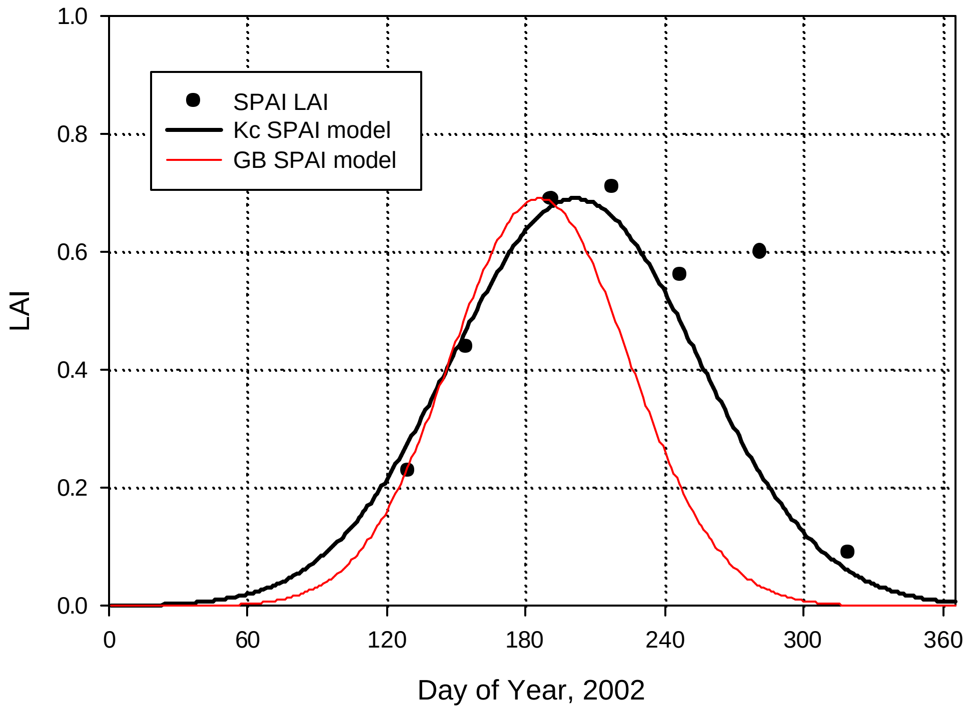

Figure 70. Measured LAI for dominant species, SPAI and DISP2, at BLK100 in 2002 and LAI models in T_{Kc} (Steinwand, 1998) and T_{GB}. Measured LAI is the mean of the four transects. Measurements taken on July 10 were used to set the maximum of the LAI models.

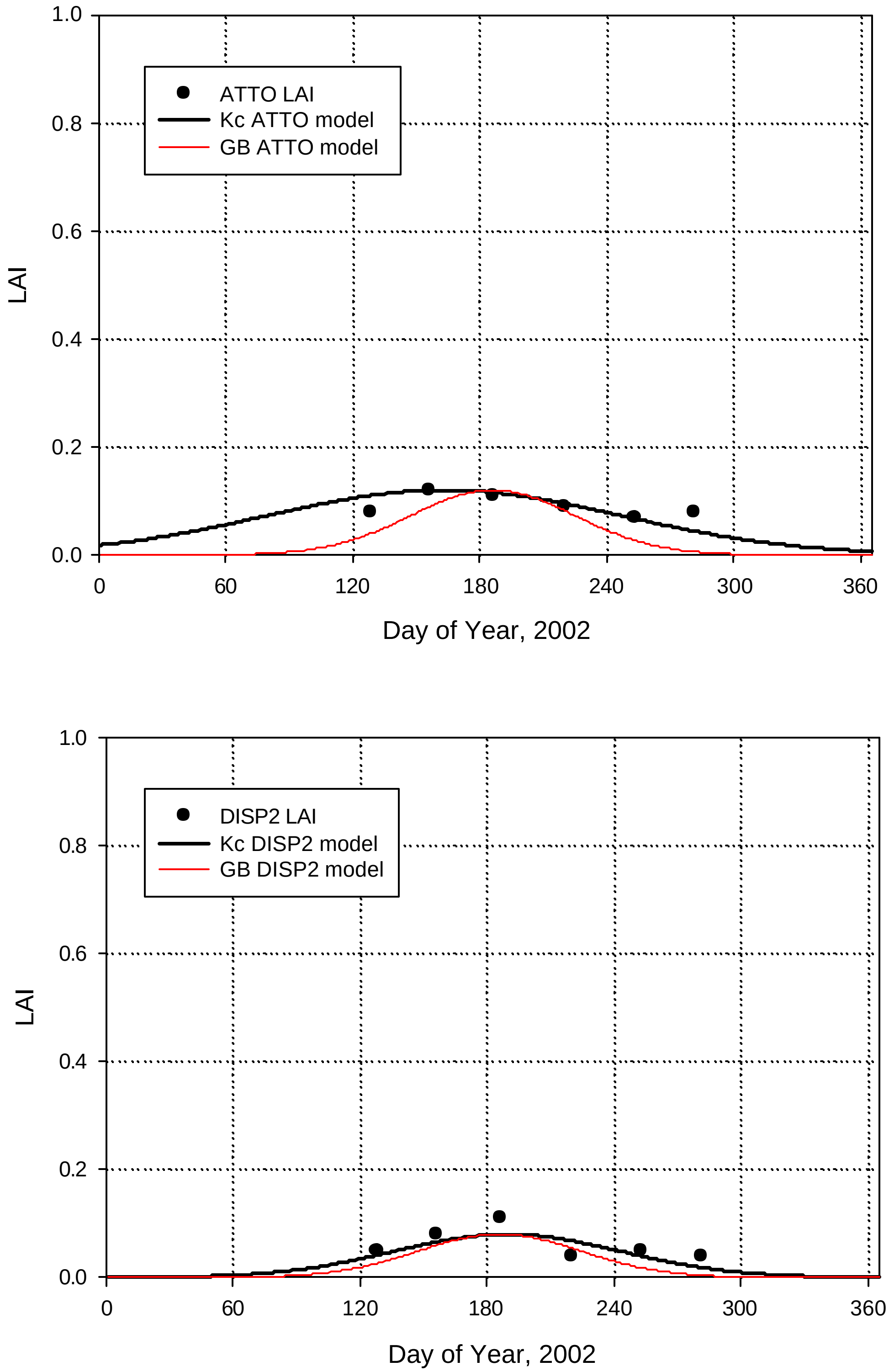

Figure 71 Measured LAI for dominant species, ATTO and DISP2, at PLC074 in 2002 and LAI model in T_{Kc} (Steinwand, 1998) and T_{GB}. Measured LAI is the mean of the four transects. Measurements taken on June 5 were used to set the maximum of the LAI models.

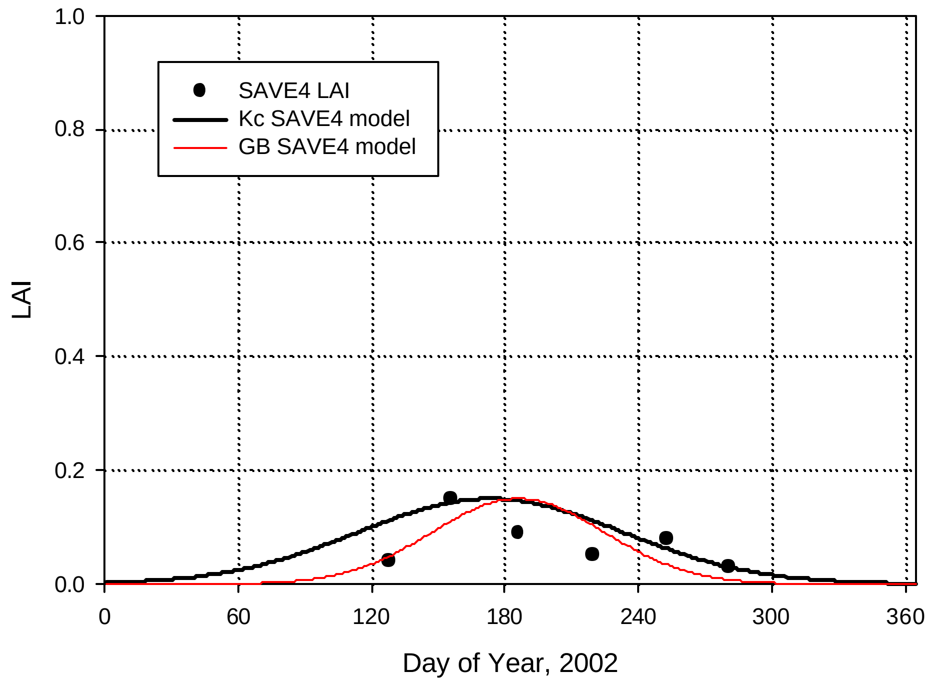

Figure 72. Measured LAI for dominant species, SAVE, at PLC074 in 2002 and LAI model in T_{Kc} (Steinwand, 1998) and T_{GB}. Measured LAI is the mean of the four transects. Measurements taken on June 5 were used to set the maximum of the LAI models.

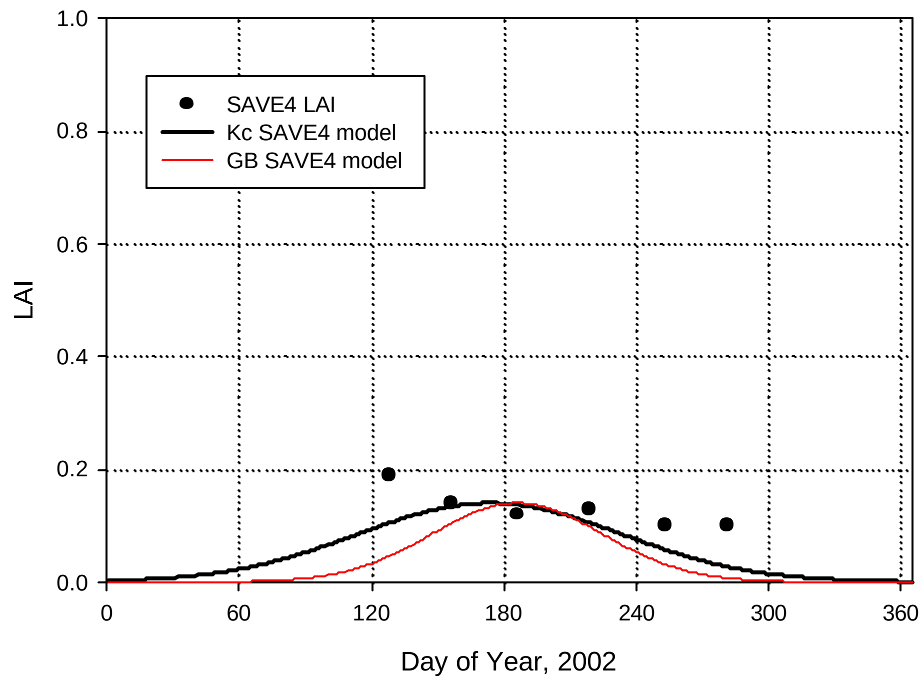

Figure 73. Measured LAI for dominant species, SAVE, at PLC185 in 2002 and LAI model in T_{Kc} (Steinwand, 1998) and T_{GB}. Measured LAI is the mean of the four transects. Measurements taken on June 5 were used to set the maximum of the LAI models.

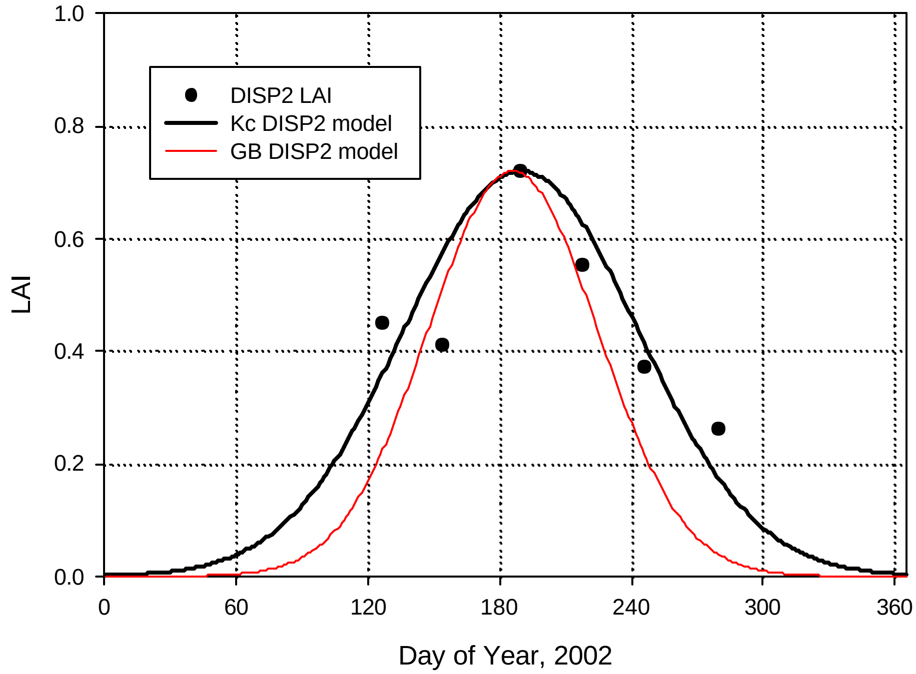

Figure 74. Measured LAI for dominant species, DISP2, at FSL138 in 2002 and LAI model in T_{Kc} (Steinwand, 1998) and T_{GB}. Measured LAI is the mean of the four transects. Measurements taken on July 8 were used to set the maximum of the LAI models.

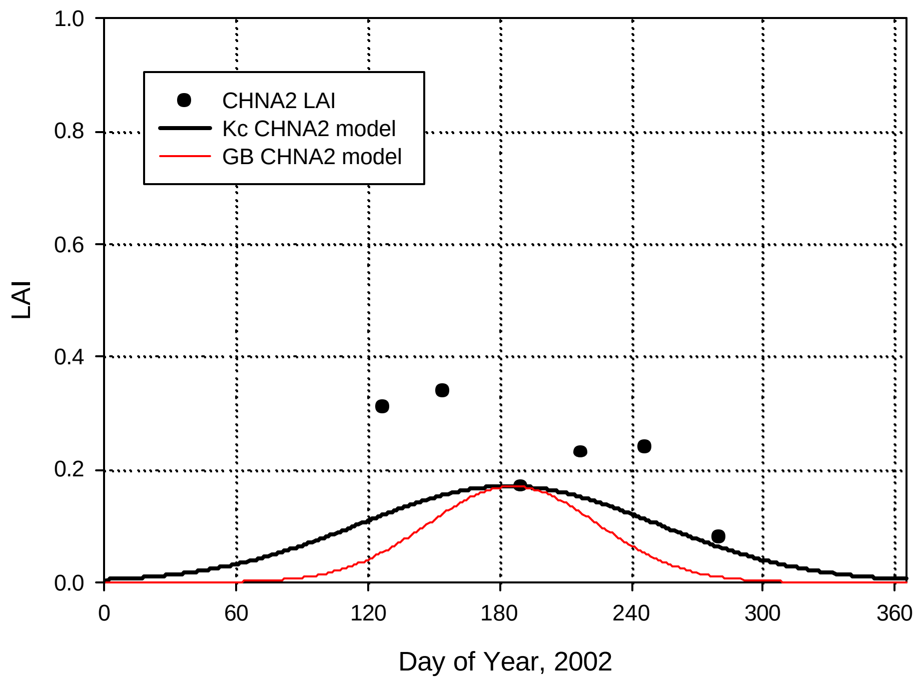

Figure 75. Measured LAI for dominant species, CHNA2, at PLC018 in 2002 and LAI model in T_{Kc} (Steinwand, 1998) and T_{GB}. Measured LAI is the mean of the four transects. Measurements taken on July 8 were used to set the maximum of the LAI models

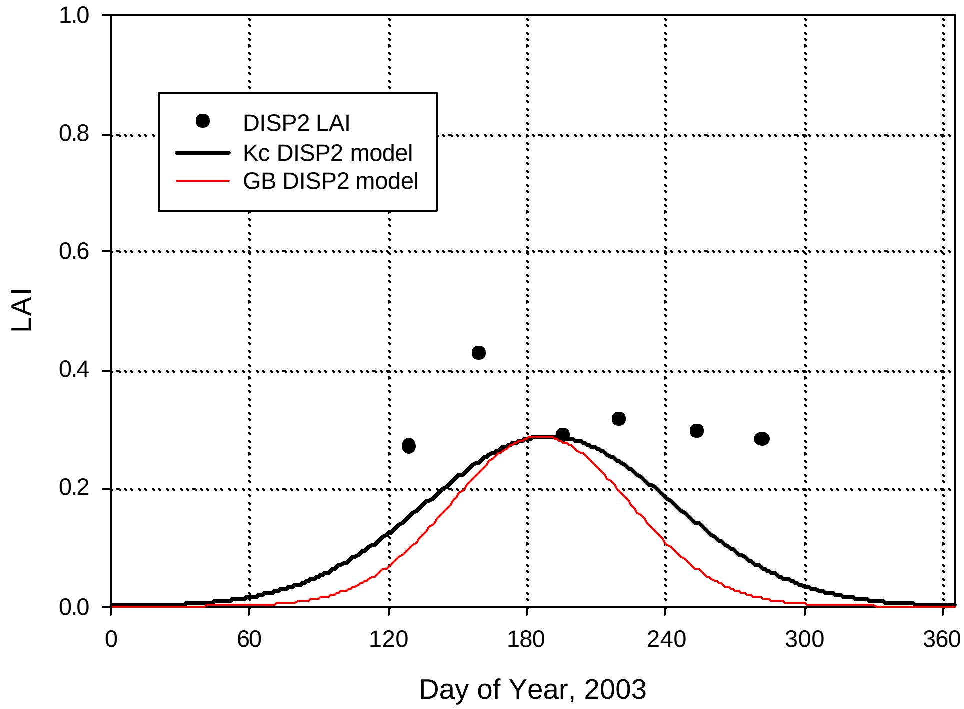

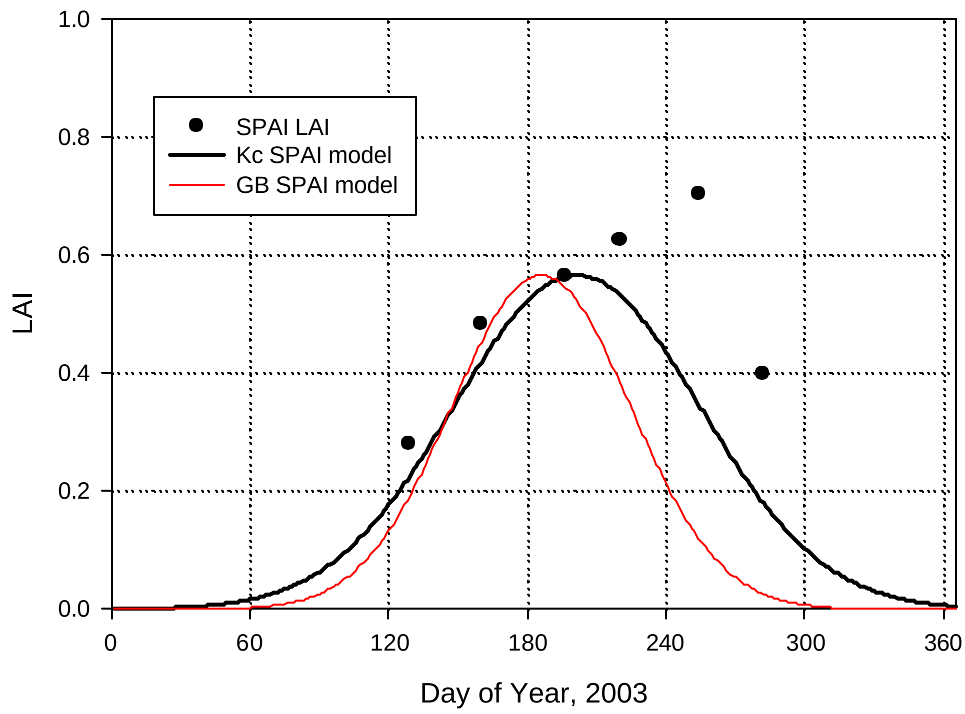

Figure 76. Measured LAI for dominant species, SPAI and DISP2, at BLK100 in 2003 and LAI models in T_{Kc} (Steinwand, 1998) and T_{GB}. Measured LAI is the mean of the four transects. Measurements taken on July 14 were used to set the maximum of the LAI models.

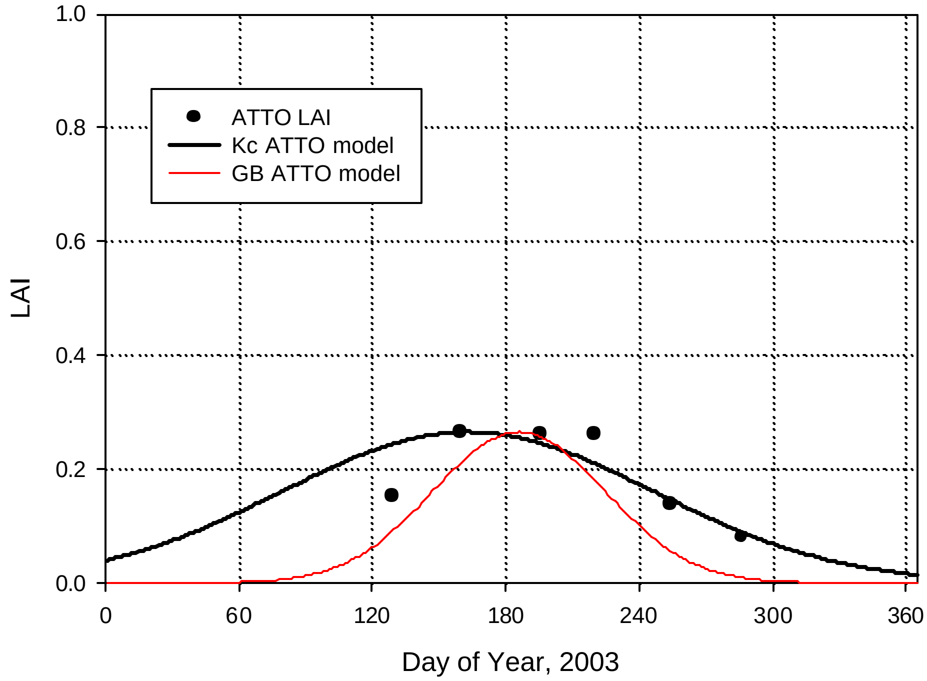

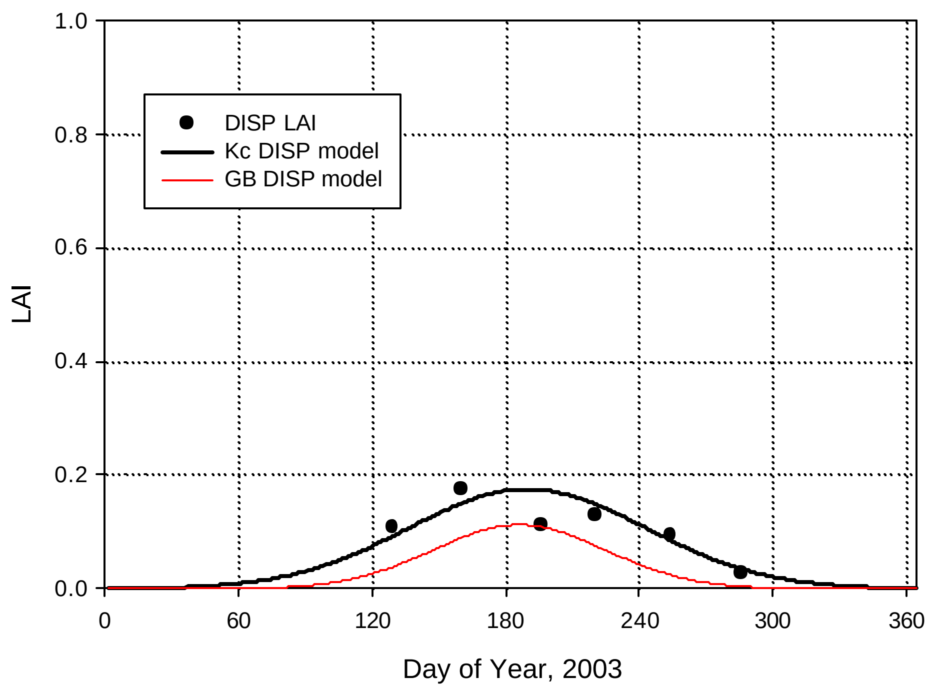

Figure 77. Measured LAI for dominant species, ATTO and DISP2, at PLC074 in 2003 and LAI model in T_{Kc} (Steinwand, 1998) and T_{GB}. Measured LAI is the mean of the four transects. Measurements taken on June 9 were used to set the maximum of the Kc LAI models and July 15 for GB models

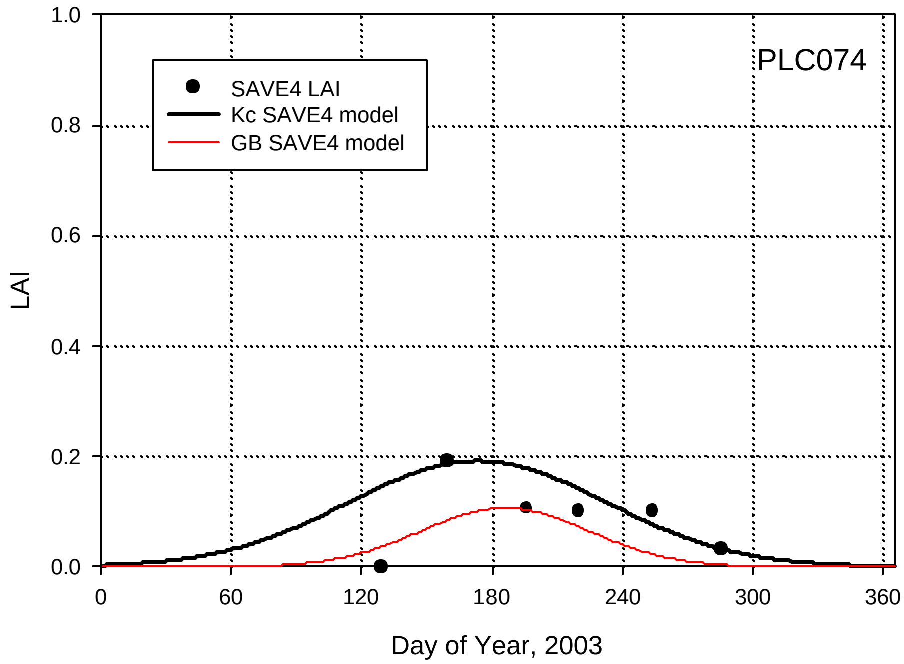

Figure 78. Measured LAI for dominant species, SAVE, at PLC074 in 2003 and LAI model in T_{Kc} (Steinwand, 1998) and T_{GB}. Measured LAI is the mean of the four transects. Measurements taken on June 9 were used to set the maximum of the Kc LAI models and July 15 for GB models

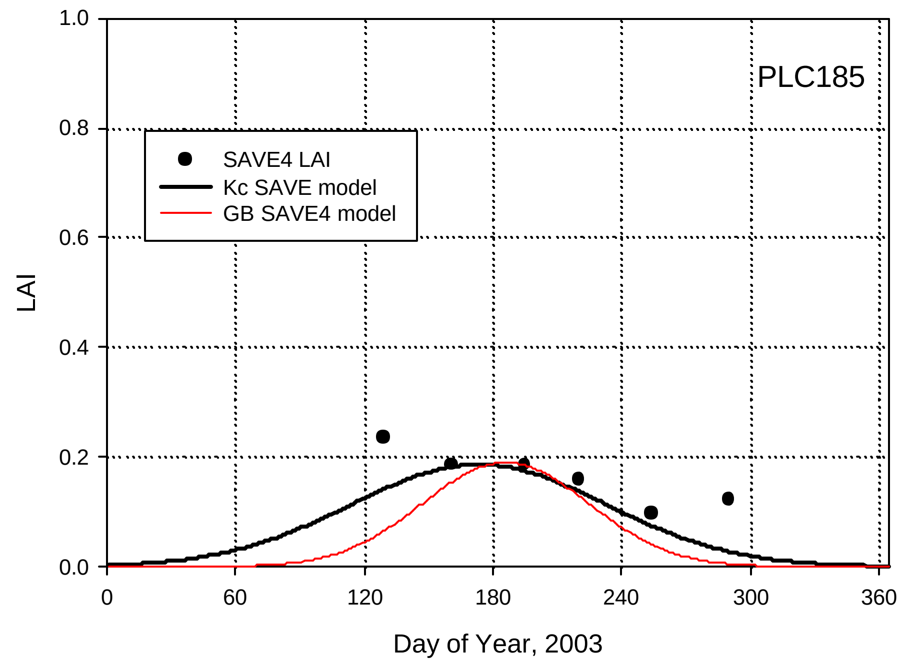

Figure 79. Measured LAI for dominant species, SAVE, at PLC185 in 2003 and LAI model in T_{Kc} (Steinwand, 1998) and T_{GB}. Measured LAI is the mean of the four transects. Measurements taken on June 10 were used to set the maximum of the Kc LAI models and July 15 for GB models

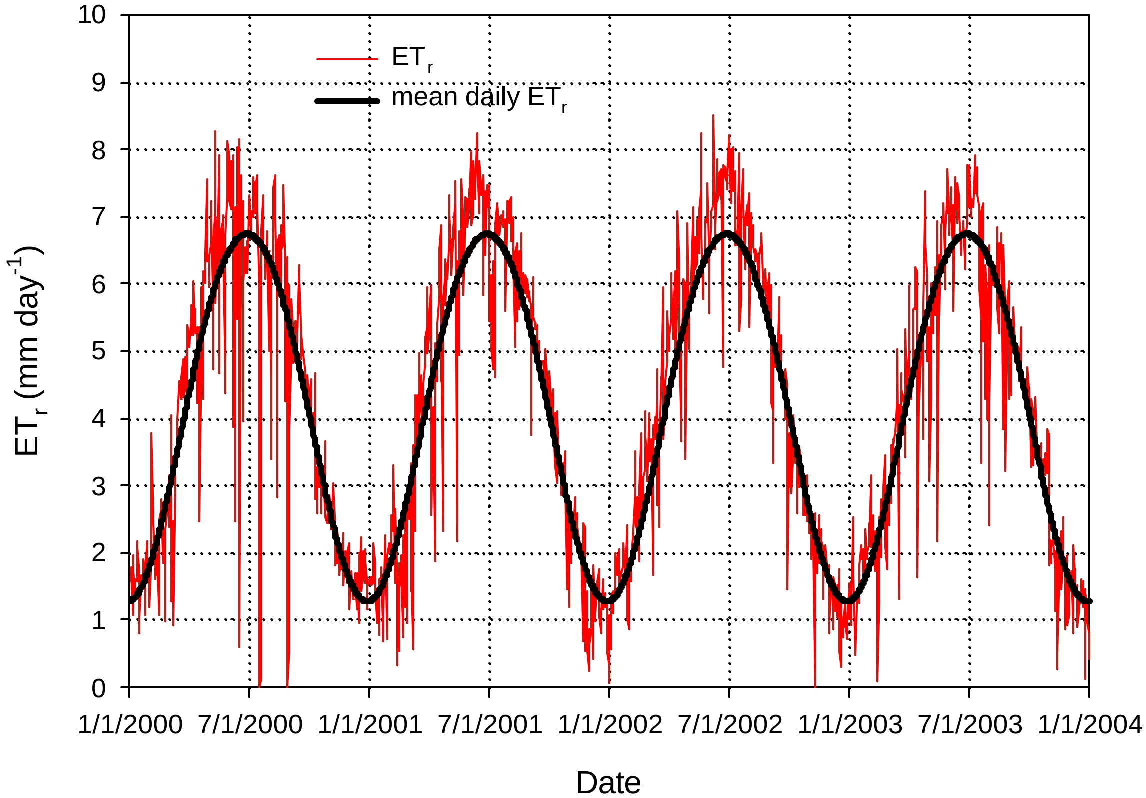

Figure 80. Mean daily ETr and daily ETr measured in 2000-2002 at the CIMIS station in Bishop, Ca.

was probably due to hotter than average temperatures. If the actual daily ET values were utilized instead of the modeled daily mean, T_{Kc} estimates increase slightly for 2001-2002, decrease slightly for 2000, and are essentially unchanged in 2003. The inclusion of ETr in the Kc model probably wasn't a large source of the deviation from ET_{corr}.

Conclusions and Recommendations

Eddy covariance measurements of ET were collected successfully during most of the growing season at seven sites over four years. Turbulent fluxes measured by the EC system, however, did not account for approximately one-third of the available energy, similar to discrepancies observed in other studies using EC methods. A comparison with a Bowen ratio station at one site was conducted to examine the energy imbalance further. During periods when the BR system obtained stable measurements, the Bowen ratios measured by the two systems substantially agreed, allowing use of the Bowen ratio measured by the EC system to correct lE and H to account for all the available energy.

The comparison of growing season ET measured by the EC systems and model predictions based on vegetation measurements did not show conclusively which model should be favored for groundwater management. Both models generally tracked the progression of ET through the growing season although the consistent underestimation early and late in the growing season suggest an inherent deficiency in the shape of the models. Usually the difference between the modeled and measured values of daily ET was smaller for the Kc model than the GB model. Likewise, the LAI models used to prepare the original Kc clearly agreed better with measured values for dominant species than the GB LAI model although performance of both sets of models often was limited by the procedure to fix maximum LAI for all species by a single midsummer measurement. Both models provide “ballpark” estimates that roughly correspond with independent ET measurements suggesting the assumptions necessary to scale up models derived from porometric data were largely met. Both the Kc and GB models, however, tended to underestimate total growing season ET, and transpiration estimates for the growing season best agreed with measured ET for essentially equal numbers of site-years with the T_{Kc} model performing marginally better. Poor predictions of actual ET occurred despite the attempt to select sites to conform with the model assumptions.

From this study, it is not obvious that either model should be favored for groundwater pumping management although the performance of the Kc models and its LAI component was marginally superior. Additional advantages of the Kc models described in previous Inyo County reports include better documentation of methods and data upon which they are based and the capability to subject the model prediction to error analysis. The relatively large average error, occasional poor performance, and frequent underestimation of actual ET suggest either model must be used with due regard for its imprecision. Ignoring prediction error in these models for pumping management is not advised.

Presentations

Steinwand, A.L., R.F. Harrington, P.J. Hubbard, and D. Martin. 2002. Transpiration coefficients and eddy covariance estimates of evapotranspiration of Great Basin phreatophytes. In Agronomy Abstracts, ASA, Madison, WI.

Steinwand, A.L., R.F. Harrington, and D. Or. 2003. Water balance closure for Owens Valley phreatophytes combining water table, eddy covariance, and soil water measurements. In Agronomy Abstracts, ASA, Madison, WI.

References

Allen, R.B., L.S. Pereira, D. Raes, and M.S. Smith. 1998. Crop ET, Irrigation, and Drainage. Paper #56. Food and Agriculture Organization of the United Nations. Rome, Italy.

Arya, S.P. 2001. Introduction to Micrometeorology, Second Edition, Academic Press.

Berger, D.L., M.J. Johnson, and M.L. Tumbusch. 2001. Estimates of Evapotranspiration from the Ruby Lake National Wildlife Refuge Area, Ruby Valley, Northeastern Nevada, May 1999-October 2000. USGS Water Resources Investigations Report 01-4234.

Bidlake, W.R. 2000. Evapotranspiration from a Bulrush-Dominated Wetland in the Klamath Basin, Oregon. J. of Amer. Water Res. Assoc. 36(6), 1309-1320.

Bidlake, W.R. 2002. Evapotranspiration from Selected Fallowed Fields on the Tule Lake National Wildlife Refuge, California, During May to October 2000, USGS Water Resources Investigations Report 02-4055.

Blake, G.R., and K.H. Hartage. 1986. Bulk density. *In* A. Klute (ed.) Methods of soil analysis. Part 1. 2nd ed. Agronomy 9:363-376.

Brutsaert, W. 1982. Evaporation into the atmosphere. D. Reidel.

Campbell Scientific Inc. 1998a. CSAT Three Dimensional Sonic Anemometer Instruction Manual, Revision 3/98.

Campbell Scientific Inc. 1998b. Eddy Covariance System Operator's Manual CA27 and KH20, Revision 7/98.

Campbell Scientific Inc. 1989. KH20 Krypton Hygrometer, Revision 11/89.

Campbell Scientific Inc. 1996. Q-7.1 Net Radiometer, Revision 5/96.

Campbell Scientific Inc. 1996. CS615 Water Content Reflectometer Instruction Manual, Version 8221-07, Revision 10/96.

Campbell Scientific Inc. 1999. HFT3 Soil Heat Flux Plate, Revision 2/99.

Campbell, G.S., and J.M. Norman. 1998. An Introduction to Environmental Biophysics, Second Edition, Springer.

CIMIS, California Irrigation Management Information System. 2003. Agric. Water Conservation Section, Dept. of Water Resources, Sacramento, CA.

Duell, L.F.W. 1990. Estimates of Evapotranspiration in Alkaline Scrub and Meadow Communities of Owens Valley, California, Using the Bowen-Ratio, Eddy-Correlation, and Penman-Combination Methods. USGS Water Supply Paper 2370-E.

Gash, J.H.C. 1986. A not on estimating the effect of a limited fetch on micrometeorological evaporation measurements. Bound.-Layer Met. 35:409-413.

Graupe, D. and D.I. Krause, 1973. On the identification of input-output noise models. Int. J. Syst. Sci. 4:617-621.

Groeneveld, DP. 1990. Deep root trench study. Report to Inyo/LA Technical Group. December 17, 1990. 44pp.

Hillel, D. 1980. Introduction to soil physics. Academic Press, Inc., London, U.K.

Jacobs, J.M., S.L. Mergelsberg, A.F. Lopera, D.A. Myers. 2002. Evapotranspiration from a wet prairie wetland under drought conditions: Paynes Prairie Preserve, Florida, USA. Wetlands. 22:374-385.

Manning, S.J., J.F. Mustard, and A.J. Elmore. 1999. Patterns of vegetation response to groundwater pumping detected with field monitoring and LandSat TM data. Ecological Society of America. August 1999. Spokane, WA. Ecological Society of America abstracts vol. 84.

Massman, W.J., D.G. Fox, K.F. Zeller, and D. Lukens. 1990.Verifying Eddy Correlation Measurements of Dry Deposition: A Study of the Energy Balance Components of the Pawnee Grasslands. USDA Rocky Mountain Forest and Range Experiment Station Research Paper RM-288.

Norman J.M. and J.L. Baker. 2002. Have eddy-flux measurements improved over thirty years. Agronomy Abstracts, American Society of Agronomy, Madison, WI.

Or, D., and D.P. Groeneveld. 1994. Stochastic estimation of plant-available soil water under fluctuating water table depths. J. Hydrol. 163:43-64.

Salas, J.D., W. Delleur, V. Yevjevich, and W.L. Lane. 1980. Applied modeling of hydrologic time series. Water Resource Publications, Fort Collins, Co.

Shuttleworth, W. J. 1993. Evaporation. In Handbook of Hydrology, ed. D. R. Maidment, McGraw-Hill.

Steinwand, A.L. 1998. Evaluation of methods to calculate vegetation water requirements for the Owens Valley, Ca. Report to the Inyo/Los Angeles Technical Group, February 28, 1998. 55pp.

Steinwand, A.L, 1999a. Transpiration coefficients for three Great Basin shrubs. Report to the Inyo/Los Angeles Technical Group, May 12, 1999. 41pp.

Steinwand, A.L. 1999b. Transpiration coefficients for two Great Basin phreatophytic grasses. Report to the Inyo/Los Angeles Technical Group, November 24, 1999. 91pp.

Steinwand, A.L. 2000a. Comparison of Green Book and Kc calculations to estimate vegetation water requirements. Report to the Inyo/Los Angeles Technical Group, February 3, 2000. 14 pp.

Steinwand, A.L. 2000b. The Effects of Kc and Green Book models for vegetation water requirements on permanent monitoring site On/Off status. Report to the Inyo/Los Angeles Technical Group, April 24, 2000. 47pp.

Steinwand, A.L., R.F. Harrington, and D.P. Groeneveld. 2001. Transpiration coefficients for three Great Basin shrubs. J. Arid Env. 49:555-567.

Steinwand, A.L, and R.F. Harrington. 2003. Water table fluctuations resulting from management under the Drought Recovery Policy and the Green Book, 1989 to 2000. Report to the Inyo/Los Angeles Technical Group, February 25, 2003. 44pp.

Steinwand, A.L. and D. Olsen. 2003. Calibration and operation of Hydrosense™ TDR for measuring soil water at shallow depths. Report to the Inyo/Los Angeles Technical Group, December 9, 2003. 10pp.

Sumner, D.M. 1996. Evapotranspiration from Successional Vegetation in a Deforested Area of the Lake Wales Ridge, Florida. USGS Water Resources Investigations Report 96-4244.

Webb, E. K., G. I. Pearman, and R. Leuning. 1980. Correction of flux measurements for density effects due to heat and water vapor transfer. Quart. J. R. Meteorol. Soc., 106, 85-100.

Zeller, K.F., W. Massman, D. Stocker, D.G. Fox, D. Stedman, and D. Hazlett. 1989. Initial Results from the Pawnee Eddy Correlation System for Dry Acid Deposition Research. USDA Rocky Mountain Forest and Range Experiment Station Research Paper RM-282.

Appendix A: Daily eddy covariance, energy balance component, and transpiration model results.

Note that some obviously erroneous data have not been culled, and the data have not be rounded to significant figures to prevent rounding errors in the future if results presented in this Appendix are utilized for another purpose.